1-29-2015 12:00 AM

Distal Humerus Hemiarthroplasty: Joint Kinematics, Stability, Congruency and Implant Design

Sagar J. Desai
The University of Western Ontario

Supervisor
Dr. Graham King
The University of Western Ontario Joint Supervisor
Dr. James Johnson
The University of Western Ontario

Graduate Program in Medical Biophysics
A thesis submitted in partial fulfillment of the requirements for the degree in Master of Science

DISTAL HUMERUS HEMIARTHROPLASTY: JOINT KINEMATICS, STABILITY, CONGRUENCY AND IMPLANT DESIGN

Integrated Article Format

by

Sagar J. Desai

Graduate Program in Medical Biophysics

A thesis submitted in partial fulfillment
of the requirements for the degree of
Master of Science

The School of Graduate and Postdoctoral Studies
Western University
London, Ontario, Canada

Abstract

Distal humeral hemiarthroplasty is a treatment option for fractures, non-unions and avascular necrosis of the distal humerus. Commercially available distal humeral implants are available; however, many unanswered questions remain regarding their role in treatment of distal humeral pathology. The optimal articular shape of the implant has not been defined, the biomechanical effects have not been reported, and contact stresses on native articular cartilage are unknown.

This work has defined the osseous anatomy and anatomic variability of the distal humeral articulation using accurate 3D reconstruction methods. A data bank of distal humeral dimensions has been created and may be effective in the development of future implants. Kinematic investigations have shown small but significant alteration in elbow joint kinematics with placement of a distal humeral hemiarthroplasty.

This work shows that currently available hemiarthroplasty implants may not be anatomically accurate, and may not reproduce native elbow kinematics. Further efforts are needed to create and test more anatomic distal humeral implants.

Keywords

Elbow hemiarthroplasty; implant design; elbow kinematics

Co-Authorship Statement

Chapter 1 Sagar J. Desai – Sole Author

Chapter 2 Sagar J. Desai - Study Design, Specimen Preparation, Data Collection, Data Analysis, Manuscript Review

Simon Deluce – Specimen Preparation, Data Collection, Data Analysis, Manuscript Review

James A. Johnson - Study Design, Manuscript Review

Louis M. Ferreira - Study Design, Data Collection, Manuscript Review

Alexandre Leclerc - Data Collection, Manuscript Review

George S. Athwal - Study Design, Manuscript Review

Graham J.W. King - Study Design, Manuscript Review

Chapter 3 Sagar J. Desai - Study Design, Specimen Preparation, Data Collection, Data Analysis, Manuscript Review

George S. Athwal - Study Design, Specimen Preparation, Manuscript Review

Louis M. Ferreira – Study Design, Specimen Preparation, Manuscript Review

Emily A. Lalone - Study Design, Specimen Preparation, Manuscript Review

James A. Johnson - Study Design, Manuscript Review

Graham J. W. King - Study Design, Specimen Preparation, Manuscript Review

Chapter 4 Sagar J. Desai - Study Design, Specimen Preparation, Data Collection, Data Analysis, Manuscript Review

Emily A. Lalone - Study Design, Specimen Preparation, Manuscript Review

George S. Athwal - Study Design, Specimen Preparation, Manuscript Review

Louis M. Ferreira – Study Design, Specimen Preparation, Manuscript Review

James A. Johnson - Study Design, Manuscript Review

Graham J. W. King - Study Design, Specimen Preparation, Manuscript Review

Chapter 5 Sagar J. Desai – Sole Author

Publication Status

Chapter 2 A version of this manuscript has been published in the Journal of Shoulder and Elbow Surgery. Permission to reprint this version of the manuscript has been granted by the publisher (See Appendix C).

Desai SJ, Deluce, S., Johnson JA, Ferreira LM, Leclerc AE, Athwal GS and King JW. An anthropometric study of the distal humerus. J Shoulder Elbow Surg. 2014 Feb;23, 463-469

Chapter 3 A version of this manuscript has been published in the Journal of Shoulder and Elbow Surgery. Permission to reprint this version of the manuscript has been granted by the publisher (See Appendix C).

Desai SJ, Athwal GS, Ferreira LM, Lalone E, Johnson JA and King GJW. Distal Humerus Hemiarthroplasty: The Effect of Implant Sizing on Elbow Joint Kinematics. J Shoulder Elbow Surg. J Shoulder Elbow Surg. 2014;23:946-954

Chapter 4 A version of this manuscript will be submitted for publication in the Journal of Shoulder and Elbow Surgery.

Acknowledgments

I would like to thank many people who were instrumental in the completion of this thesis. Firstly, I would like to thank my supervisors Dr. Graham King and Dr. James Johnson. Dr. Johnson, thank you for your constant support and direction during this process. You always were available and took countless hours of your own time to allow me to achieve this goal of mine. Dr. King, thank you for all your support over the past five years. You have been instrumental in my development both as a surgeon and researcher. You have been a true inspiration to me and made me realize that it is possible to be a technically sound surgeon, great educator AND a master researcher.

I would also like to express my gratitude to the researchers at the Hand and Upper Limb Center Bioengineering laboratory. Louis Ferreira, Simon Deluce, Hannah Shannon, Emily Lalone and Mark Walsh – you have been instrumental in my success in completing this Masters degree. Your hard work, long hours, and expertise helped me tremendously in all aspects of my research – from study design to manuscript review. Thank you so much, I could not have completed this without your help. Dr. George Athwal was also instrumental during this process. Thank you for your help from the first to the last day of this process. My many conversations and emails with you were instrumental in progressing through this research. Similar to Dr. King, you have played an instrumental role in my development as both a surgeon and scientist.

I would also like to thank the Department of Medical Biophysics for being so accommodating during the process of completing my Masters. Thank you for understanding

the challenges of completing a Masters during a challenging surgical residency, and being accommodating with course selection and exams.

Finally, I would like to thank my family. My parents and my wife have always been great supporters of all my life's endeavors. Thank you for all your support and understanding during a very difficult residency period and for the time and commitment it took to complete a Masters degree on top of this. The extra nights and weekends in addition to a surgical residency schedule were always met with support and understanding. Thank you. I simply would not have been able to complete this without you.

Sincerely,

Sagar J. Desai

Table of Contents

List of Figures

List of Tables

Chapter 1

Introduction

Overview

The purpose of this thesis is to evaluate the anatomy of the distal humerus, and the effect of elbow hemiarthroplasty on joint kinematics and joint congruency. As an introduction, this chapter will focus on the anatomy and kinematics of the elbow. The role and current state of knowledge on elbow hemiarthroplasty will also be reviewed. The objective, hypothesis, rationale and outline of the thesis are highlighted.

1.1 The Elbow

The primary function of the elbow is to position and stabilize the hand in space (1, 2). The elbow consists of three bones, as well as various ligaments and muscles which provide stability and assist in movement of the elbow joint.

1.1.1 Osteology

The human elbow consists of the articulation between three bones: the humerus, radius and ulna. These bones make up the three articulations of the elbow: the ulnohumeral joint, the radiocapitellar joint and the proximal radioulnar joint. The ulnohumeral joint consists of the greater sigmoid notch of the ulna, which articulates with the trochlea of the distal humerus (Figure 1.1).

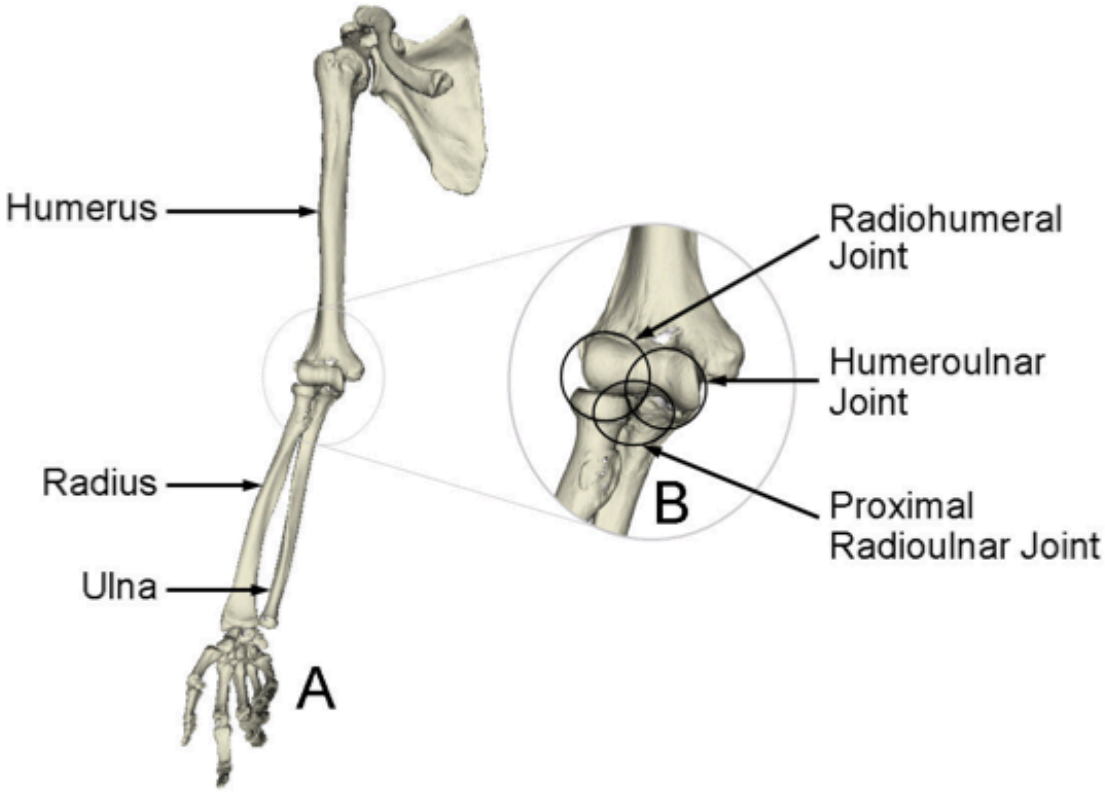

Figure 1.1 Osteology of the Elbow. (A) Upper extremity, consisting of the scapula, clavicle, humerus, radius, ulna, carpals, metacarpals and phalanges. (B) The elbow under magnification, demonstrating the three articulations of the elbow: the ulnohumeral joint, radiohumeral joint and proximal radioulnar joint.

All figures in this thesis have been created/taken at the Roth|McFarlane Hand and Upper Limb Centre laboratory, London, Ontario, Canada unless otherwise specified.

The ulnohumeral joint allows for flexion/extension of the elbow and is responsible for the majority of the stability of the elbow. Forearm rotation can also occur in the form of pronation and supination. During rotation, the ellipsoid-like capitellum rotates against the lesser sigmoid notch of the ulna (Figure 1.2).

The flexion-extension (F-E) axis of the distal humerus is defined by the geometric centers of the capitellum and the trochlear groove. A line connecting these two points represents the F-E axis (Figure 1.3). The F-E axis is in valgus with respect to the humerus and is internally rotated with respect to the epicondylar axis (Figure 1.4).

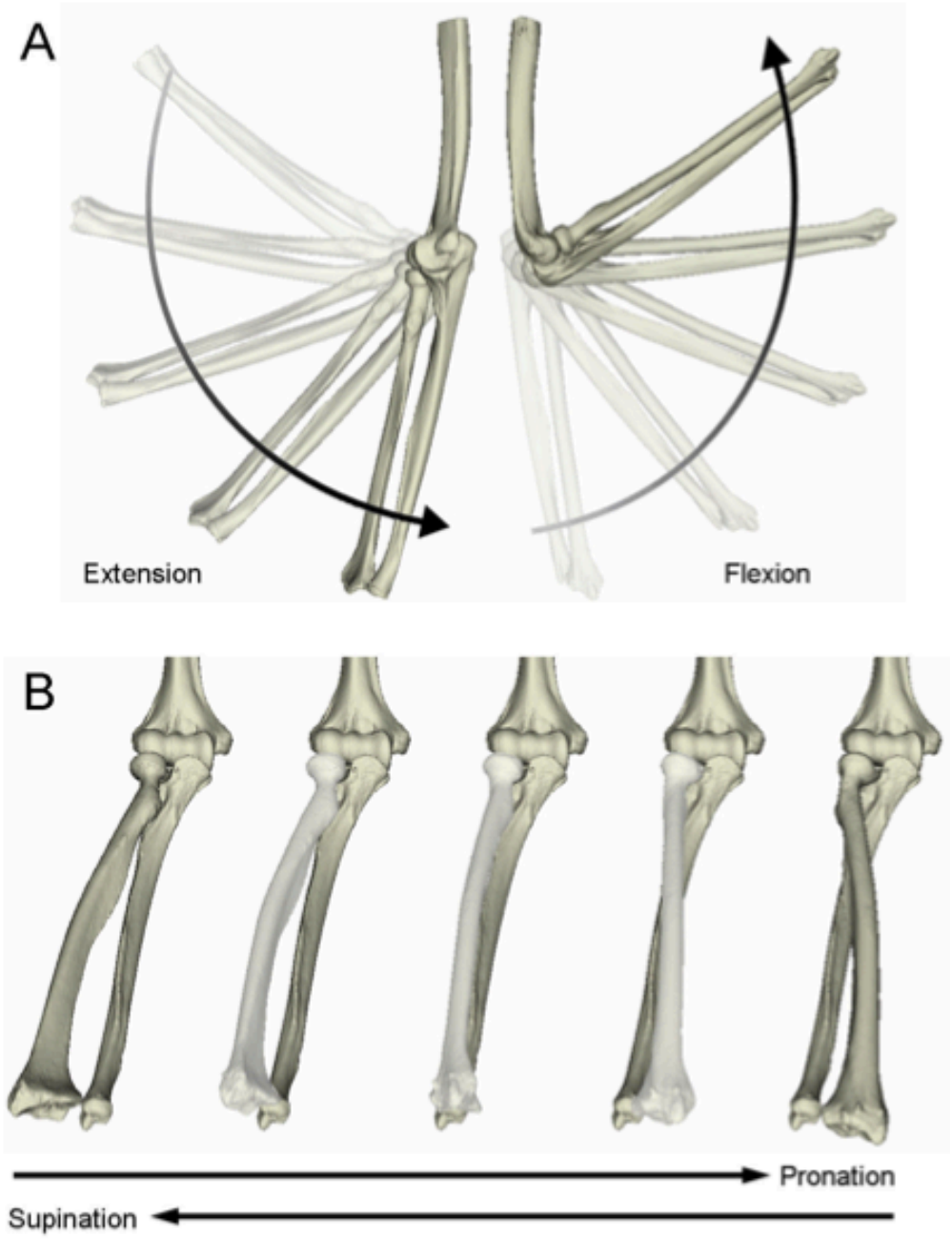

Figure 1.2: Elbow motions: (A) Elbow flexion and extension. (B) Forearm pronation and supination.

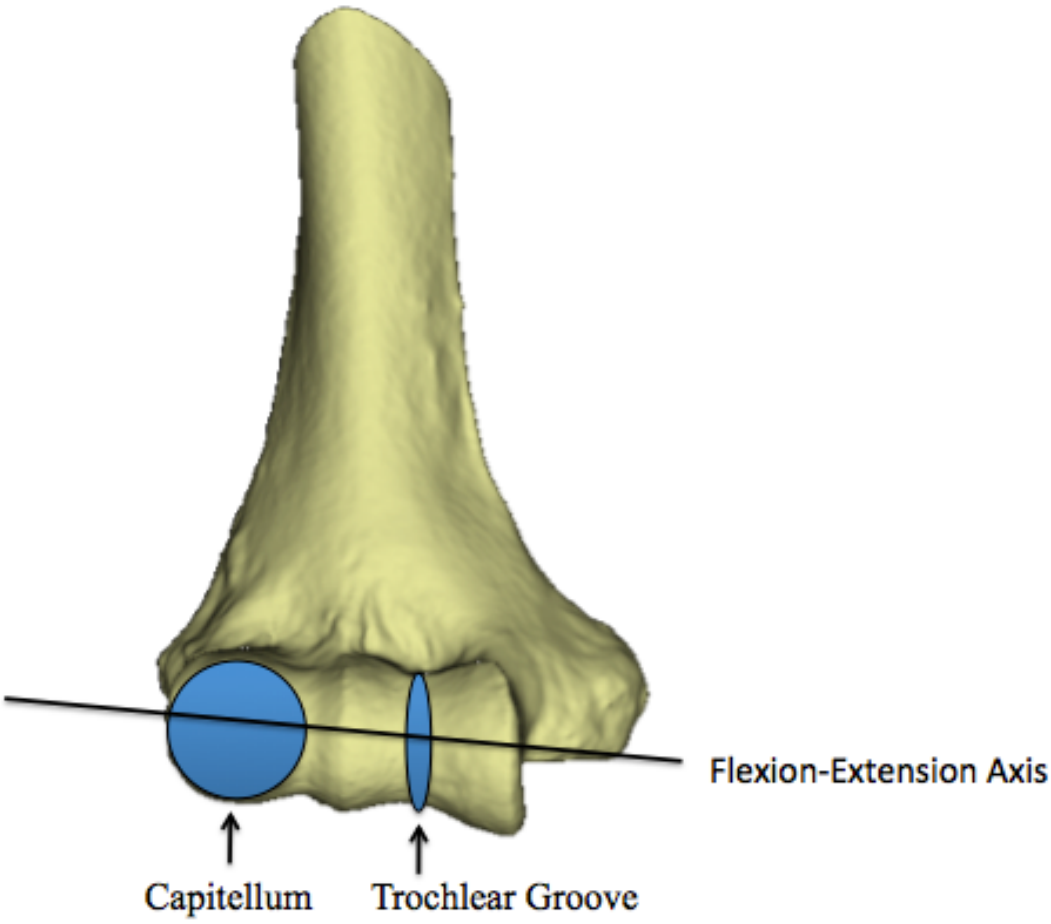

Figure 1.3: Flexion-extension (F-E) axis of the elbow. The F-E axis of the elbow is defined by a line connecting the geometric centre of the capitellum and the trochlea.

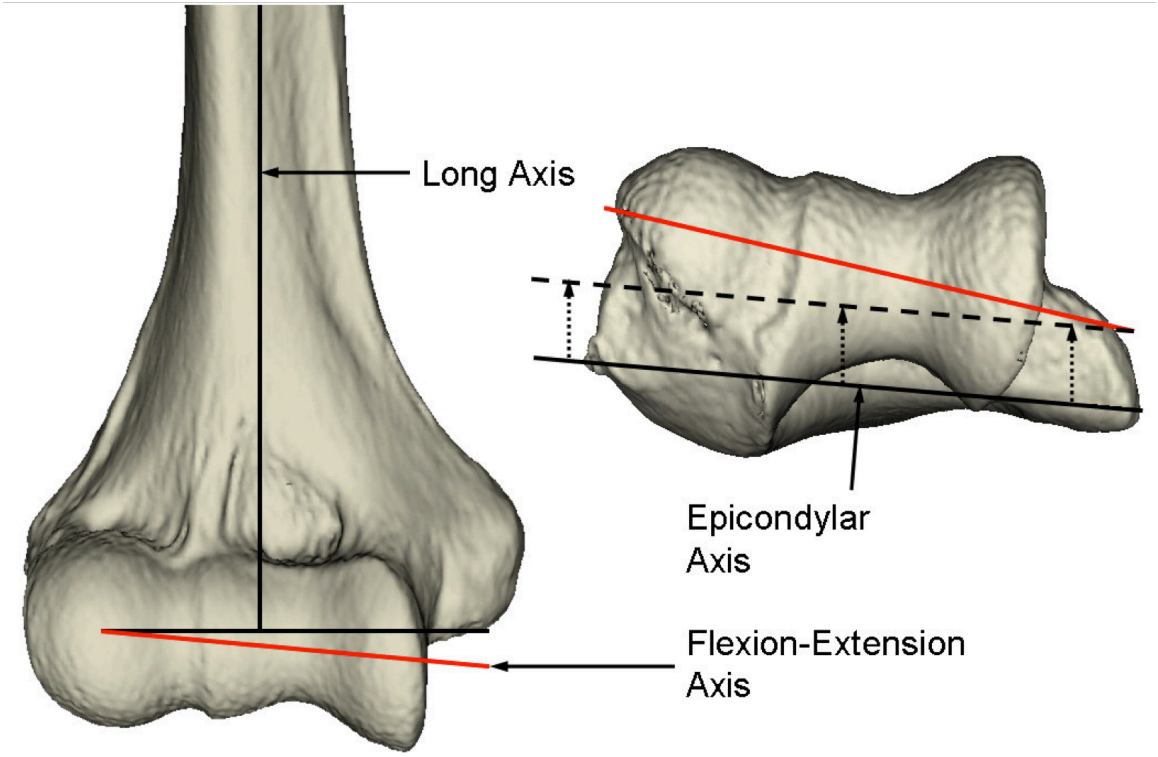

Figure 1.4: Alignment of flexion-extension (F-E) axis of the elbow. The F-E axis of the elbow is approximately 6-8^{o} of valgus with respect to the long axis of the humerus and 5-7^{o} of internal rotation with respect to the epicondylar axis of the distal humerus.

1.1.2 Ligaments and Joint capsule

Elbow stability is conferred by inherent bony stability as a consequence of the interlocking shape of the articulation and is reinforced by capsuloligamentous structures. Two of the main sources of stability are the lateral collateral ligamentous complex and the medial collateral ligament (MCL). The lateral complex consists of the lateral ulnar collateral ligament (LUCL), annular ligament, radial collateral ligament (RCL) and accessory ligament. The MCL consists of three bands: Anterior band, posterior band and transverse band (Figure 1.5). The elbow joint capsule attaches proximal to the coronoid and radial fossa on the anterior portion of the humerus, and above the olecranon fossa on the posterior humerus (3). The elbow capsule encloses all three major articulations of the elbow.

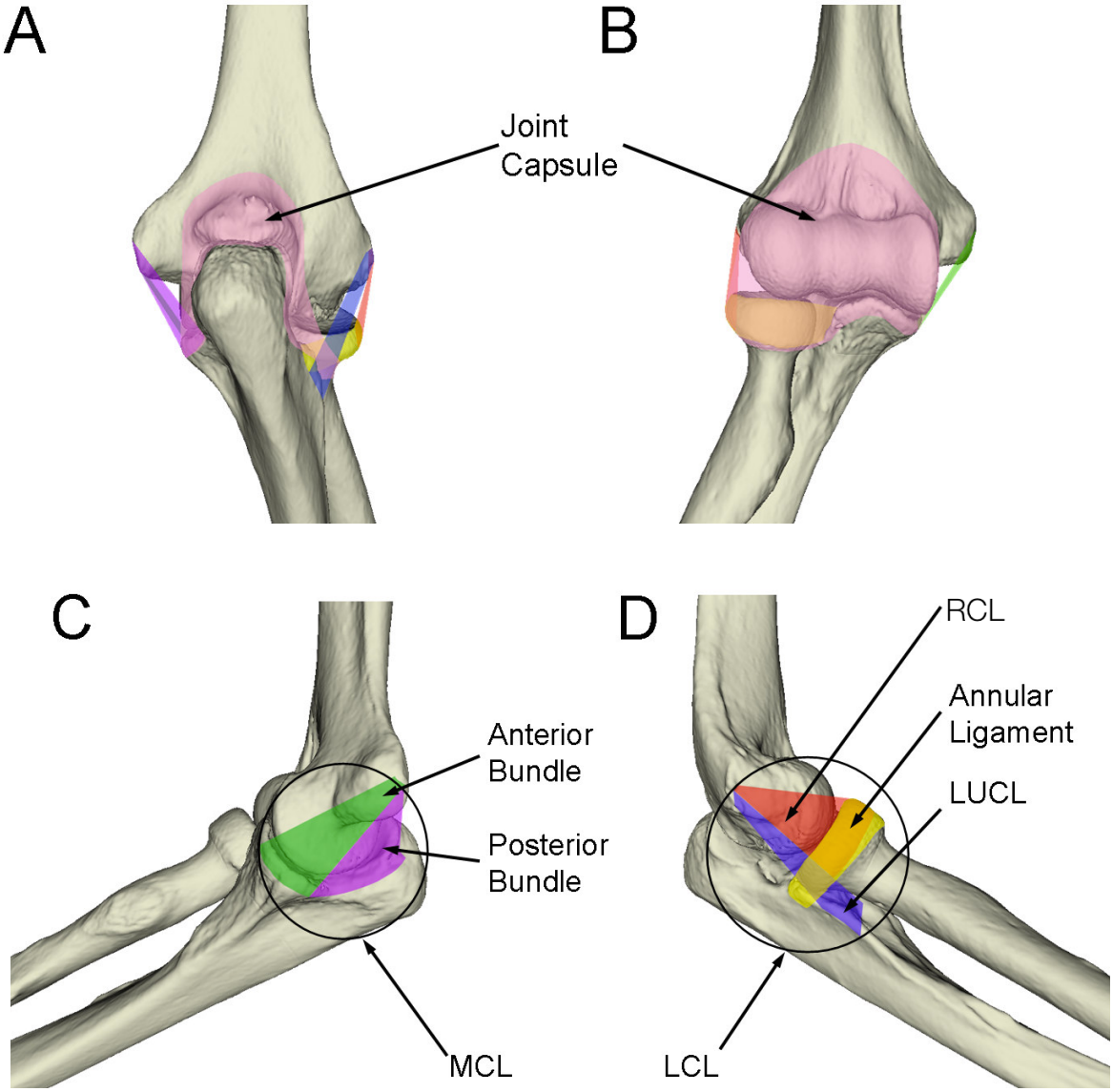

Figure 1.5: Ligaments and capsule of the elbow: (A) Posterior view and (B) anterior view of the elbow showing capsular attachment (pink. (C) Medial view showing the MCL with the anterior (green) and posterior (violet) bundle. (D) Lateral view showing the LCL and three of its components – RCL (red), annular ligament (yellow) and LUCL (purple).

1.1.3 Musculature

Numerous muscles crossing the elbow joint contribute to elbow motion and stability. The motions produced are elbow flexion, elbow extension, forearm pronation and forearm supination. Some muscles controlling the hand and wrist motion also originate proximal to the elbow (Figure 1.6).

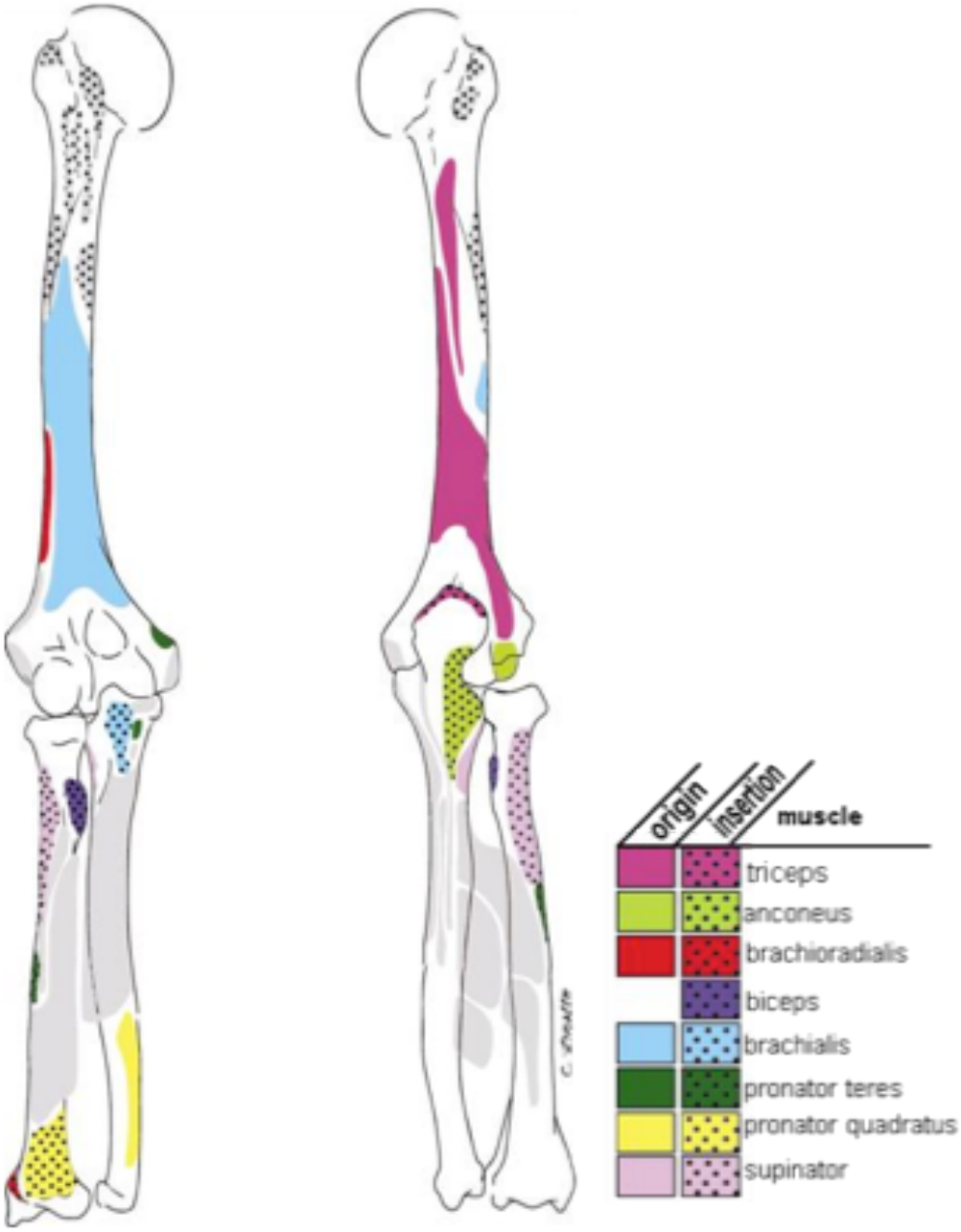

Figure 1.6: Muscles of the elbow. The main muscles crossing the elbow, including their origin and insertion, are displayed. These muscles play a role in elbow motion and stability (4)

1.1.3.1 Elbow Flexors

Three muscles contribute to flexion of the elbow: biceps, brachialis and brachioradialis. The biceps consists of the long head and short head. The long head of the biceps originates on the supraglenoid tubercle of the scapula while the short head originates from the coracoid process. Both heads of the biceps insert into the bicipital tuberosity of the radius via the biceps tendon and the fascia of the forearm via the lacertus fibrosis. The brachialis originates on the anterior-distal aspect of the humerus and attaches to the coracoid process, ulnar tuberosity and anterior capsule of the elbow. The brachioradialis muscle originates on the lateral supracondylar ridge of the humerus and inserts distally into the radial styloid at the wrist.

1.1.3.2 Elbow Extensors

The triceps is the main extensor of the elbow. The triceps has three heads: long, medial and lateral. The long head originates from the intraglenoid tubercle of the scapula, the lateral head from the humerus distally and the intermuscular septum, and the medial head from the posteromedial humerus and medial intermuscular septum. These heads coalesce and form the triceps tendon which inserts into the olecranon (3).

1.1.3.3 Forearm Supinators

Forearm supination is produced by two muscle groups: the biceps brachii and the supinator. The biceps is primarily responsible for supination during elbow flexion, while the supinator is more active throughout elbow range of motion. The supinator originates on the lateral epicondyle, lateral collateral ligament and the crista supinatorum of the ulna and inserts on the proximal radius.

1.1.3.4 Forearm Pronators

The pronator teres and the pronator quadratus are the two muscles primarily responsible for forearm pronation. The pronator quadratus is present distally at the wrist. It originates on the volar surface of the radius and inserts on the volar surface of the ulna. The quadratus is a weak pronator and also stabilizes the distal radioulnar joint (3). The main pronator of the forearm is the pronator teres muscle. The pronator teres has origins on both the medial epicondyle and the coronoid process. It inserts on the middle-proximal third of the radius.

1.2 Elbow Kinematics, Biomechanics and Stability

1.2.1 Elbow Kinematics

As previously mentioned, the F-E axis of the distal humerus is defined by the geometric centers of the capitellum and the trochlear groove. A line connecting these two points represents the F-E axis (Figure 1.3). This axis is positioned anterior to the humeral shaft. Normal range of motion of the elbow is from approximately 0^o extension to 145^o flexion. This can vary greatly between individuals based on amount of soft tissue present, prior injury or inherent ligamentous laxity. Forearm rotation involves the radius pronating and supinating around a relatively fixed ulna. Normal range of motion is approximately $150\text{-}160^o$ (3). In addition to flexion-extension and pronation-supination, the ulna also rotates and flexes with respect to the humerus (3). The ulna internally rotates with pronation, and externally rotates with supination (3).

1.2.2 Elbow Stability

Elbow stability is conferred by inherent bony stability and is reinforced by capsuloligamentous structures. The primary stabilizers of the elbow are the ulnohumeral articulation, anterior band of the MCL and the LUCL. The secondary stabilizers of the elbow are the common flexor muscles, common extensor muscles, the radio-capitellar articulation and the joint capsule.

Bony stability is derived from the congruency of the articular surfaces. The greater sigmoid notch closely conforms to the trochlea. The coronoid process is an important buttress to prevent posterior subluxation of the ulna on the humerus. The

olecranon contributes to stability in both varus and valgus directions. The radial head plays an important role as a secondary stabilizer, particularly in valgus in the case of a deficient MCL (3).

The anterior bundle of the MCL originates from the anteroinferior aspect of the medial epicondyle, inferior to the axis of rotation, and inserts on the sublime tubercle at the base of the coronoid process. The anterior bundle is of prime importance in elbow stability. It is the primary stabilizer of the elbow from 20-120^{o} flexion. The main restraint is to valgus angulation. The LUCL originates at isometric point on the lateral epicondyle and attaches to supinator crest of proximal ulna. The LUCL functions as an important restraint to varus angulation.

The elbow joint capsule plays a role in elbow stability, particularly in full extension and is less important in flexion (3). The elbow capsule prevents hyperextension of the elbow and provides coronal stability.

1.3 Elbow Hemiarthroplasty

Total joint replacement is one of the most commonly performed procedures in orthopaedic surgery. Total knee and hip replacements are amongst the most successful orthopaedic procedures. Total elbow arthroplasty (TEA) is a procedure which is becoming increasingly popular, and may be utilized for the management of primary osteoarthritis (5), post-traumatic osteoarthritis (6), stiffness (7), fractures (8), rheumatoid arthritis (9) and bone tumours (10). Similar to hip and knee arthroplasty, elbow replacements have been shown to improve pain and function. However, the success rate of elbow arthroplasty has thus far been inferior to hip and knee arthroplasty. This may be related to the extensive surgical approaches required for implantation as well as suboptimal implant designs and implantation techniques (11).

A.  B. 

Figure 1.8: Total elbow arthroplasty: Total elbow arthroplasty consists of a humeral component and an ulnar component. Some designs also include the ability to place a radial head replacement (Latitude, Tornier, Stafford, TX).

As a result of the problems associated with TEA, there has been an increased interest in elbow hemiarthroplasty (Figure 1.9). This partial replacement may be ideal in situations where only one portion of the elbow joint is affected. This may be particularly useful in the situation of comminuted distal humerus fractures that are not amenable to open reduction internal fixation. Other potential pathologic conditions which may benefit are avascular necrosis or non-unions of the distal humerus. Hemiarthroplasty has the advantage of less invasive surgical approaches, potentially less patient morbidity, and preservation of bone stock for potential future procedures. Furthermore it avoids problems of polyethylene wear which is common with TEA.

A.

B.

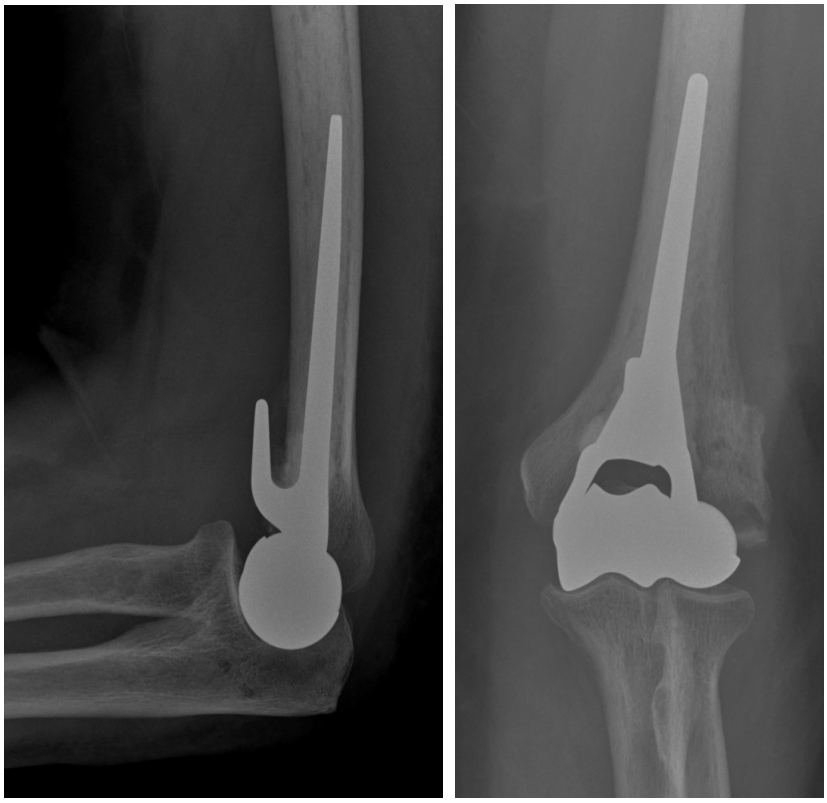

Figure 1.9: (A) Distal humeral implant. (B) Lateral and anterior-posterior radiographs of a distal humeral replacement (Latitude Anatomic, Tornier, TX)

1.3.1 Distal Humerus Fractures

Approximately 7% of all adult fractures involve the elbow, one third of which involve the distal humerus (12,13). Therefore, it can be estimated that approximately 2% of all adult fractures involve the distal humerus. There is a bi-model age distribution, with hi-energy injuries occurring mainly in young, and lower energy injuries mainly in elderly. The overall incidence of distal humerus fractures has steadily increased. Palvanen et al. (12) found a two-fold increase in age-adjusted incidence of distal humerus fracture from 1970 (12/100,000) to 1995 (28/100,000), and predicted a three-fold increase by 2030. These fractures remain extremely challenging to manage, particularly in elderly patients with osteoporotic bone. These patients may present with significant intraarticular comminution (Figure 1.10). Because of the complex anatomy of the joint surface, displaced intraarticular fragments that are not perfectly reduced may alter the kinematics of the joint. This will lead to post traumatic osteoarthrosis and subsequent stiffness and pain. While sometimes it is possible to recreate the joint surface, imperfections may be unavoidable considering the severity of the initial trauma. Furthermore, healing of the fractures can be problematic, particularly in the elderly. As a result of these issues with internal fixation, TEA has become a popular option to manage these fractures in older low demand patients (8) (Figure 1.8). Although some studies have shown good short-term and mid-term results (14,15), long-term concerns, such as polyethylene wear and aseptic loosening persist. There are also significant restrictions in weight bearing, often limited to only 5 lbs. Due to these concerns, the interest in distal humeral hemiarthroplasty has increased in recent years.

Figure 1.10: Distal humerus fracture. Example of a comminuted, intra-articular distal humerus fracture in an elderly patient. This type of fracture would be extremely challenging to fix by conventional open reduction internal fixation.

1.3.2 Role of Hemiarthroplasty in Distal Humerus Fractures

The role of hemiarthroplasty has been well established for humeral neck fractures of the shoulder (16) and femoral neck fractures of the hip (17). To date there has been very little in the literature on treatment of acute distal humerus fractures with hemiarthroplasty (18-20). The majority of the literature on distal humeral hemiarthroplasty involves clinical studies limited to either case controls or studies with small sample sizes (21-25). In 1947 Mellex and Phalen (21) were the first to describe the use of hemiarthroplasty in the elbow. They presented a series of 4 patients who underwent distal humeral replacement with an acrylic prosthesis. These patients had been involved in significant trauma, and presented months after the initial trauma with significant deformity. They were able to provide each patient with good pain relief, but unpredictable function and range of motion. In 1965, Barr and Eaton (22) placed a custom prosthesis in a patient with a prior distal humerus fracture. They had a good functional result at four year follow-up; however, some bone resorption had occurred and the distal screw in the construct had broken. Shifrin and Johnson (23) presented a case report on a 19 year old patient who received a custom distal humeral prosthesis after suffering from post-traumatic arthritis secondary to a distal humerus fracture. After 21 years of observation, a painless, stable range of motion was established. Swoboda and Scott (24) evaluated early results of distal humeral hemiarthroplasty of 5 young, rheumatoid arthritis patients. The patients had good pain relief, but the post-operative range of motion was not predictable. The largest early series of distal humerus hemiarthroplasty was reported by Street and Stevens (25) in 1974. They described their results in 10 patients: 5 with post-traumatic lesions, 3 with rheumatoid arthritis, and 2

with ankylosis secondary to hemophilia. They found poor results in patients with inflammatory arthritis or hemophilia, and stable, painless range of motion in 4 of 5 patients with post-traumatic arthrosis.

More recently, Adolfsson and Hammer (18) reported the short-term outcome of 4 elderly female patients (average age 80 years) treated with a distal humeral hemiarthroplasty for complex intraarticular distal humerus fractures. At an average of 10 months, 3 patients had excellent results and one patient had a good result according to the Mayo elbow performance score. Parsons et al. (19) reported the outcome of 8 patients treated with a distal humeral prosthesis. Of these patients 4 were treated for acute fractures and 4 treated non-acutely. Patients treated for acute fractures had a better range of motion and lower pain post-operatively. Malone et al. (20) presented their results in 30 patients (mean age 65) who underwent hemiarthroplasty for distal humeral fractures considered unreconstructable or for salvage of failed internal fixation. They also reported their acute cases had better outcomes than salvage cases. A re-operation on 16 patients (53%) was required for various reasons; including aseptic loosening, periprosthetic fracture, prominent hardware and ulnar nerve symptoms. Seven had cement lucencies >1 mm; one was loose but acceptable. Two elbows had degenerative changes and 15 an osteophytic lip on the medial trochlea (20).

1.3.3 Hemiarthroplasty Concerns

Although hemiarthroplasty appears in theory to be a good option in certain cases, there are some concerns. While the risk of bearing wear is eliminated, their remains concern regarding the fate of the adjacent cartilage. Cruess et al. (26) studied hemiarthroplasty in the hips of dogs, and followed changes in acetabular cartilage up to

24 weeks. They found early loss of protoglycan, articular damage and progressive degenerative changes. They suggested the articular cartilage maintains its structural integrity for only a brief period following the hemiarthroplasty. Dalldorf et al. (27) took biopsy specimens of cartilage and subchondral bone in patients who were undergoing revision from a hemiarthroplasty to a total hip replacement. They also took similar samples from patients of similar age undergoing a total hip replacement for femoral neck fracture. Significant degeneration of acetabular cartilage in those with a previous hemiarthroplasty was found. A direct correlation was made with the duration of hemiarthroplasty use.

The mechanism of cartilage erosion in hemiarthroplasty is not well defined; however, several possible causes have been proposed. Factors may include improper implant sizing or geometric conformity, abnormal contact pressures and the activity level of the patient (28,29). In their case study, McGibbon et al. (29) found that areas experiencing increased contact pressures were associated with increased severity of cartilage degeneration. There is also suggestion that degenerative enzymes may accelerate cartilage breakdown. Moon et al. (30) noted that abnormal stresses and reduced contact area between the implant and native cartilage promotes the secretion of degenerative enzymes which induce softening and reduced elasticity in the articular cartilage. The resulting biomechanical changes may destroy the existing cartilage, causing further degeneration at the articulation.

1.4 Rationale

There is a clear lack of clinical literature regarding the use of hemiarthroplasty of the elbow. All studies to date are small studies, with limited samples sizes, poor long-term follow-up, inconsistent indications for surgery, and variable implant materials and design (18-25). In addition to lack of clinical information in the literature, there is a complete void of information regarding the biomechanics, kinematics, and articular contact stresses of these devices. Altered elbow kinematics may result in implant loosening and accelerated wear of the native articulation. In addition to the need to define the influence on kinematics, there is also a lack of information regarding the implant characteristics. Current hemiarthroplasty implants available are presumed to re-create normal anatomy. However, these implants may not be optimally designed based on the lack of anthropometric data currently available (31,32). The effect of these implants on articular contact mechanics on native cartilage has also not been reported. Given that surgeons estimate the optimal implant size at surgery, the effect of incorrect implant sizing on joint kinematics and contact is also of clinical interest.

1.5 Objectives

The objectives of this thesis were as follows:

1. To quantify the osseous anatomy of the distal humerus and define anatomic variability using three-dimensional (3D) imaging techniques;
2. To determine the influence of distal humeral hemiarthroplasty and implant size on joint kinematics and stability *in-vitro*;
3. To determine the influence of distal humeral hemiarthroplasty on joint congruency *in-vitro*.

1.6 Hypothesis

Based on the above objectives, these hypotheses have been generated:

1. The morphology of the distal humerus would be consistent in shape but vary in size between elbows. A family of distal humeral implant sizes could be developed to closely replicate the anatomical shape of the distal humerus.
2. The kinematics of the elbow with an optimally sized hemiarthroplasty will best recreate the kinematics and stability of the elbow.
3. Distal humeral hemiarthroplasty with an optimally sized hemiarthroplasty will demonstrate the greatest joint congruency.

Thesis Overview

Chapter 2 defines the anatomy and anatomic variability of the distal humerus using 3D imaging techniques. Chapter 3 examines the influence of distal humeral hemiarthroplasty and implant size on joint kinematics and stability *in-vitro*. Chapter 4 quantifies the effects of hemiarthroplasty on joint congruency. Chapter 5 provides a general discussion, summary and potential areas of future work.

1.7 References

1. Morrey BF, Askew LJ, Chao EY. A biomechanical study of normal fuctional elbow motion. J Bone Joint Surg Am, 1981;63:872-7

2. Morrey BF. The Elbow / Anatomy and Surgical Approaches. In: Morrey BF, Buckwalter K, editors. Reconstructive Surgery of the Joints. New York: Churchill Livingstone; 1996. p. 461-9

3. Morrey, B.F. (2008) The Elbow and Its Disorders. Saunders Elsevier.

4. Stacpoole, R.A. (2002) Biomechanical Considerations Related to the Fixation and Kinematics of Radial Head Arthroplasty. Master of Science Western University.

5. Cheung EV, Adams R, Morrey BF. Primary osteoarthritis of the elbow: current treatment options. J Am Acad Orthop Surg 2008;16:77-87

6. Moro JK, King GJ. Total elbow arthroplasty in the treatment of posttraumatic conditions of the elbow. Clin Orthop Relat Res 2000:102-14

7. Mansat P, Morrey BF. Semiconstrained total elbow arthroplasty for ankylosed and stiff elbows. J Bone Joint Surg Am 2000;82:1260-8

8. Kamineni S, Morrey BF. Distal humeral fractures treated with noncustom total elbow replacement. J Bone Joint Surg Am 2004;86:940-47

9. Gill DR, Morrey BF. The Coonrad-Morrey total elbow arthroplasty in patients who have rheumatoid arthritis. A ten to fifteen-year follow-up study. J Bone Joint Surg Am 1998;80:1327-35

10. Athwal GS, Chin PY, Adams RA, Morrey BF. Coonrad-Morrey total elbow arthroplasty for tumours of the distal humerus and elbow. J Bone Joint Surg Br 2005;87:1369-74.

11. Gschwend N. Present state-of-the-art in elbow arthroplasty. Acta Orthop.Belg. 2002;68:100-17.

12. Palvanen M, Kannus P, Niemi S, Parkkari J. Secular trends in the osteoporotic fractures of the distal humerus in elderly women. Eur J Epidemiol 1998;14(2):159-164

13. Rose SH, Melton LJ 3rd, Morrey BF, et al. Epidemiologic features of humeral fractures. Clin Orthop Relat Res 1982 Aug(168):24-30

14. Gambirasio R, Riand N, Stern R, et al. Total elbow replacement for complex fractures of the distal humerus. An option for the elderly patient. J Bone Joint Surg Br 2001; 83(7):974-78

15. Garcia JA, Mykula R, Stanley D. Complex fractures of the distal humerus in the elderly. The role of total elbow replacement as primary treatment. J Bone Joint Surg Br. 2002; 84(6):812-816

16. Shah N, Iqbal HJ, Brookes-Fazakerley S, Sinopidis C. Shoulder hemiarthroplasty for the treatment of three and four part fractures of the proximal humerus using Comprehensive(R) Fracture stem. Int Orthop. 2010 Jul 14

17. Miller D, Choksey A, Jones P, Perkins R. Medium to long term results of the Exeter bipolar hemiarthroplasty for femoral neck fractures in active, independent patients. 5-13 year follow-up. Hip Int. 2008 Oct-Dec;18(4):301-6

18. Adolfsson L and Hammer R. Elbow hemiarthroplasty for acute reconstruction of intraarticular distal humerus fractures. Acta Orthop. 2006;77(5):785-787

19. Parsons M, O'Brien R, Hughes J. Elbow hemiarthroplasty for actue and salvage reconstruction of intra-artiular distal humerus fractures. Tech Shoulder and Elbow Surg 2005; 6 (2): 87-97

20. Malone AA, Zarkadas P, Jansen S, Hughes JS. Elbow hemiarthroplasty for intra-articular distal humerus fracture. J Bone Joint Surg Br 2009;91-B Supp 256

21. Mellex RH, Phalen GS. Arthroplasty of the elbow by replacement of the distal portion of the humerus with an acrylic prosthesis. J Bone Joint Surg Am. 1947;29:348-353

22. Barr JS, Eaton RG. Elbow reconstruction ith a new prosthesis to replace the distal end of the humerus: A case report. J Bone and Joint Surg Am. 1965:47:1408-1413

23. Shifrin PG and Johnson DP. Elbow hemiarthroplasty with 20-year follow-up study. Clin Orthop Relat Res. 1988;254:128-133

24. Swoboda B and Scott R. Humeral hemiarthroplasty of the elbow joint in young patients with rheumatoid arthritis. J of Arthro. 1999;14(5)553-59

25. Street DM and Stevens PS. A humeral prosthesis for the elbow: results in ten elbows. J Bone Joint Surg Am. 1974;56:1147-1158

26. Cruess RL, Kwok DC, Duc PN, Lecavalier MA, Dang GT. The response of articular cartilage to weight-bearing against metal. A study of hemiarthroplasty of the hip in the dog. J.Bone Joint Surg.Br. 1984;66:592-7

27. Dalldorf PG, Banas MP, Hicks DG, Pellegrini VD. Rate of degeneration of human acetabular cartilage after hemiarthroplasty. J Bone Joint Surg Am. 1995;77:877-882.

28. McCann L, Ingham E, Jin Z, Fisher J. An investigation of the effect of conformity of knee hemiarthroplasty designs on contact stress, friction and degeneration of articular cartilage: a tribological study. J.Biomech. 2009;42:1326-31

29. McGibbon CA, Krebs DE, Trahan CA, Trippel SB, Mann RW. Cartilage degeneration in relation to repetitive pressure: case study of a unilateral hip hemiarthroplasty patient. J.Arthroplasty 1999;14:52-8.

30. Moon KH, Kang JS, Lee TJ, Lee SH, Choi SW, Won MH. Degeneration of acetabular articular cartilage to bipolar hemiarthroplasty. Yonsei Med.J. 2008;49:719-24

31. Shiba R, Sorbie C, Siu DW, Bryant JT, Cooke TDV and Wevers HW. Geometry of the Humeroulnar Joint. J of Orthop Res 1988; 6(6): 897-906

32. Yokley TR and Churchill SE. Archaic and modern human distal humeral morphology. J Hum Evol. 2006 Dec;51(6):603-16

Chapter 2

An Anthropometric Study of the Distal Humerus

Overview

The optimal articular shape for distal humeral hemiarthroplasty has not been defined due to a paucity of data quantifying the morphology of the normal distal humerus. This chapter explores the osseous anatomy and anatomic variability of the distal humerus using three-dimensional (3D) imaging techniques.

A version of this work has been published:

Desai SJ, Deluce, S., Johnson JA, Ferreira LM, Leclerc AE, Athwal GS and King JW. An anthropometric study of the distal humerus. J Shoulder Elbow Surg. 2014 Feb;23, 463-469 (See Appendix C).

2.1 Introduction

Hemiarthroplasty of the distal humerus was reported as early as 1927. It has only recently become more commonly used as devices specifically designed for this indication have become commercially available. This procedure may be ideal in situations where only one portion of the elbow joint is affected, including distal humerus fractures not amenable to open reduction internal fixation, avascular necrosis and non-unions. The optimal shape of hemiarthroplasty implants has not been established due to a lack of data quantifying the morphology of the normal distal humerus (1,2). Anthropometric information is available for the shoulder (3-6) and has played an important role in optimizing the design of these implants. The purpose of the present study was to quantify the osseous anatomy of the distal humerus and define anatomic variability using three-dimensional (3D) imaging techniques. The data bank of distal humeral dimensions created may improve the designs of future distal humeral hemiarthroplasty implants.

2.2 Materials and Methods

2.2.1 Specimen Preparation

This three dimensional (3D) computer tomography (CT) anatomic study of the distal humerus utilized 50 unpaired normal human cadaveric elbows. There were 34 male donors and 16 female donors, with an average age of 72 ± 12.5 years. CT scans were acquired using a 64-slice clinical scanner (GE Light Speed Ultra, New Berlin, WI, USA) at a slice thickness of 0.625mm. The humeri were manually segmented from the CT images using semi-automated methods and a fixed threshold of 148 Hounsfield Units (HU) using Mimics software (Materialize NV, Leuven, Belgium). Three dimensional surface models were generated. A series of custom programs created using the Visualization ToolKit (VTK, Kitware Inc., Clifton Park, NY, USA) were used to measure each model. To simplify the measuring process, all left-sided models were mirrored before the measurements were taken.

2.2.2 Axis Determination

On the 3D surface model, nine points were manually chosen on the capitellum, six points on the trochlear groove, and 2 points on the posterior surface of humerus. Using a semi-automated algorithm, point clouds were created on the surface of the capitellum and along the trochlear groove. This algorithm ensured precision and consistency of point placement. These points were used to define the geometric center of the spherical capitellum and the circular trochlear groove (Figure 2.1).

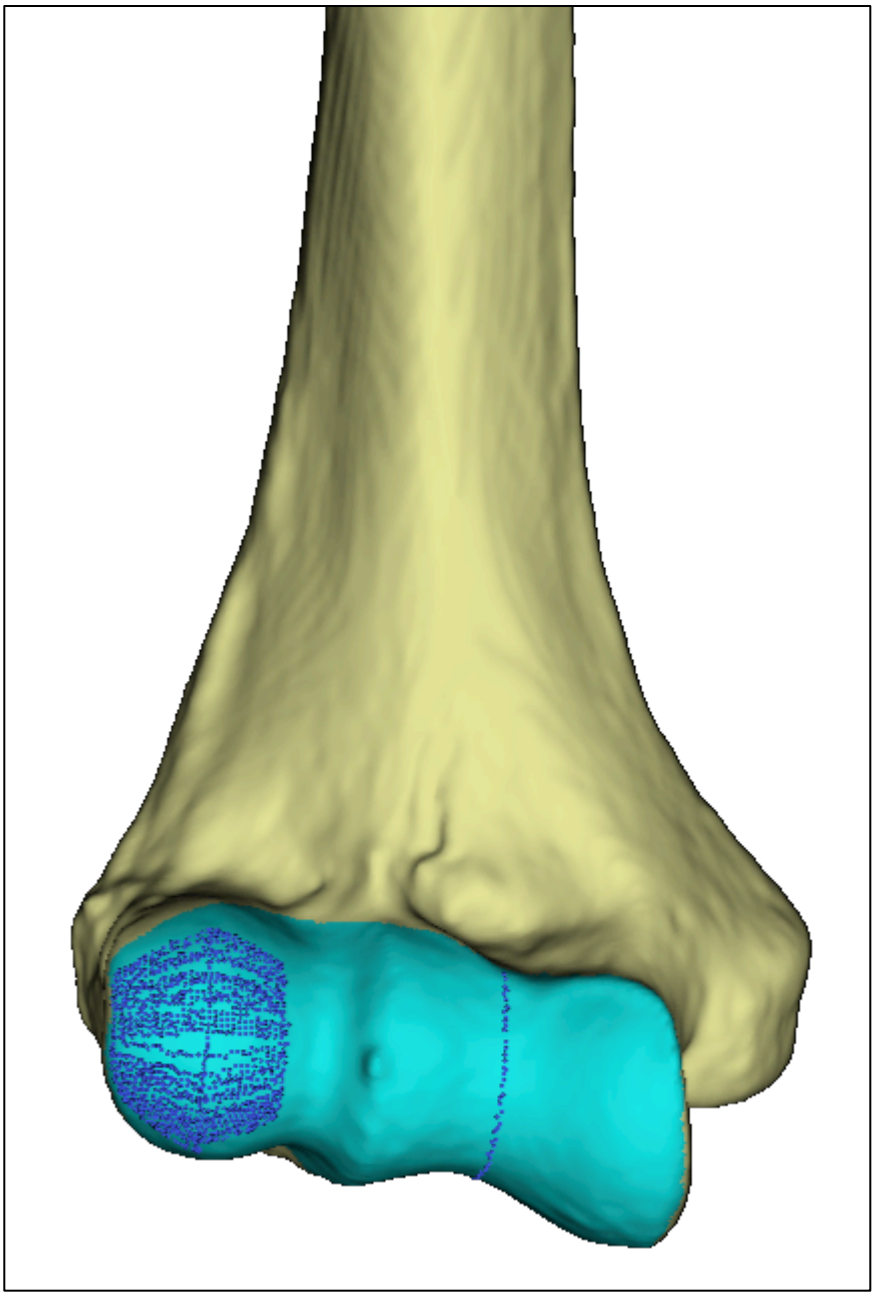

Figure 2.1: 3D surface models of the distal humeri. Coordinate systems were established by choosing nine points on the capitellum, six points on the trochlear groove, and 2 points on the posterior surface of humerus (not shown). Using a semi-automated algorithm, point clouds were created over the surface of the capitellum and along the trochlear groove. These points were used to define the geometric center of the spherical capitellum and the circular trochlear groove. These points, along with the posterior points selected, were used to create the co-ordinate system.

A line connecting these center points defined the flexion-extension (FE) axis. A humeral coordinate system, aligned with the FE axis, was created in order to provide a measurement reference frame. The axial direction was determined using two points chosen on the distal aspect of the posterior humeral shaft, one located distally and one mid-shaft, respectively. The distally pointing axial vector was defined as the x-axis and the laterally pointing axis defined as the z-axis. The y-axis was determined using the cross-product and pointed anteriorly (Figure 2.2). The process of selecting points and creation of the coordinate system was repeated by the primary author (SJD) on 20 of the specimen models to ensure intra-observer reliability. The process was also repeated on twenty models by another author (AL) to ensure inter-observer reliability. These were quantified using intra-class correlations of absolute agreement.

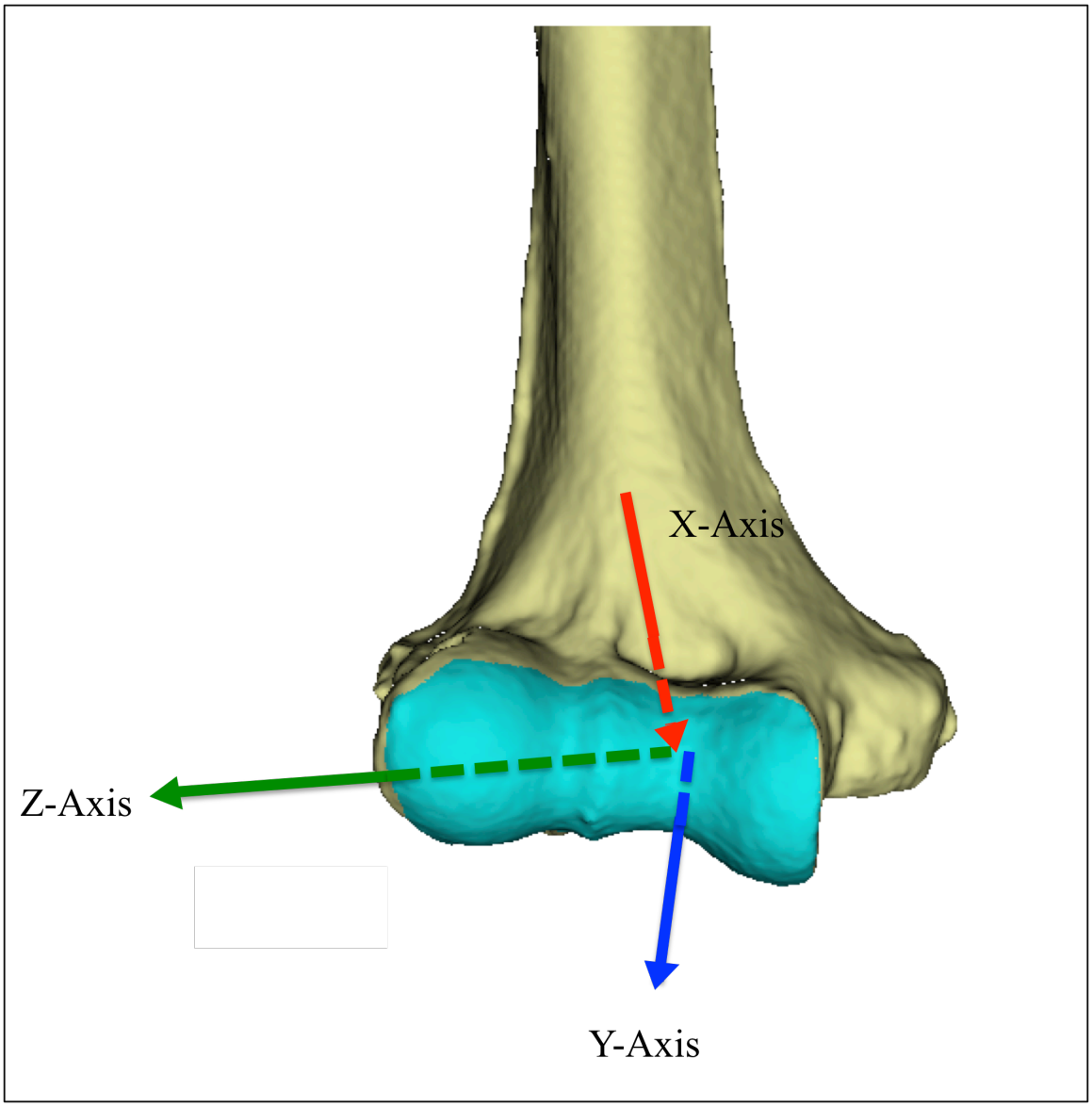

Figure 2.2: 3D surface model of the articular surface of the distal humerus with co-ordinate system used to determine measurements. The distally pointing vector (red) was defined as the x-axis, the lateral pointing vector (green) represented the z-axis and the anteriorly pointing axis (blue) was y-axis.

2.2.3 "C-Line"

Using the FE axis as an initial reference direction vector, transverse cross sections of the articular surface were automatically segmented at 0.1 mm increments, and then circle-fitted using a least-squares method. A best-fit line through these centers of all the cross sections was generated as per method of Shiba et al. (1), who defined this as the C-Line. Cross sections with fewer than 30 points were automatically ignored in order to ensure a sufficient number of points at each slice to obtain an accurate circle fit. This process was iterated again, using the C-Line as the reference vector, thus refining the final C-Line by ensuring that it was defined solely by the articular surface cross sections. The reference coordinate system was aligned with the refined C-Line and its origin was defined as the center of the most medial slice. The distance between the most medial and lateral slices defined the width of the articulation. The purpose of the algorithm was to determine the C-Line, articular width and coordinate system. The final cross-sections were obtained between the medial and lateral slices at increments of 1% of the measured articular width. The 3D location and radius of the fitted circle was recorded for each of these 100 cross-sections (Figure 2.3). The data was transferred into Microsoft Excel Spreadsheet (Microsoft, Redmond, WA, USA) where pre-defined anatomic measurements were calculated (Figure 2.4).

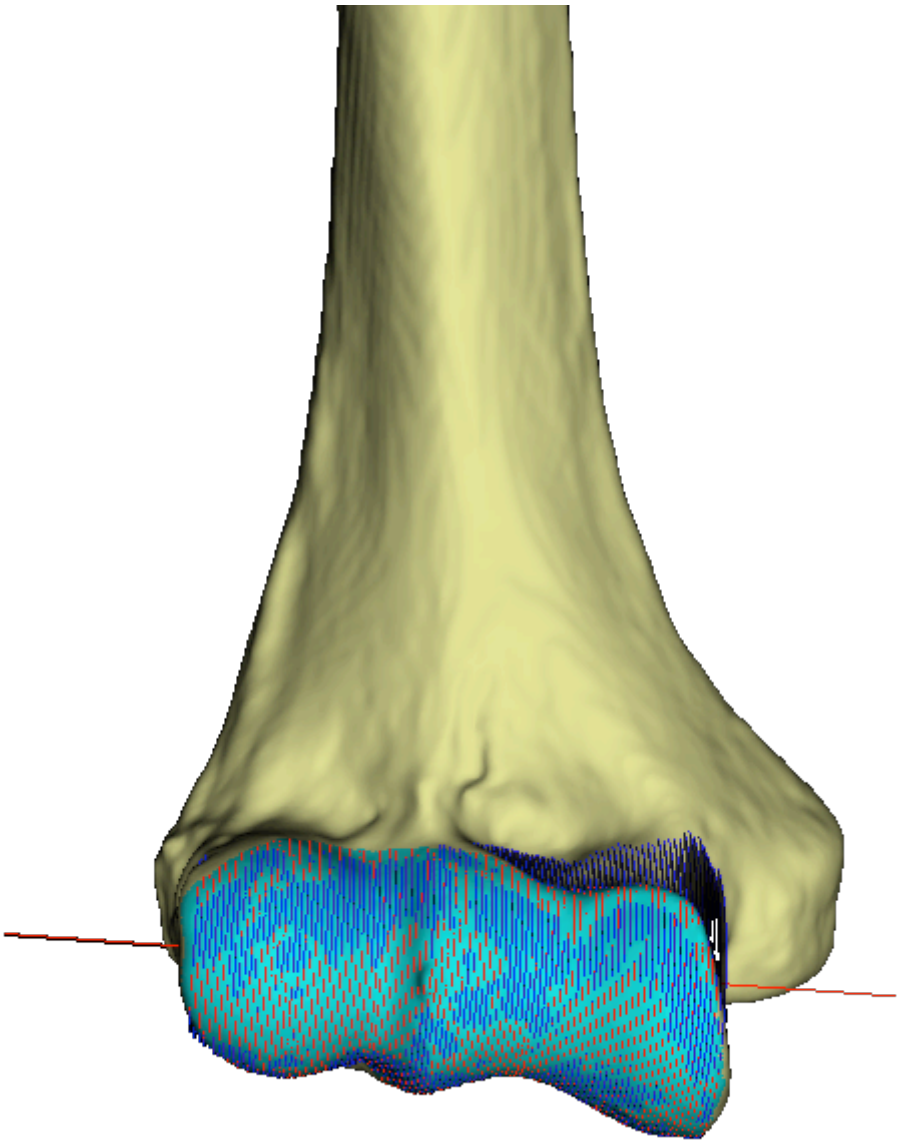

Figure 2.3: 3D reconstruction of the distal humerus with 100 circle-fitted transverse slices. The red line represents the joint axis (i.e. C-Line) as defined by the centres of the least squares circle fits.

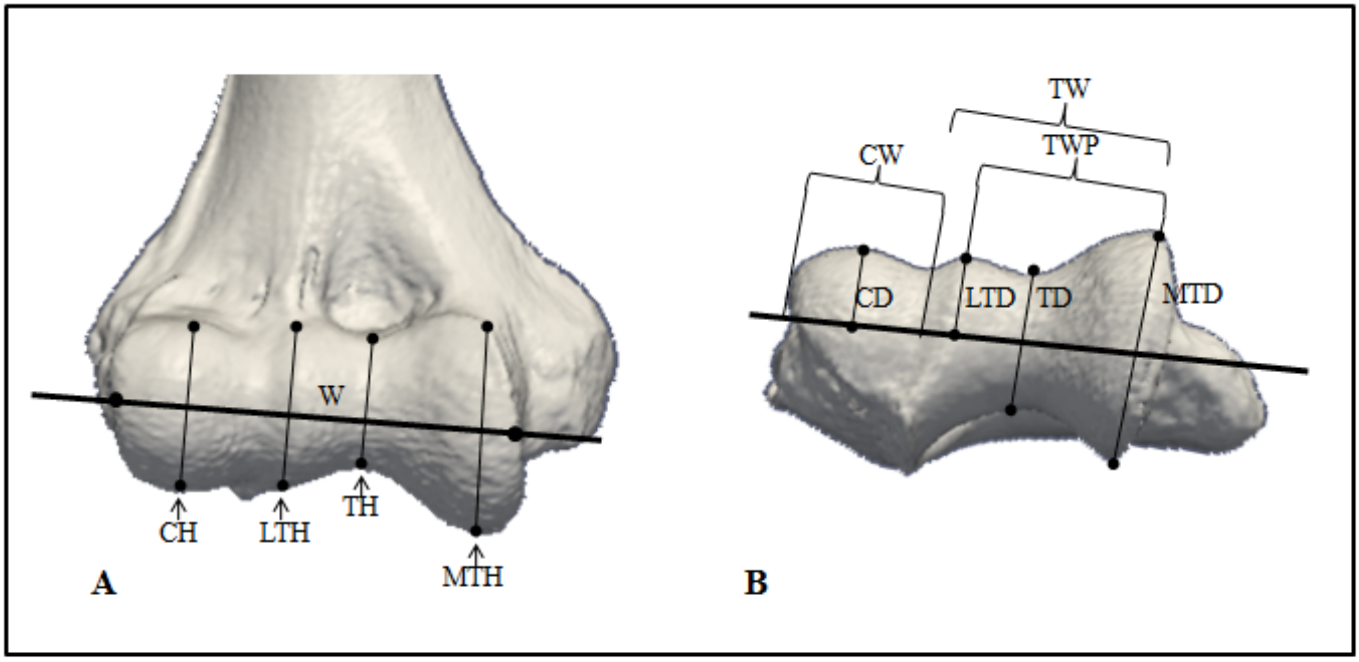

Figure 2.4: (A) Measurements taken from anterior-posterior view, perpendicular to the C-Line. (B) Measurements taken from the axial view, also perpendicular to the C-Line.

(A) The **capitellar height (CH)** is the diameter of the capitellar circle with the largest radius in the AP plane; **lateral trochlear height (LTH)** is the diameter of the most lateral circle on the trochlea ridge with the largest diameter; **trochlear height (TH)** is the height of the trochlear groove, the diameter of the circle with the smallest radius in the trochlear groove; **medial trochlear height (MTH)** is the diameter of the most medial circle on the trochlea ridge with the largest radius. **Articular width (W)** is the width of the distal humeral articulation, from the medial most circle on the trochlea to the lateral most circle on the capitellum.

(B) The **capitellar width (CW)** is the distance along C-Line from the depth of the groove between the capitellum and trochlea, to the lateral edge of capitellum; **trochlear width (TW)** is the distance along the C-Line from the medial trochlear ridge to the groove between the capitellum and trochlea; **trochlear width proper (TWP)** is the distance along the C-Line from the medial trochlear ridge to lateral trochlear ridge; **capitellar depth (CD)** is from the most anterior point on the capitellum to the C-Line; **lateral trochlear depth (LTD)** is from the most anterior point on the lateral trochlear ridge to the most posterior point; **trochlear groove depth (TD)** is measured from the most anterior point of the trochlear groove to the most posterior point; **medial trochlear depth (MTD)** is measured from the most anterior point of the medial trochlear ridge to the most posterior point.

2.3 Results

2.3.1 Summary of results

The results of all measurements, including various ratios, are presented in Table 1. Intra-observer reliability for the manual steps of coordinate system creation, had intra-class correlations of 0.9 (95% confidence interval [95% CI], 0.2 – 1.0). Inter-observer reliability had intra-class correlations of 0.9 (95% confidence interval [95% CI] 0.5 – 1.0).

	Age (yrs)	CW	CH	TW	TWP	LTH	TH	MTH	CD	LTD	TD	MTD	W	CW/CH	TW/CW	MTH/LTH	W/TH
All (n=50)																	
Average (mm)	72.3	17.2	23.3	25.3	21.0	21.6	17.8	29.9	9.0	21.9	17.8	30.0	42.5	0.7	1.4	1.7	2.4
Standard Deviation (mm)	12.5	1.9	2.3	3.2	2.6	2.2	2.0	4.1	1.0	2.3	2.0	4.1	4.6	0.1	0.1	0.2	0.2
Max/Min	97/46	21.1/12.1	27.6/18.2	33.8/19.6	27.4/15.8	25.2/17.1	22.3/13.4	43.6/23.7	11.4/6.9	25.5/17.4	22.3/13.4	43.6/23.8	53.6/33.2				
Men (n=34)																	
Average (mm)	72.8	18.1	24.4	26.9	22.1	22.6	18.6	31.5	9.4	23.0	18.6	31.6	45.0	0.7	1.5	1.7	2.4
Standard Deviation (mm)	11.1	1.4	1.8	2.5	2.1	1.6	1.6	3.6	0.8	1.6	1.6	3.6	3.2	0.0	0.1	0.2	0.2
Max/Min (mm)	93/48	21.1/15.7	27.6/20.4	33.8/22.3	27.4/17.2	25.2/19.7	22.3/14.8	43.6/27.0	11.4/7.6	25.5/19.9	22.3/14.8	43.6/27.0	53.6/38.2				
Women (n=16)																	
Average (mm)	65.7	15.5	20.7	23.5	19.3	19.4	16.1	26.4	8.2	19.7	16.0	26.5	38.9	0.7	1.3	1.4	2.1
Standard Deviation (mm)	23.9	6.0	8.1	8.9	7.2	7.5	6.2	9.7	3.2	7.6	6.2	9.8	15.0	0.3	0.5	0.5	0.8
Max/Min (mm)	97/46	17.5/12.1	23.3/18.2	25.9/19.6	22.1/15.8	23.5/17.1	19.1/13.4	36.0/23.7	9.7/6.9	23.7/17.4	18.8/13.4	36.0/23.8	42/33.2				

Table 2.1: Average measurements for all specimens, men only and women only. CW: Capitellar width; CH: Capitellar height; TW: Trochlear width; TWP: Trochlear width proper; LTH: Lateral trochlear height; TH: Trochlear height; MTH: Medial trochlear height; CD: Capitellar depth; LTD: Lateral trochlear depth; TD: Trochlear groove depth; MTD: Medial trochlear depth; W: Articular width.

2.3.2 Flexion-Extension Axis

The anatomic FE axis of the distal humerus was 0.85 ± 0.70 degrees from the C-Line (range 0.07-3.17 degrees) in the coronal plane and 1.57 ± 1.45 degrees (range 0.04-7.47 degrees) in the axial plane.

2.3.3 Distal humeral dimensions

The mean width of the capitellum (CW) was 17.2 ± 1.9 mm, while the height (CH) was 23.3 ± 2.3 mm. A paired T-test revealed that the width and height were significantly different ($p < 0.001$). The Pearson correlation coefficient between CW and CH was 0.772, representing a significant correlation ($p < 0.001$) (Figure 2.5). The average trochlear width proper (TWP) was 21.6 ± 2.6 mm, and the correlation with CW was 0.676, also representing a significant correlation ($p < 0.001$) (Figure 2.6). The average trochlear height (TH) was 17.8 ± 2.0 mm. TWP and TH were significantly correlated with a Pearson correlation coefficient of 0.454 ($p < 0.05$) (Figure 2.7).

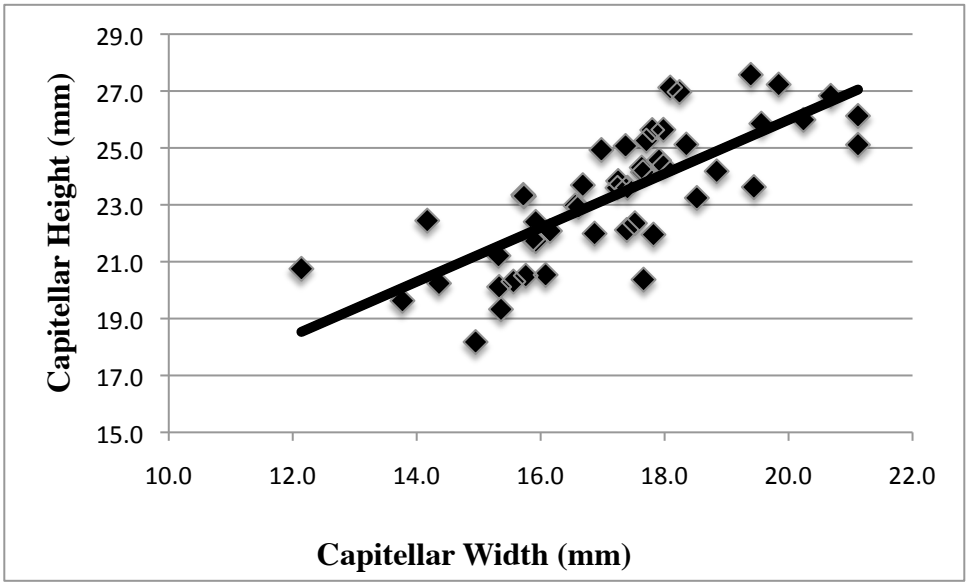

Figure 2.5: Correlation of capitellar height (CH) with capitellar width (CW). ($R = 0.772$, $p < 0.001$)

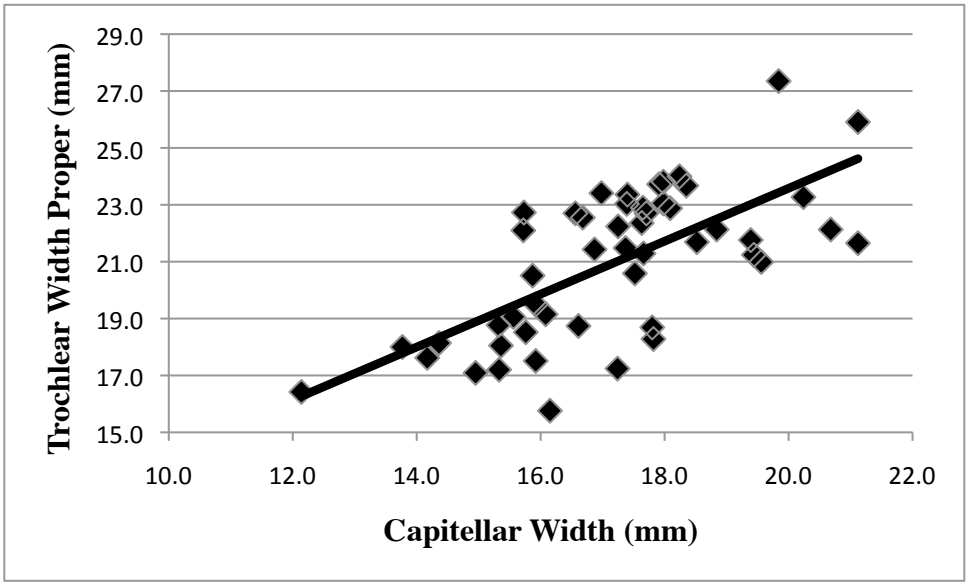

Figure 2.6: Correlation of trochlea width proper (TWP) with capitellar width (CW). ($R=0.676, p < 0.001$)

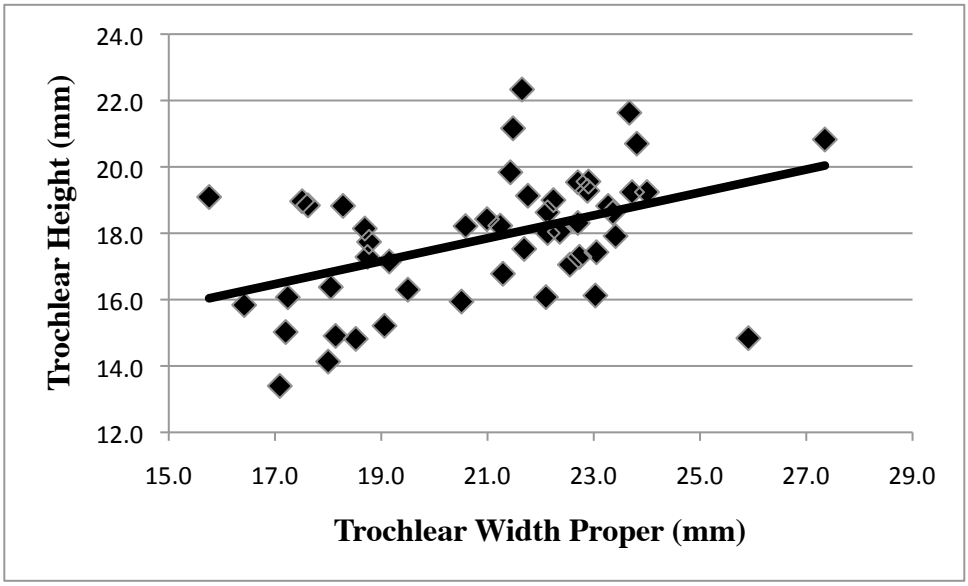

Figure 2.7: Correlation of trochlear height (TH) with trochlear width proper (TWP). ($R= 0.454$, $p < 0.05$)

The mean lateral trochlear height (LTH) was 21.6 ± 2.2 mm, while the mean medial trochlear height was significantly larger at 29.9 ± 4.1 mm ($p < 0.001$). Likewise, the lateral trochlear depth (LTD) was 21.9 ± 2.3 mm, while the average medial trochlear depth (MTD) was significantly larger at 30.0 ± 4.1 mm ($p <0.001$). Refer to Appendix C for complete set of measurements from all specimens.

2.3.4 Gender comparison

When comparing men and women, the capitellar width (CW), capitellar height (CH), trochlear width (TW), trochlear width proper (TWP), lateral trochlear height (LTH), trochlear height (TH), medial trochlear height (MTH), capitellar depth (CD), lateral trochlear depth (LTD), medial trochlear depth (MTD), and articular width (W) were significantly larger in men ($p<0.001$). The morphological ratios: CW/CH, TW/CW, MTH/LTH and W/TH were not significantly different between men and women ($p>0.05$).

2.3.5 Graphical representation

The average diameter of each of the 100 circle fits was calculated. This was done for all 50 donor arms, as well as for men and women groups. This is presented in both the distal-proximal (coronal) and anterior-posterior (axial) projections in Figure 2.8.

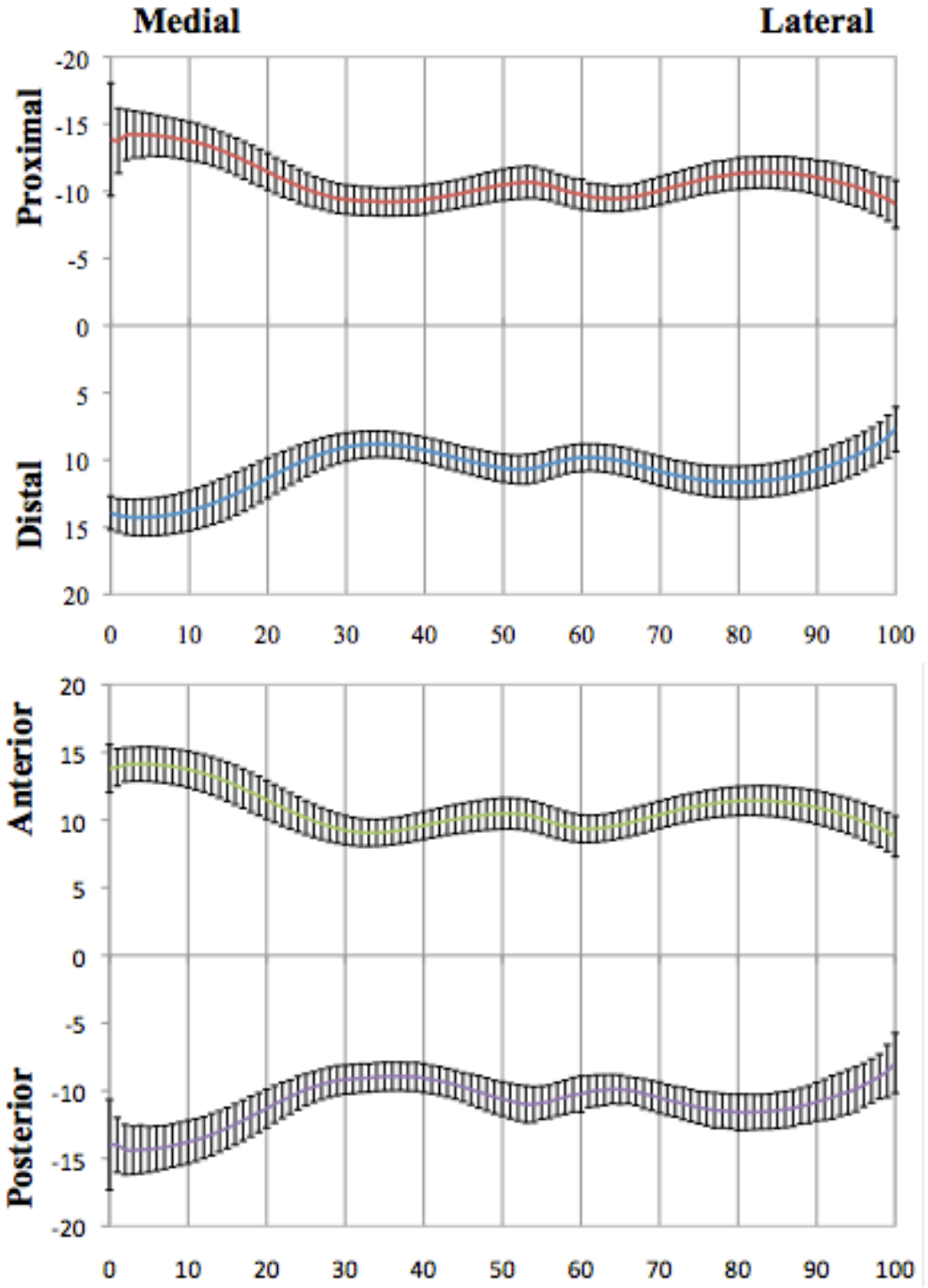

Figure 2.8: Average diameter of each of the 100 slices in millimeters (mm) of all specimens. X-axis represents the 100 slices, Y-axis represents diameter in mm. Top figure represents distal to proximal projections (coronal plane). Bottom figure represents anterior to posterior projections (axial plane).

2.3.6 Implant Sizes

Using the data on the various morphological measurements collected (Table 2.1), seven implant sizes were developed – Sizes 1-7. The average morphological size for all 50 specimens was used as the middle size (i.e. Size 4). The implant which is one size larger (Size 5) was created by adding 2 mm to overall width (W). An additional 2 mm was added to the width to create Size 6, and an additional 2 mm to create size 7. Likewise, the implant which is one size smaller (Size 3), was created by subtracting 2 mm from the width (W). An additional 2 mm was subtracted from the width to create Size 2, and an additional 2 mm to create Size 1. The remainder of the measurements (Figure 2.4) were calculated proportionally based on various morphological ratios (W/CW, W/TW, CW/CH, TW/CW, etc).

Implant Size	W	CW	CH	TW	TH	TWP	MTH	LTH	TD	MTD	LTD	CD
1	48.5	19.6	26.6	28.9	20.4	23.9	34.1	24.7	20.3	34.2	25.0	10.2
2	46.5	18.8	25.5	27.7	19.5	22.9	32.7	23.7	19.5	32.8	24.0	9.8
3	44.5	18.0	24.4	26.5	18.7	22.0	31.3	22.6	18.6	31.4	23.0	9.4
4	42.5	17.2	23.3	25.3	17.8	21.0	29.9	21.6	17.8	30.0	21.9	9.0
5	40.5	16.4	22.2	24.2	17.0	20.0	28.5	20.6	17.0	28.6	20.9	8.6
6	38.5	15.6	21.1	23.0	16.2	19.0	27.1	19.6	16.1	27.2	19.9	8.1
7	36.5	14.8	20.0	21.8	15.3	18.0	25.7	18.6	15.3	25.8	18.8	7.7

Table 2.2: Seven implant sizes (in mm) create based on average measurements from the 50 specimens. Refer to Figure 2.4 for diagram and abbreviations.

2.4 Discussion

Implants used for elbow hemiarthroplasty aim to recreate the normal distal humeral articular anatomy. A thorough knowledge of the distal humerus morphology is necessary to create anatomic implants which will help to optimize elbow kinematics and maximize contact area with the proximal radius and ulna.

Shiba et al. (1) were the first to thoroughly quantify the anatomy of the ulnohumeral joint. Four human cadaveric elbows were used in their study. The humeri were cut in 0.76mm thick slices perpendicular to the transepidondylar line (line joining the medial and lateral epicondyles). The geometry was examined using surface analysis by creating circle fits of each slice and determining a center and radius of each circle. The centers of each circle generally were on a straight line they referred to as the C-Line (1). They performed similar measurements on the trochlea and reported ranges of sagittal radii of the lateral trochlear flange, trochlear groove and medial trochlear flange of 9.6-11.6mm, 8.4-9.0mm and 11.8-14.7mm, respectively. This is similar to the results of the present study which found sagittal diameter of the lateral trochlear height (LTH), trochlear height (TH) and medial trochlear height (MTH) to be 22 ± 2 mm, 18 ± 2 mm, and 30 ± 4 mm, respectively.

Sabo (7) performed a morphological analysis of the capitellum on fifty cadaveric elbows using CT scan images and similar measurements to the present study. They found an average capitellar height of 23.2 ± 2.8 mm (range, 18.0-29.5 mm) with a mean width of 13.9 ± 2.3 mm (range, 9-19 mm). Wevers (2) sectioned 6 distal humeri in the sagittal plane and performed circle-fits to characterize the shape of the distal humeral

articulation. They found a range in capitellar width from 14.5 to 21.5 mm. They did not specifically report on capitellar height, but suggested the size for the height of the capitellar portion ranging from 19.2 to 23.7mm (2). Shiba (1) also measured sagittal radius of the capitellum, and reported a range from 9.8-12.0 mm. The present study's results are consistent with the results from the previous three studies. The current study found a mean capitellar width of 17 ± 2 mm (range, 12-21 mm), and a mean capitellar height of 23 ± 2 mm (range, 18-27 mm). In addition, we found that the capitellar width and height were statistically different. This indicates that the capitellum is ellipsoid, not spherical, and consistent with a recent report on capitellar morphology (7).

The measures taken in the present study were referenced from the C-Line as described by Shiba et al. (1). In the current study, the C-Line was defined as the line of best fit connecting the geometric centres of each of the 100 circle fits of the distal humerus. The FE axis of the distal humerus is defined by the geometric center of the capitellum approximated as a sphere, and the geometric center of the trochlear, approximated as a circle (8-12). We found that on average, these lines differed by 1 ± 1^{o} (range $0\text{-}3^{o}$) in the coronal plane and 2 ± 1^{o} (range $0\text{-}7^{o}$) in the axial plane ($p < 0.0001$). These large standard deviations and large ranges demonstrate the variability between the C-Line and the FE axis. This information becomes significant in implant design, as the measurements found in this study are referenced to the C-Line; therefore, any implant produced from these measurements must also be referenced to the C-Line, not the anatomic FE axis.

The circle fit method used in the present study created 100 circles in the sagittal plane. Diameter of each is presented in schematic form in both anterior-posterior and

axial projections in Figures 2.8. This provides a detailed description of the articular shape of the distal humerus which could prove useful when developing a distal humeral hemiarthroplasty. Additionally, seven implant sizes have been proposed based on the average morphological size of the specimens studied. The average size of all 50 specimens was used as the middle implant (Size 4). The remainder of the sizes were based on adding or subtracting 2 mm from the middle implant. The range of 2 mm between sizes was chosen for a number of reasons. First, the industry standard for hemiarthroplasty of the shoulder and hip is also approximately 2 mm between sizes. Second, the thickness of articular cartilage is between 1.0 and 2.0 mm (13), therefore, 2 mm compensates for this slight mismatch. Third, most of the other morphological parameters are less than 2 mm between sizes; the width is the largest measurement. Fourth, the only commercially available implant has six sizes; therefore, adding an extra size is not unreasonable. Finally, by using this method, 96% of cadaveric specimens used fell within a 2 mm range of the implant sizes.

The present study has limitations. First, the sample size is relatively small to define such a complex articulation which has such high variability between subjects. Second, we defined the anatomy of the distal humerus based on 3D CT reconstructions. CT scans do not include articular cartilage; therefore, the measurements taken reflect only the osseous anatomy of the distal humerus. Schub et al. demonstrated that the thickness of cartilage was not uniform in their MRI study (13). They selected eight points along the distal humeral articular surface, including three points on the lateral capitellum, three points on the medial capitellum and two points along the trochlear groove. They found the cartilage thickness of the lateral capitellum ranged from 1.06mm

to 1.49mm, the medial capitellum ranged from 0.87mm to 1.63mm and the trochear groove from 0.78mm to 1.32mm (13). These differences may affect the calculation of the FE axis and C-Line. In spite of this, the previously cited studies which included articular cartilage in their analysis demonstrated relatively consistent measurements with the present study (1,2). Finally, we used a circle fit algorithm to define the morphology of the capitellum and trochlea. Neither of these structures conforms to perfect geometric shapes, such as spheres or ellipses; therefore, this may result in measurement error in some cases.

The strengths of this the present study are that we examined the morphology of the distal humerus using modern 3-dimensional techniques, with high intra- and inter-observer reliability. We used similar principles to the study performed by Shiba (1); however, because of the technology used, we were able to analyse many more specimens, and used a software program which is very accurate (<1.0 mm measurement error). Other studies using the similar software report high accuracy of <0.5 mm discrepancy between measurements taken on CT scan and direct measurements on the anatomical specimens (14). We were also able to define our circle fits based on slices perpendicular to the C-Line, whereas Shiba (1) initially created circle fits perpendicular to the transepicondylar axis, which has considerable variability between subjects.

2.5 Conclusion

The present study characterizes the osseous anatomy and anatomic variability of the distal humeral articulation using accurate 3D reconstruction methods. Despite not including the articular cartilage thickness in our measurements, a data bank of distal humeral dimensions has been created and may be effective in the development of future distal humeral hemiarthroplasty implants. Seven implant sizes based on average morphological measurements have been proposed. A more anatomic implant may optimize elbow kinematics and maximize contact on the native ulna and radius, which may ultimately increase function and improve longevity of the implant.

2.6 References

1. Shiba R, Sorbie C, Siu DW, Bryant JT, Cooke TDV and Wevers HW. Geometry of the Humeroulnar Joint. J of Orthop Res 1988; 6(6): 897-906 DOI: 10.1002/jor.1100060614

2. Wevers HW, Broekhoven LH, Sorbie C. Resurfacing elbow prosthesis: shape and sizing of the humeral component. J Biomed Eng 1985;7: 241-6. DOI: 10.1016/0141-5425(85)90026-3

3. Boileau P, Walch G. The three-dimensional geometry of the proximal humerus. Implications for surgical technique and prosthetic design. J Bone Joint Surg Br 1997;79:857-65

4. Hertel R, Knothe U, Ballmer FT. Geometry of the proximal humerus and implications for prosthetic design. J Shoulder Elbow Surg 2002;11:331-8 DOI: 10.1067/mse.2002.124429

5. Pearl ML, Volk AG. Coronal plane geometry of the proximal humerus relevant to prosthetic arthroplasty. J Shoulder Elbow Sur 1996 Jul-Aug;5(4):320-6

6. Robertson DD, Yuan J, Bigliani LU, Flatow EL, Yamaguchi K. Three-dimensional analysis of the proximal part of the humerus: relevance to arthroplasty. J Bone Joint Surg Am 2000;82: 1594-602

7. Sabo MT, McDonald CP, Ng J, Ferreira LM, Johnson JA and King JW. A morphological analysis of the humeral capitellum with an interest in prostheses design. J Shoulder Elbow Surg 2011;In press 1-5 DOI: 10.1016/j.jse.2011.01.007

8. Bottlang M, O'Rourke MR, Madey SM, Steyers CM, Marsh JL, Brown TD. Radiographic determinants of the elbow rotation axis: experimental identification and quantitative validation. J Orthop Res 2000;18:821-8.

9. Deland JT, Garg A, Walker PS. Biomechanical basis for elbow hinge-distractor design. Clin Orthop Relat Res 1987:303-12.

10. Ericson A, Arndt A, Stark A, Wretenberg P, Lundberg A. Variation in the position and orientation of the elbow flexion axis. J Bone Joint Surg Br 2003;85:538-44. DOI: 10.1302/0301-620X.85B4.13925

11. London JT. Kinematics of the elbow. J Bone Joint Surg Am 1981; 63:529-35.

12. Morrey BF, Chao EY. Passive motion of the elbow joint. J Bone Joint Surg Am 1976;58:501-8.

13. Oka T, Moritomo H, Goto A, Sugamoto K and Yoshikawa H. Accuracy analysis of three dimensional bone surface models of the forearm constructed from multidetector computed tomography. Int J Med Robot 2009;5:452-7. doi:10.1002/rcs.277 DOI: 10.1002/rcs.277

Chapter 3

The Effect of Implant Size on Kinematics and Stability

Overview

Distal humeral hemiarthroplasty is a treatment option for distal humerus fractures, non-unions and avascular necrosis. The biomechanical effects, however, have not been reported. The purpose of this chapter is to quantify the effects of hemiarthroplasty and implant size on elbow joint kinematics using in vivo techniques.

A version of this work has been published:

Desai SJ, Athwal GS, Ferreira LM, Lalone E, Johnson JA and King GJW. Distal Humerus Hemiarthroplasty: The Effect of Implant Sizing on Elbow Joint Kinematics. J Shoulder Elbow Surg. J Shoulder Elbow Surg. 2014;23:946-954 (See Appendix C).

3.1 Introduction

While described and reported many years ago, there has been recent interest in elbow hemiarthroplasty as a less invasive alternative to total elbow arthroplasty (TEA). Hemiarthroplasty may be ideal in situations where only one portion of the elbow joint is affected, such as distal humerus fractures not amenable to open reduction internal fixation, non-unions or avascular necrosis. Hemiarthroplasty has the advantage of less invasive surgical approaches, less patient morbidity, avoidance of polyethylene wear concerns and preservation of bone stock for future reconstructive procedures (1).

There is a paucity of literature regarding hemiarthroplasty of the elbow. Clinical studies to date are few, with limited samples sizes, short-term follow-up, inconsistent indications for surgery, and variable implant materials and designs (2-9). In addition to lack of clinical information, there is a complete void of information regarding the biomechanics of these devices. Altered elbow kinematics may result in symptomatic instability from mal-tracking, implant loosening and accelerated wear of the native articulation. Given that surgeons estimate the optimal implant size at surgery, the effect of incorrect implant sizing on joint kinematics and mechanics is unknown. Therefore, the purpose of the present study was to determine the influence of distal humeral hemiarthroplasty and implant size on joint kinematics and stability *in-vitro*.

3.2 Materials and Methods

3.2.1 Specimen Preparation

This *in vitro* study quantifying the effects of hemiarthroplasty on elbow joint mechanics utilized eight fresh, previously frozen male cadaveric arms (76 ± 6.4 years) amputated at the mid-humerus. Each arm underwent 64-slice, computed tomography (CT) (GE LightSpeed Ultra; General Electric, New Berlin, Wisconsin). A three-dimensional (3D) surface model was generated (Visualization Toolkit, VTK; Kitware, Clifton Park, New York) from CT scan DICOM data.

The optimal size distal humeral implant was determined by measurements taken from the 3D CT reconstruction. Points were defined on the surface of the trochlea and capitellum with a semi-automated algorithm using initial boundary points selected by a single user (Figure 3.1). The geometric center of the capitellum and trochlea was found using a sphere-fit of the capitellum and a circle-fit of the trochlear groove**.** The distance from the geometric center of the trochlear groove to the geometric center of the capitellum was measured for each 3D model. To match the implant to the specimen, comparative measurements were taken from 3D models of the six distal humeral implants (Latitude Anatomic, Tornier, Inc, Stafford, Texas).

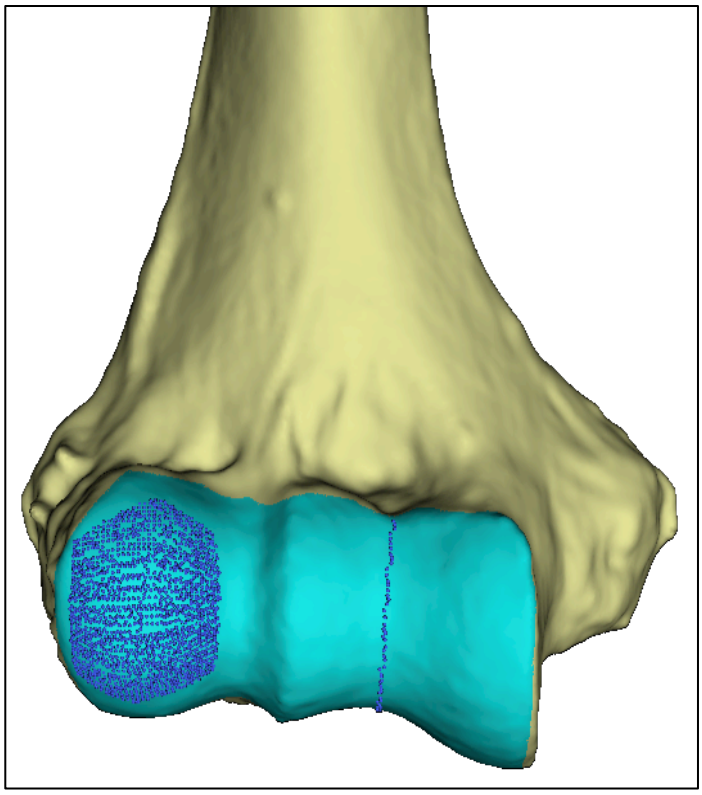

Figure 3.1: Three dimensional (3D) reconstruction of the distal humerus. Nine points were selected on the surface of the capitellum and six points along the trochlear groove. Using a semi-automated algorithm, a point cloud was created over the surface of the capitellum and along the trochlear groove. These points were used to define the geometric center of the spherical capitellum and the circular trochlear groove.

Specimens were thawed at room temperature (mean 22 ± 2 °C) for eighteen hours prior to testing. The specimen was kept hydrated throughout the preparation and testing protocol using normal saline. The tendons of the biceps, triceps and brachialis were sutured using a locking Krackow repair (10). All skin incisions were closed using #2 Vicryl (Ethicon Inc, USA). A Steinmann pin was placed through the third metacarpal, through the carpus and into the distal radius to fix the wrist in neutral flexion and extension. Two fully threaded 3.5 mm cortical screws were placed across the distal radio-ulnar joint to fix the forearm in neutral rotation.

3.2.2 Elbow Simulator

The distal humerus was mounted in an *in-vitro*, unconstrained elbow simulator previously developed in our laboratory (11). The sutures were connected to servomotors via braided Dacron® cords. The servomotors applied forces to the tendons which moved the elbow from full extension to full flexion or vice versa at a controlled rate (10 degrees/second). The motion simulation was based on electromyographic data and muscle cross-sectional area (12,13). Established muscle loading protocols were used during active motion, as reported by Ferreira et al. (2010) (11). The simulator allowed for testing in the dependent (vertical), horizontal, varus and valgus positions (Figure 3.2). The motion of the ulna with respect to the humerus was quantified with the use of an electromagnetic tracking system (trakSTAR, Ascension Technology, Burlington, Vermont). Accuracy reported by the manufacturer is 1.8 mm and 0.5^{o} root-mean-squared deviation. A tracker receiver was rigidly fixed to the ulna, while the tracking transmitter was mounted on the simulator rigidly with respect to the humerus.

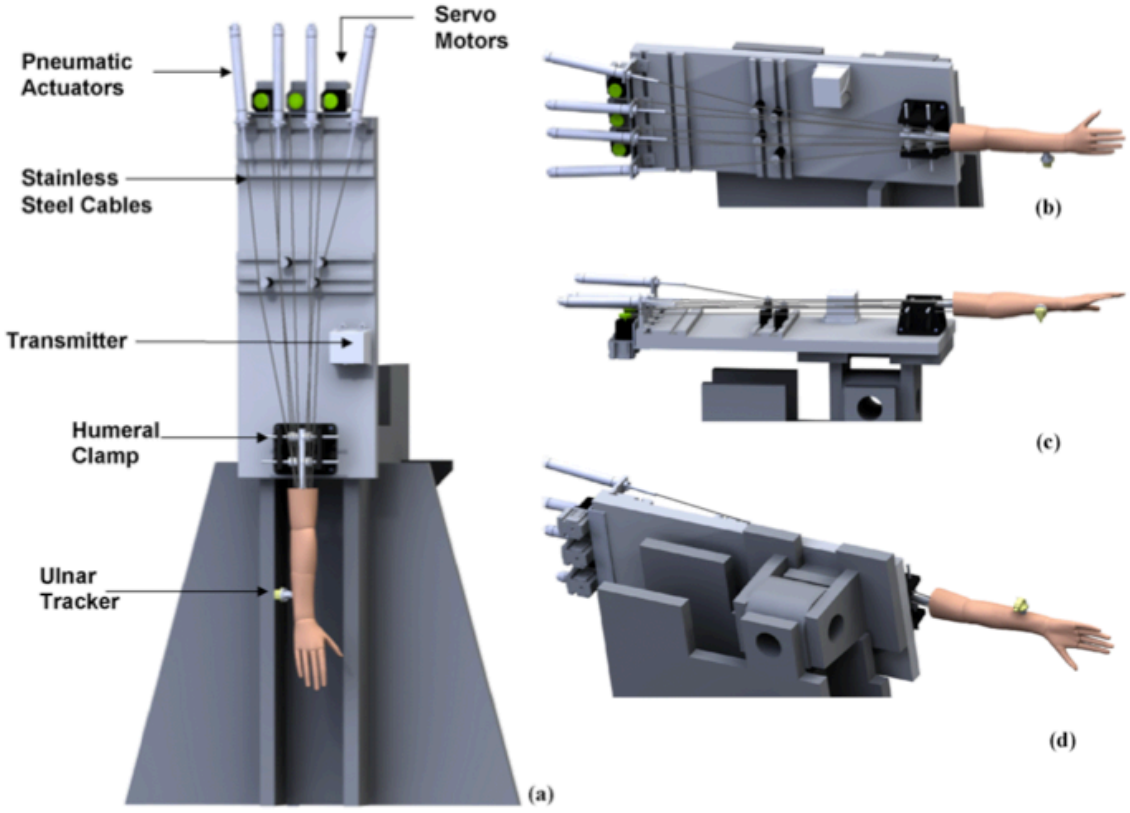

Figure 3.2. Schematic diagram of the elbow motion simulator showing the mounted specimen. The simulator is shown in the (a) vertical, (b) valgus, (c) dependant, and (d) varus positions.

3.2.3 Experimental Testing Protocol

The testing began with the intact arm. The various elbow orientations, including varus, valgus, dependent and horizontal positions were tested in random order both actively and passively in flexion and extension. Passive flexion was performed by one investigator (SJD) slowly moving the arm through a full arc of motion. The elbow was then surgically exposed through a midline posterior incision. Medial and lateral fasciocutaneous flaps were created and the subcutaneous border of the ulna was identified. A chevron-type olecranon osteotomy was performed to gain access to the distal humerus. The osteotomy was fixed with a pre-contoured olecranon plate and locking screws (Accumed Llc, Hillsboro, Oregon). The collateral ligaments were left intact. The testing protocol with the native articulation was repeated following the osteotomy and fixation to act as a control in order to determine if there were any kinematic changes due to the osteotomy alone.

A medium humeral stem (Latitude, Tornier, Texas, USA) was shortened for ease of placement into the humeral canal. The stem was shortened in order to optimize articular alignment by avoiding stem impingement with the humeral canal (14). The shortened stem was placed under computer navigation, which has been shown to improve accuracy and reproducibility of humeral component placement (15). This step was performed by first digitizing the native elbow's distal humerus articular surface using a 3D optical tracking system (Optotrak Certus®, NDI, Waterloo, ON, Canada). This was accomplished by using a stylus and tracing the native distal humeral articular surface. Based on the point cloud created, a 3D surface model was generated. The humeral stem was calibrated to the tracking system and its location was tracked in real-time during

navigation relative to the humeral anatomy. The stem location was visualized by viewing the CAD model of the implant spool. During navigation, the spool was not actually attached to the stem; however its virtual representation aided navigation by aligning it to the virtual humeral articular surface (Figure 3.3). Navigation was performed as the stem was cemented in the humeral canal.

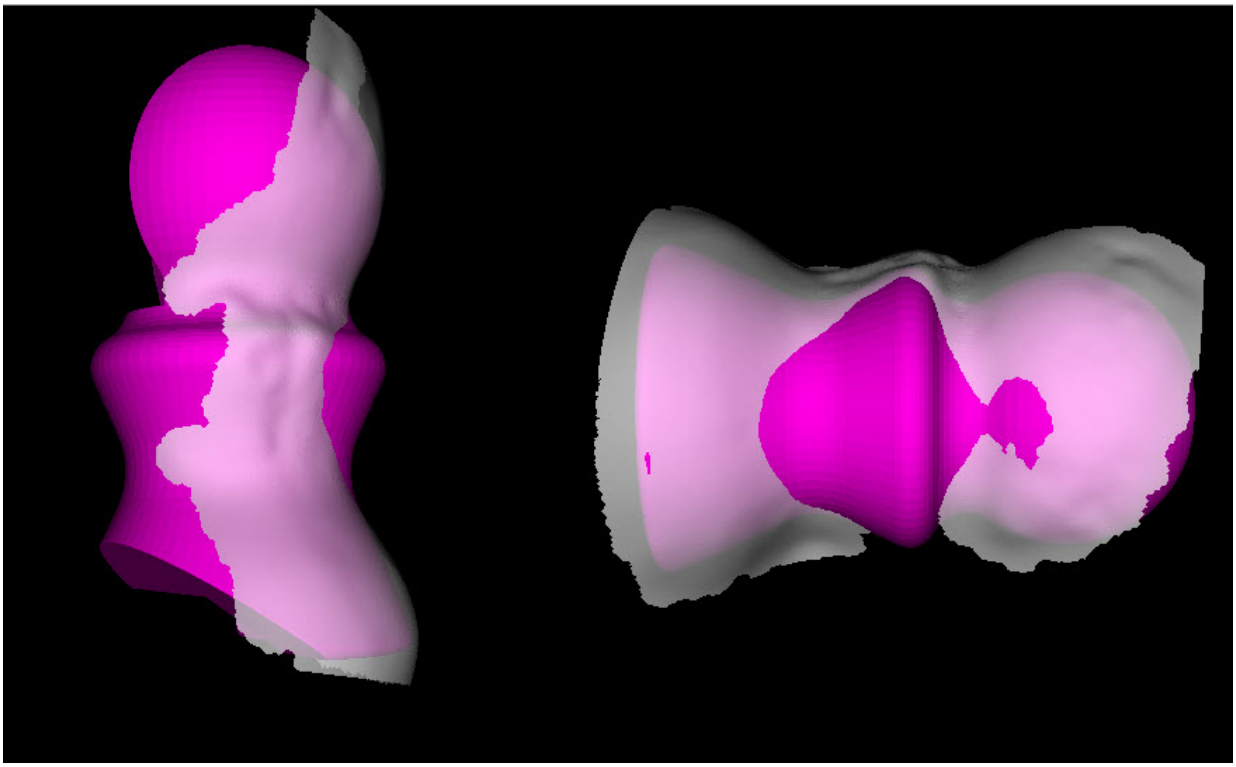

Figure 3.3: Navigation of the distal humeral implant. The distal humerus was digitized, and a virtual humeral surface was created (light). The implant CAD model (dark) was also visualized and tracked in real-time. The implant stem was navigated by closely matching the implant and humeral virtual surfaces. Differences in surface shape between the native articulation and the humeral implant can be seen.

The optimally sized implant, which was pre-determined based on the 3D CT measurements and the implant which was one size too large and one size too small were tested in random order (Figure 3.4). The stem was custom designed to fit all three implants using a locking mechanism; therefore, only a single stem was cemented throughout the duration of the testing protocol. Loosening of the stems were not observed in any of the tested elbows; all were well fixed at the conclusion of the testing protocol. Just prior to testing, a fellowship trained elbow surgeon estimated the size of the implant based on direct visualization of the native distal humerus. This allowed us to determine any trends in accuracy of implant size selection.

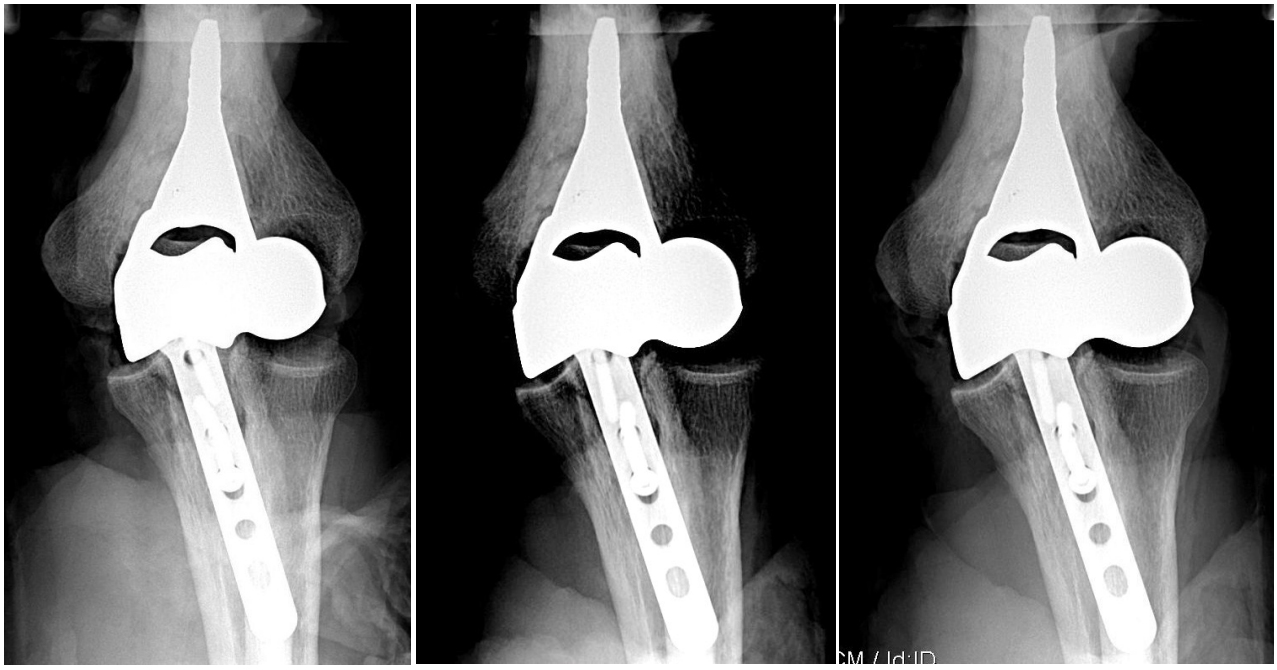

A **B** **C**

Figure 3.4: Radiographs of the three implants *in-situ*: (A) Under-sized (B) Optimal (C) Oversized-sized.

3.2.4 Statistical Analysis

A two-way repeated-measures analysis of variance was used comparing flexion angle and implant size for varus-valgus angulation and internal-external rotation. Significance was defined as $p < 0.05$.

3.3 Results

3.3.1 Varus/Valgus Angulation

3.3.1.1 Olecranon Osteotomy

Small but significant increases in valgus angulation occurred after the olecranon osteotomy with the arm oriented in the valgus position for active and passive motion, $1.4^{o} \pm 0.96^{o}$ ($p < 0.05$) and $1.4^{o} \pm 0.95^{o}$ ($p < 0.05$), respectively. In the varus position, there were no differences in varus angulation for either active ($p = 0.8$) or passive ($p = 0.2$) motion.

As a result of the small differences in kinematics after the olecranon osteotomy, the post osteotomy state was used as the control for all further analyses.

3.3.1.2 Dependent and Horizontal Position

There was no difference in varus-valgus angulation between the intact, post-osteotomy, optimally sized, over-sized and under-sized hemiarthroplasty groups in either active ($p > 0.05$**)** or passive ($p > 0.05$) motion in both the dependent ($p > 0.05$**)** and horizontal positions ($p > 0.05$**)**.

3.3.1.3 Valgus Position

When compared to the post-osteotomy state, there was a significant increase in valgus angulation for all implant sizes in both active ($p < 0.05$) and passive motion ($p < 0.05$), respectively (Figure 3.5). The optimal implant had an increase in valgus angulation of $3.0^{o} \pm 1.3^{o}$ ($p = 0.003$), the over-sized increased angulation by $3.0^{o} \pm 1.7^{o}$ ($p = 0.01$), and the under-sized by $4.4^{o} \pm 2.2^{o}$ ($p = 0.01$). In passive motion, the optimal

implant increased valgus angulation $2.6^{o} \pm 0.7^{o}$ ($p < 0.001$), the over-sized by $2.9^{o} \pm 1.8^{o}$ ($p = 0.02$), and the under-sized by $4.4^{o} \pm 2.3^{o}$ ($p = 0.01$).

When comparing individual implant sizes, there were no differences between the optimally-sized implant, and either the over-sized or under-sized implant ($p > 0.05$) (Figure 3.6). However, the under-sized implant had a significant increase in valgus angulation of $1.3^{o} \pm 0.8^{o}$ ($p=0.02$) and $1.5^{o} \pm 0.7^{o}$ ($p=0.006$) in active and passive motion respectively when compared to the over-sized implant.

3.3.1.4 Varus Position

When compared to the post-osteotomy state, there was a significant increase in varus angulation for the optimally-sized and under-sized implants in both active and passive motion ($p < 0.05$) (Figure 3.7). The optimal implant had an increase in varus angulation of $2.6^{o} \pm 1.4^{o}$ ($p = 0.01$) and the under-sized implant had an increase by $3.2^{o} \pm 1.2^{o}$ ($p = 0.001$). There was no difference in varus angulation between the over-sized implant and the post-osteotomy control ($p = 0.2$). During passive motion, the optimal implant had an increase in varus angulation of $2.1^{o} \pm 1.4^{o}$ ($p = 0.04$) and the under-sized increased by $3.0^{o} \pm 1.3^{o}$ ($p = 0.004$). There was no difference in varus angulation between the over-sized implant and the control ($p = 0.8$).

When comparing individual implant sizes to each other, there were no differences between the optimally-sized implant, and either the over-sized or under-sized implant in active motion ($p > 0.05$). In passive motion, the under-sized implant had an increase in varus angulation of $0.9^{o} \pm 0.5^{o}$ ($p=0.01$) when compared to the optimally sized implant.

In both active and passive motion, there were kinematic differences between the over-sized and under-sized implants. The under-sized implant had an increase in varus angulation of $1.6^{o} \pm 0.7^{o}$ ($p=0.004$) in active motion when compared to the over-sized implant. In passive motion, the under-sized implant had an increase in varus angulation of $1.9^{o} \pm 0.8^{o}$ ($p=0.003$) when compared to the over-sized implant.

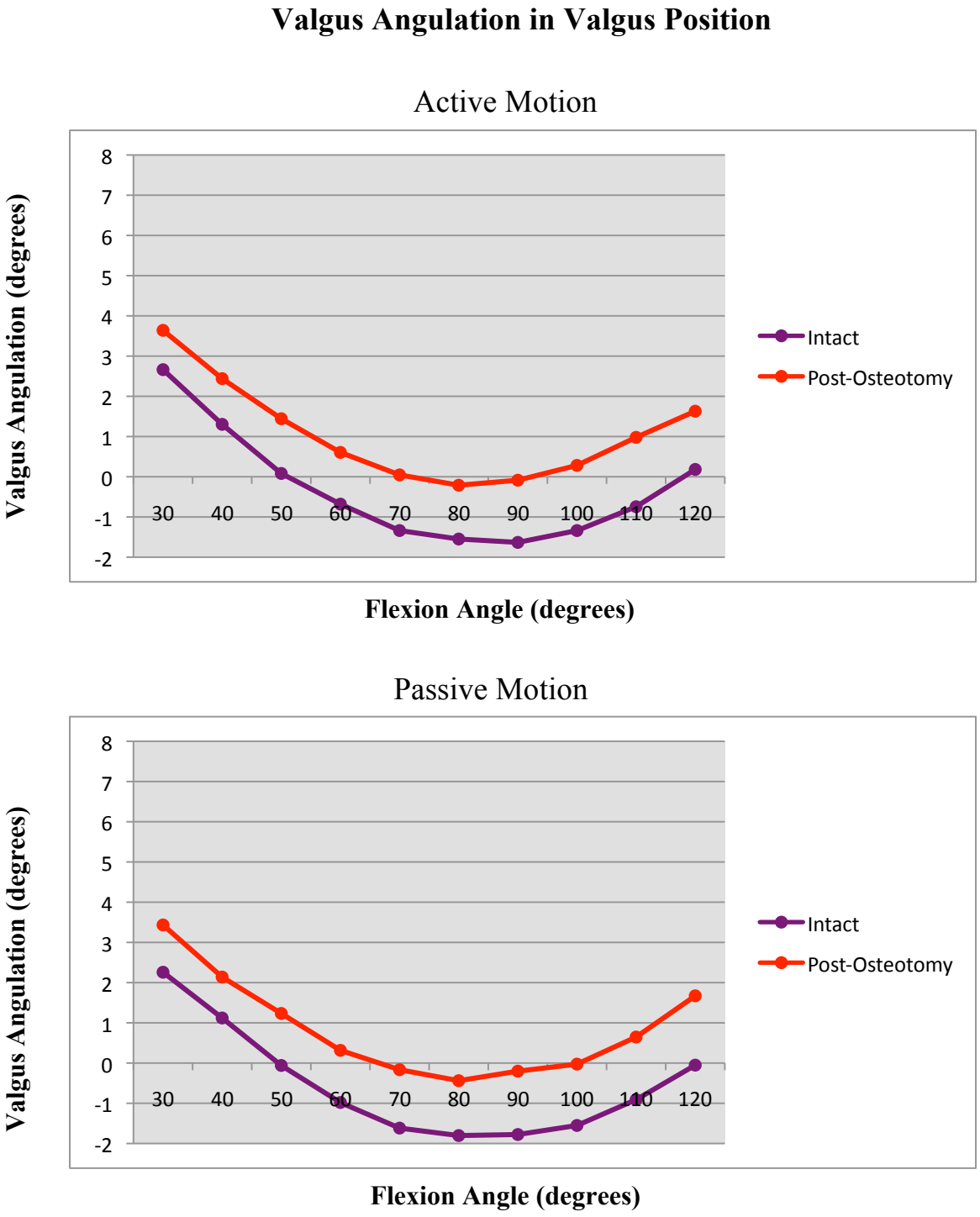

Figure 3.5: Mean valgus angulation for active and passive motion with the arm oriented in valgus. There was an increase in valgus angulation after olecranon osteotomy throughout range of motion ($p < 0.05$). During passive motion, there was also a significant increase in valgus angulation ($p < 0.05$).

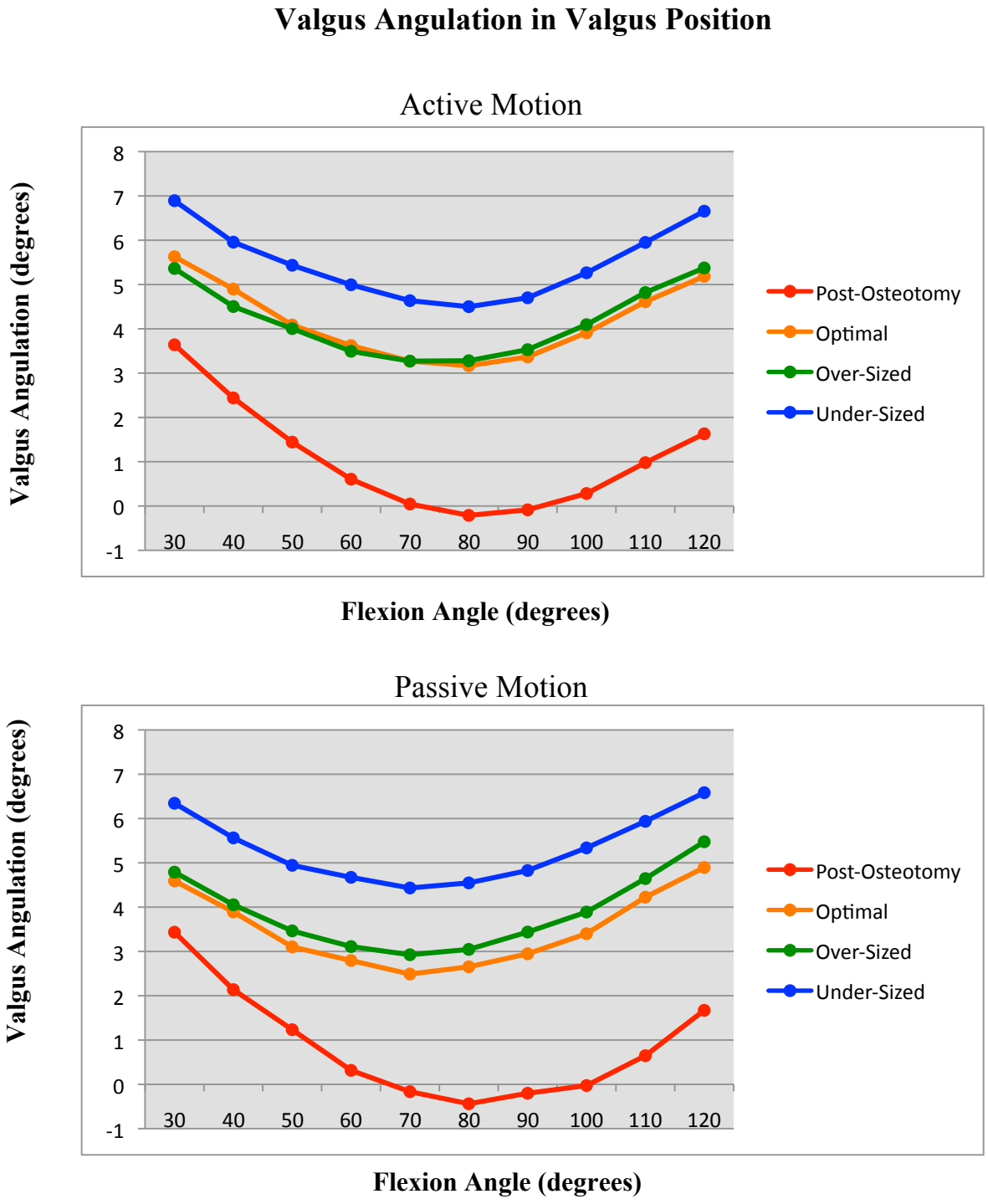

Figure 3.6: Mean valgus angulation for a) active motion and b) passive motion with arm oriented in valgus position. There was an increase in valgus angulation for all implant sizes throughout range of motion ($p < 0.05$).

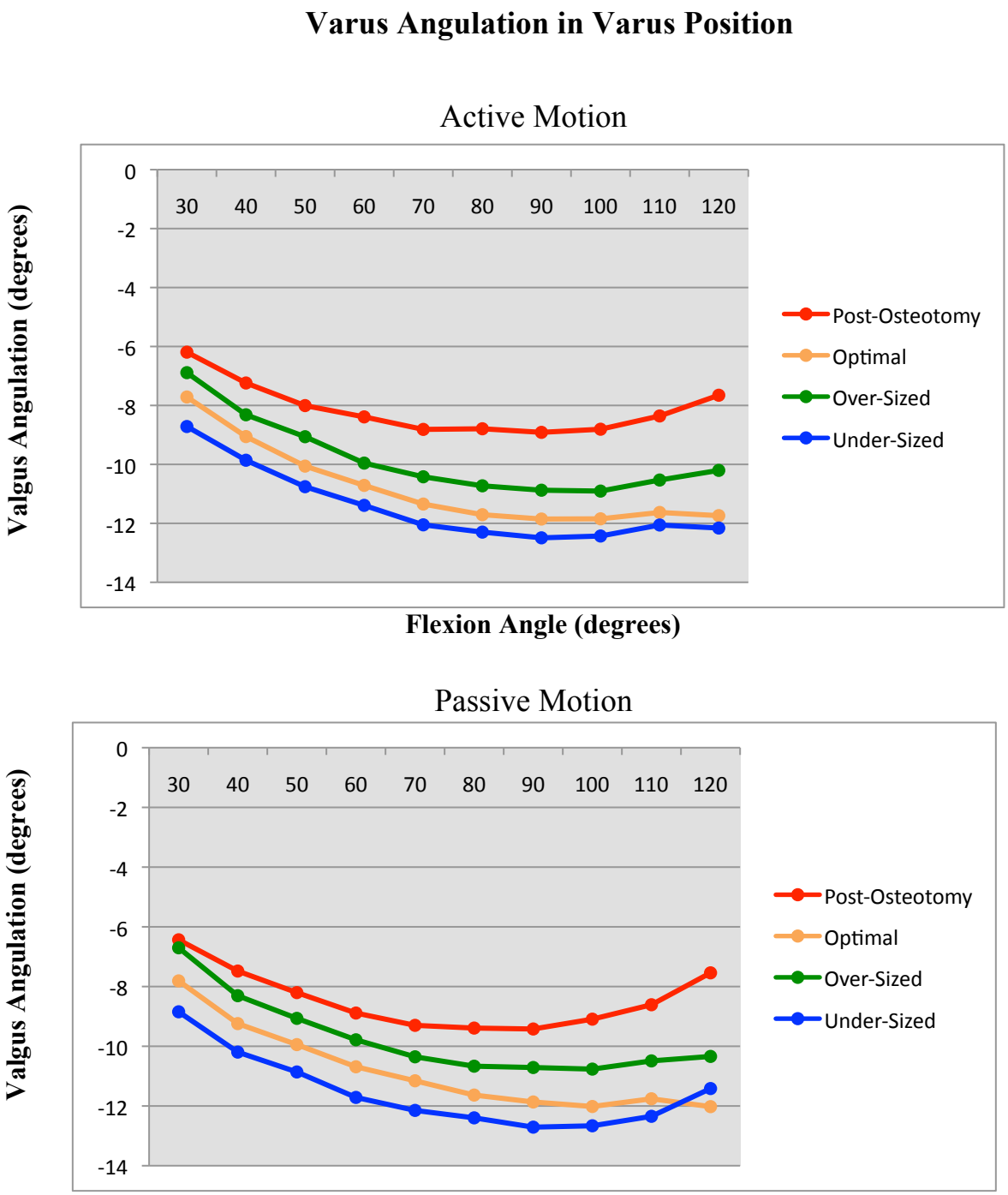

Figure 3.7: Mean varus angulation for a) active motion and b) passive motion with arm oriented in varus position. When compared to the post-osteotomy state, there was an increase in varus angulation for the optimally sized and under-sized implant. There was no difference in varus angulation between the over-sized implant and the control ($p = 0.2$). When comparing the over-sized to the under-sized implants, the undersized implant had an increase in varus angulation in both active and passive motion ($p < 0.05$).

3.3.2 Ulnohumeral Rotation

3.3.2.1 Olecranon Osteotomy

Significant changes in ulnohumeral rotation occurred after the olecranon osteotomy with the arm in valgus position. During active motion, there was a significant increase in external rotation of $2.1^{o} \pm 0.98^{o}$ ($p = 0.005$) after the olecranon osteotomy. During passive motion, there was also a significant increase in external rotation of $2.2^{o} \pm 0.7^{o}$ ($p < 0.0001$). No changes in ulnohumeral rotation were present in the varus position in either active or passive motion.

During passive motion in the dependent position, there was an increase in external rotation of $1.8^{o} \pm 1.0^{o}$ ($p = 0.01$) after the olecranon osteotomy. No changes were found in active motion. Due to the alterations in kinematics after the olecranon osteotomy, this was used as the control for analysis.

3.3.2.2 Dependent and Horizontal Position

There was no difference in ulnohumeral rotation between the intact, post-osteotomy, optimally sized, over-sized and under-sized hemiarthroplasty groups in either active ($p > 0.05$) or passive ($p > 0.05$) motion in either the dependent or horizontal position.

3.3.2.3 Valgus Position

There was no difference in ulnohumeral rotation between the intact, post-osteotomy, optimally sized, over-sized and under-sized hemiarthroplasty groups in either active ($p > 0.05$) or passive ($p > 0.05$) motion in the valgus position.

3.3.2.4 Varus Position

Significant changes in ulnohumeral rotation occurred with the arm in the varus position. When compared to the post-osteotomy state, there was an increase in ulnohumeral internal rotation for the optimally sized and under-sized implant in passive motion. The optimal implant had an increase in internal rotation of $3.2^{o} \pm 2.1^{o}$ ($p = 0.04$) and the under-sized implant increased by $3.7^{o} \pm 2.0^{o}$ ($p = 0.01$). There was no difference in varus angulation between the over-sized implant and the post osteotomy state ($p = 0.1$). No differences were present during active motion**.**

Prior to performing the humeral cuts, the size of the optimal implant was estimated by a fellowship trained elbow surgeon. This size was compared to the optimal implant size chosen based on 3D CT measurements. In three of the eight specimens, an incorrect size was chosen. In all cases, an under-sized implant was selected.

3.4 Discussion

The olecranon osteotomy did not precisely recreate the native kinematics after repair and as such was not a perfect control. The surgical technique for the osteotomy involved leaving all major stabilizing ligaments intact, including the anterior band of the medial collateral ligament and the lateral ulnar collateral ligament. However, the surgical exposure sacrificed the accessory stabilizers of the elbow, including the postero-lateral capsule and the posterior portion of the posterior band of the medial collateral ligament (pMCL). This likely resulted in a subtle increase in elbow instability as previously reported (16). Interestingly, there was no difference in varus angulation or ulnohumeral internal rotation in the varus position after the olecranon osteotomy in either active ($p > 0.05$) or passive ($p > 0.05$) motion. A possible explanation is the relatively greater contribution to elbow stability of the pMCL when compared to the postero-lateral capsule. Another possible explanation is the olecranon osteotomy, which was fixed with a pre-contoured locking plate, may not have been repaired in an anatomic position in spite of our best efforts.

The present study demonstrates that distal humeral hemiarthroplasty alters elbow joint kinematics, regardless of the implant size in both varus and valgus positions. This difference in kinematics between the post-osteotomy elbow and the elbows with the hemiarthroplasty implant may, in part, be related to the navigation technique. The distal humeral implant was navigated into position by visually matching the digitized surface of the native distal humerus with the surface of the humeral implant. Navigation of distal humeral implants has been shown to increase accuracy; however, inaccurate placement still occurs due to errors in registration and optical implant tracking and due to the

subjective nature of the navigation attempting to match the surface contours. This error in navigation may result in a mismatch in flexion-extension (FE) axis between the implant and the native distal humerus. The anatomic FE axis of the distal humerus is defined by the geometric center of the capitellum approximated as a sphere, and the geometric center of the trochlear, approximated as a circle (17-21). As mentioned, the navigation was performed by matching the surface of the implant with the native distal humeral surface, not the native FE axis. This resulted in a difference between the FE axis of the native distal humerus and the navigated implant of $7^{o} \pm 3^{o}$ ($p < 0.001$). Also, even the optimally sized distal humeral implant shape did not precisely match the shape of the native distal humerus, indicating the implant may not precisely recreate normal anatomy. This may further explain the alteration in joint kinematics.

When comparing individual implant sizes, not surprisingly, the under-sized implant was consistently more lax than the over-sized implant in both the valgus and varus positions. The optimally sized implants would be expected to best recreate physiologic tension in the soft tissues and restore normal stability. In the present study, a fellowship trained elbow surgeon chose an implant size based on the size of the native distal humerus. In three of the eight distal humeri, the size was underestimated by the surgeon when compared to the CT-derived optimal dimensions. The results of this study suggest that intra-operatively, when uncertainty exists in choosing between sizes, the surgeon should choose the larger implant, as this may reduce post-operative instability and provide more favourable contact mechanics. However, the effect this may have on articular cartilage contact area, loading and wear is not known.

The present study has limitations. First, we performed an olecranon osteotomy to insert the implant whilst leaving the stabilizing ligaments intact. This is a common technique to insert a hemiarthroplasty clinically and also closely models other surgical approaches where the collateral ligaments are taken down and repaired or epicondyle fractures are internally fixed around the implant. Second, we used the width between the center of the capitellum and the center of the trochlea to determine the size of the distal humeral implant. Sizing the implant using a different technique such as using the diameter of the capitellum and trochlea may have lead to a different size for the optimal implant, explaining the finding that the oversized implant best recreated normal kinematics. Further studies are needed to evaluate the optimal shape of distal humeral implant designs. Third, the implant size determined from CT scan did not account for articular cartilage. Our approach to determine optimal size, using the width between the center of the capitellum and the center of the trochlea, would not be affected by the thickness of the articular cartilage. Therefore, lack of incorporation of articular cartilage would not have an affect on implant sizing. Fourth, we used an *in vitro* elbow motion simulator which may not precisely replicate the clinical scenario. Fifth, our protocol involved prolonged testing with four positions and multiple conditions, which may have resulted in changes in the mechanical behaviour of the soft tissues. However, previous studies suggest that these changes may be minor in relation to the experimental effects of interest (22). Finally, we have quantified the differences in varus-valgus angulation and ulnohumeral rotation; however, we are unsure of how much alterations in angulation or rotation are clinically significant in elbow hemiarthroplasty. Additionally, these results

can only be applied to the hemiarthroplasty implants tested and should not be generalized to other designs.

3.5 Conclusion

The current study showed an alteration in elbow joint kinematics with placement of a distal humeral hemiarthroplasty, regardless of implant size, when compared to the control group. The kinematic alterations were small; therefore it is difficult to deduce whether patients would have symptomatic instability. Clinical studies are required to further assess this hypothesis. The modest changes in joint kinematics will cause significant changes in articular contact and loading (23), which may result in pain, accelerated cartilage degeneration and arthritis. Also, within the hemiarthroplasty group, the implant which is too small showed the greatest alteration in joint kinematics and stability. This suggests that intra-operative sizing has an important role in joint stability. Intra-operatively if a surgeon is faced with uncertainty, the larger implant may be a better option, at least from the perspective of joint kinematics and stability.

3.6 References

1. Athwal GS, Goetz TJ, Pollock JW and Faber KJ. Prosthetic replacement for distal humerus fractures. Orthop Clin North Am. 2008 Apr;39(2):201-12, vi

2. Adolfsson L and Hammer R. Elbow hemiarthroplasty for acute reconstruction of intraarticular distal humerus fractures. Acta Orthop. 2006;77(5):785-787

3. Barr JS, Eaton RG. Elbow reconstruction ith a new prosthesis to replace the distal end of the humerus: A case report. J Bone and Joint Surg Am. 1965:47:1408-1413

4. Malone AA, Zarkadas P, Jansen S, Hughes JS. Elbow hemiarthroplasty for intra-articular distal humerus fracture. J Bone Joint Surg Br 2009;91-B Supp 256

5. Mellex RH, Phalen GS. Arthroplasty of the elbow by replacement of the distal portion of the humerus with an acrylic prosthesis. J Bone Joint Surg Am. 1947;29:348-353

6. Parsons M, O'Brien R, Hughes J. Elbow hemiarthroplasty for actue and salvage reconstruction of intra-artiular distal humerus fractures. Tech Shoulder and Elbow Surg 2005; 6 (2): 87-97

7. Shifrin PG and Johnson DP. Elbow hemiarthroplasty with 20-year follow-up study. Clin Orthop Relat Res. 1988;254:128-133

8. Street DM and Stevens PS. A humeral prosthesis for the elbow: results in ten elbows. J Bone Joint Surg Am. 1974;56:1147-1158

9. Swoboda B and Scott R. Humeral hemiarthroplasty of the elbow joint in young patients with rheumatoid arthritis. J of Arthro. 1999;14(5)553-59

10. Howard RF, Ondrovic L, Greenwald DP. Biomechanical analysis of four-strand extensor tendon repair techniques. J Hand Surg Am. 1997;22:838-42

11. Ferreira, L.M., Johnson, J.A., and King, G.J. Development of an active elbow flexion simulator to evaluate joint kinematics with the humerus in the horizontal position. J.Biomech. 2010;43[11], 2114-2119.

12. Funk DA, An KN, Morrey BF, Daube JR. Electromyographic analysis of muscles across the elbow joint. J Orthop Res. 1987;5:529-38

13. Johnson JA, Rath DA, Dunning CE, Roth SE, King GJ. Simulation of elbow and forearm motion in vitro using a load controlled testing apparatus. J Biomech 2000:May;33(5):635-9

14. McDonald CP, Johnson JA, Peters TM, King GJ. Image-based navigation improves the positioning of the humeral component in total elbow arthroplasty J Shoulder Elbow Surg 2010 19, 533-543

15. McDonald CP, Peters TM, Johnson JA, King GJ. Stem abutment affects alignment of the humeral component in computer-assisted elbow arthroplasty. J Shoulder Elbow Surg. 2011 Sep;20(6):891-8

16. Pollock JW, Brownhill J, Ferreira LM, McDonald CP, Johnson JA, King GJ. Effect of the posterior bundle of the medial collateral ligament on elbow stability. J Hand Surg Am. 2009 Jan;34(1):116-23

17. Bottlang M, O'Rourke MR, Madey SM, Steyers CM, Marsh JL, Brown TD. Radiographic determinants of the elbow rotation axis: experimental identification and quantitative validation. J Orthop Res 2000;18:821-8.

18. Deland JT, Garg A, Walker PS. Biomechanical basis for elbow hinge-distractor design. Clin Orthop Relat Res 1987:303-12.

19. Ericson A, Arndt A, Stark A, Wretenberg P, Lundberg A. Variation in the position and orientation of the elbow flexion axis. J Bone Joint Surg Br 2003;85:538-44.

20. London JT. Kinematics of the elbow. J Bone Joint Surg Am 1981; 63:529-35.

21. Morrey BF, Chao EY. Passive motion of the elbow joint. J Bone Joint Surg Am 1976;58:501-8.

22. King GJ, Pillon CL, Johnson JA. Effect of in vitro testing over extended periods on the low-load mechanical behaviour of dense connective tissues. J Orthop Res. 2000;18:678-81

23. Lalone EA, Giles JW, Alolabi B, Peters TM, Johnson JA, King GJ. Utility of an image-based technique to detect changes in joint congruency following simulated joint injury and repair: an in vitro study of the elbow. J Biomech. 2013 Feb 22;46(4):677-82.

Chapter 4

The Effect of Implant Size on Joint Congruency

Overview

Distal humeral hemiarthroplasty is a treatment option for distal humerus fractures, non-unions and avascular necrosis. The effect on native articular cartilage, however, have not been reported. The purpose of this chapter is to quantify the effects of hemiarthroplasty and implant size on elbow joint congruency using in vivo techniques.

4.1 Introduction

There has been a recent increased interest in distal humeral hemiarthroplasty as a less invasive alternative to total elbow arthroplasty (TEA). Distal humeral hemiarthroplasty may be ideal in situations where only the distal humerus is affected. This includes distal humerus fractures not amenable to open reduction internal fixation, avascular necrosis and non-unions. Distal humeral hemiarthroplasty has the advantage of being a less invasive surgical approach, decreasing patient morbidity, avoiding concerns surrounding polyethylene wear and preserving the bone stock for future reconstructive procedures (1).

The current literature on distal humeral hemiarthroplasty is limited. Clinical studies to date have small samples sizes, short-term follow-up and inconsistent indications for surgery (2-11). Articular wear from abnormal contact of the metallic implant on the proximal radius and ulna is a long-term concern. A recent biomechanical study on distal humeral hemiarthroplasty demonstrates its limitations in restoring normal elbow kinematics (12). The purpose of the present study was to determine the influence of distal humeral hemiarthroplasty and implant size on joint congruency *in vitro*.

4.2 Materials and Methods

4.2.1 Specimen Preparation

This *in vitro* study examined the effect of distal humeral hemiarthroplasty on joint congruency using five fresh, previously frozen male cadaveric arms (74.1 ± 6.4 years) amputated at the mid-humerus. A 64-slice, computed tomography (CT) scan was performed on each arm (GE LightSpeed Ultra; General Electric, New Berlin, Wisconsin). A three-dimensional (3D) surface model was generated (Visualization Toolkit, VTK; Kitware, Clifton Park, New York) from CT scan DICOM data. A pre-operative surgical plan was conducted using the 3D reconstructed bone model. The distal humerus hemiarthroplasty component size was selected using the geometric center of the capitellum and trochlea based on the 3D model. Points were identified on the capitellar and trochlea surface and a semi-automated algorithm created a point cloud over the capitellum and trochlear groove. The geometric center was found using a sphere-fit of the capitellum and a circle-fit of the trochlear groove. The size of the native distal humerus was based on the distance between these two points, and then compared to the six available implants to determine the optimal implant size (Latitude Anatomic, Tornier, Inc, Stafford, Texas).

Prior to testing, specimens were thawed at room temperature (mean 22 ± 2 °C) for eighteen hours. Normal saline was used throughout the testing protocol to keep the specimen well hydrated. The tendons of the biceps, triceps and brachialis were sutured using a locking Krackow technique (13). A Steinmann pin was placed through the third metacarpal into the distal radius to fix the wrist in neutral flexion and extension. The

forearm was also fixed in neutral rotation by placing two fully threaded 3.5mm cortical screws across the distal radio-ulnar joint.

4.2.2 Elbow Simulator

An *in-vitro* unconstrained elbow simulator was used (14). The humerus was mounted in the simulator. The tendons sutures were connected to servomotors via braided Dacron® cords. The servomotors applied forces to the tendons which moved the elbow from full extension to full flexion and vice versa at a controlled rate (10 degrees/second). The motion simulation was based on electromyographic data and muscle cross-sectional area (15,16). Elbow motion was simulated with the arm in the horizontal position. Two optical position sensors were used. One sensor was rigidly fixed to the ulna using a bone-fixated mounting pedestal, while the other sensor was mounted on the base of the simulator adjacent to the humerus.

4.2.3 Experimental Testing Protocol

The distal humeral hemiarthroplasty stem was then surgically implanted. The elbow was approached through a midline posterior incision. The subcutaneous border of the ulna was identified and a chevron-type olecranon osteotomy was performed to access the distal humerus while maintaining the integrity of the collateral ligaments. The distal humeral cuts were made as per manufacturers protocol. A medium humeral stem (Latitude, Tornier, Texas, USA) was shortened for ease of placement into the humeral canal. The stem was cemented under computer navigation as previously described (12), in order to the maximize accuracy and reproducibility of stem placement (17). The optimal sized implant, along with the implant which was one size too small and one size too large, were tested in random order. The stem was cemented and used for the entire

testing protocol. The stem had a custom locking mechanism which allowed the various humeral articular components to be locked to the same stem. The osteotomy was secured with a pre-contoured olecranon plate and locking screws (Accumed Llc, Hillsboro, Oregon).

Active and passive flexion were performed on each specimen with the three implant sizes in the horizontal position. Established muscle load protocols were used during active motion, as reported by Ferreira et al. (2010). Passive flexion was performed by one investigator (SJD) slowly moving the arm through a full arc of motion. The optical tracking system recorded motion of the ulna with respect to the stationary humerus throughout elbow flexion (Optotrak Certus®, NDI, Waterloo, ON, Canada).

At the conclusion of testing, each specimen was denuded of all soft tissue structures and the distal humerus was isolated. Coordinate systems were created by digitizing anatomical landmarks using a calibrated tracked stylus (16). Four delrin spherical 19 mm fiducials were attached to the humerus in a previously described configuration (18). Each fiducial was digitized using a calibrated stylus to record the precise position of each fiducial marker with respect to the bone optical sensor (18).

A post-test CT scan was then performed using the same CT parameters used on the pre-testing CT scan. Landmark registration and determination of ulnohumeral joint congruency, a surrogate of joint contact, was examined using a previously reported image-based proximity mapping technique (19).

4.2.4 Statistical Analysis

In order to determine the statistical differences between joint congruency for each level of proximity (inter-surface distance less than 3.5mm, 2.5mm, 1.5m and 0.5mm), a three-way repeated-measures analysis of variance was performed. Variables include implant size (optimal, oversized, undersized), joint loading (active, passive), and flexion angle (30^{o}-120^{o}). Statistical significance was set at $p < 0.05$, then corrected with a Bonferroni correction factor to account for the multiple comparisons.

4.3 Results

4.3.1 Implant Size

Overall, the optimal-sized implant demonstrated the greatest joint congruency with the ulna, followed by the oversized implant, then the undersized implant at all levels of proximity (Figure 4.1). The three-way ANOVA revealed a significant effect of implant size on joint congruency at an inter-surface distance less than 3.5mm ($p = 0.008$). Pairwise comparisons demonstrated significant differences in joint congruency between the optimal sized implant and the undersized implant ($p = 0.036$), as well as the oversized implant and the undersized implant ($p = 0.001$) (Figure 4.2).

There were no differences in joint congruency between implants at 2.5mm ($p = 0.077$), 1.5mm ($p = 0.133$), and 0.5mm ($p = 0.445$) levels of proximity.

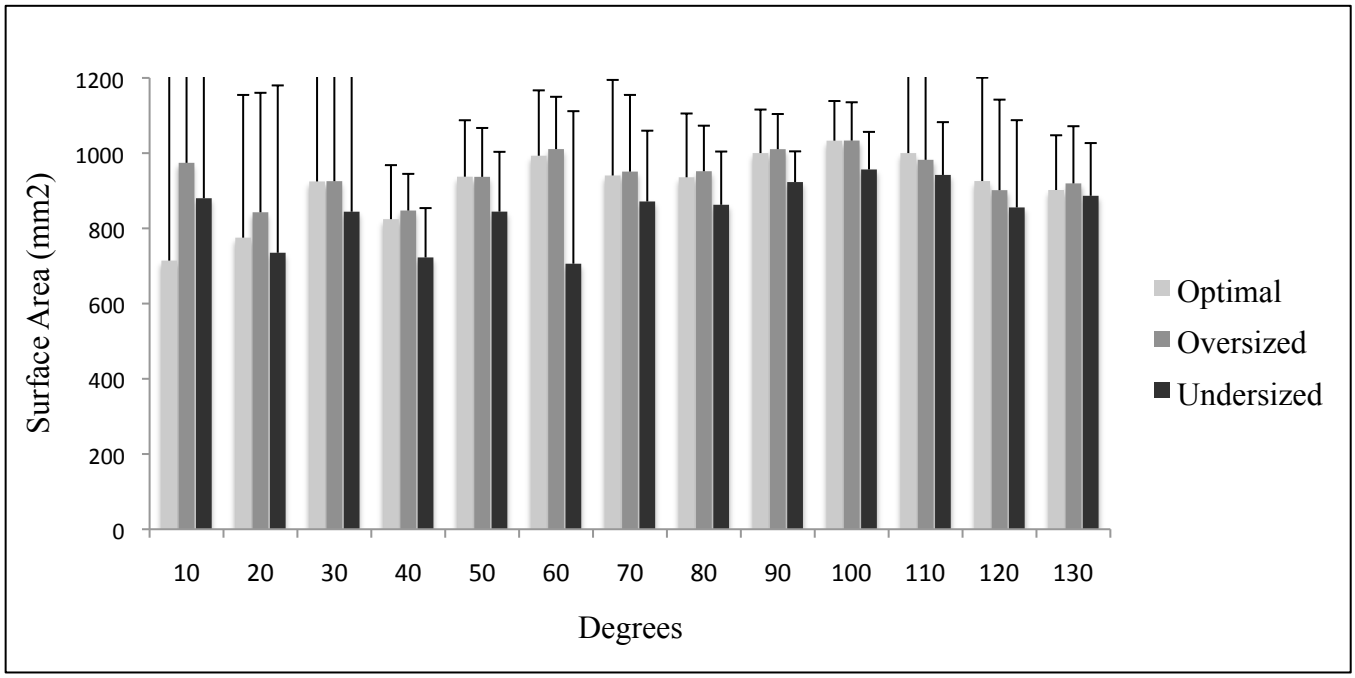

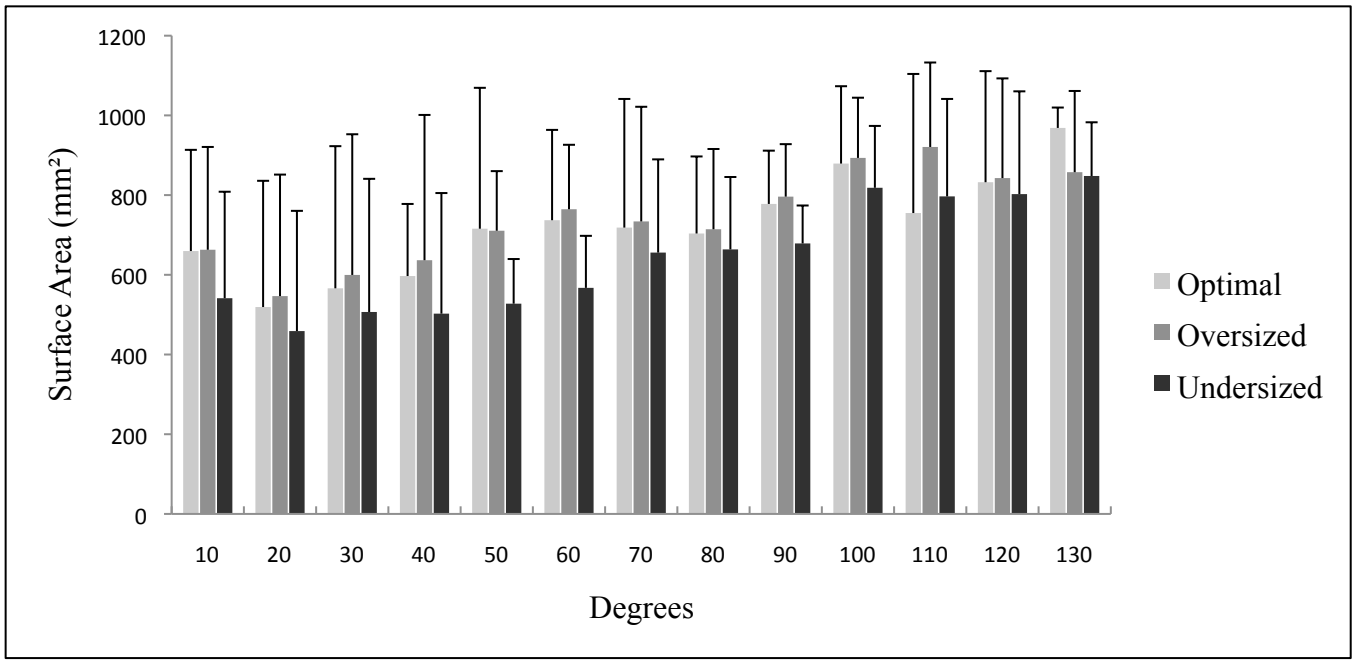

Figure 4.1: Surface area graphs for optimal, oversized and undersized implants and each level of flexion at 3.5mm of proximity for (a) active and (b) passive flexion. Optimal and oversized implants consistently demonstrate higher surface area contact compared to the undersized implant. This was also found at all other levels of proximity for both active and passive flexion.

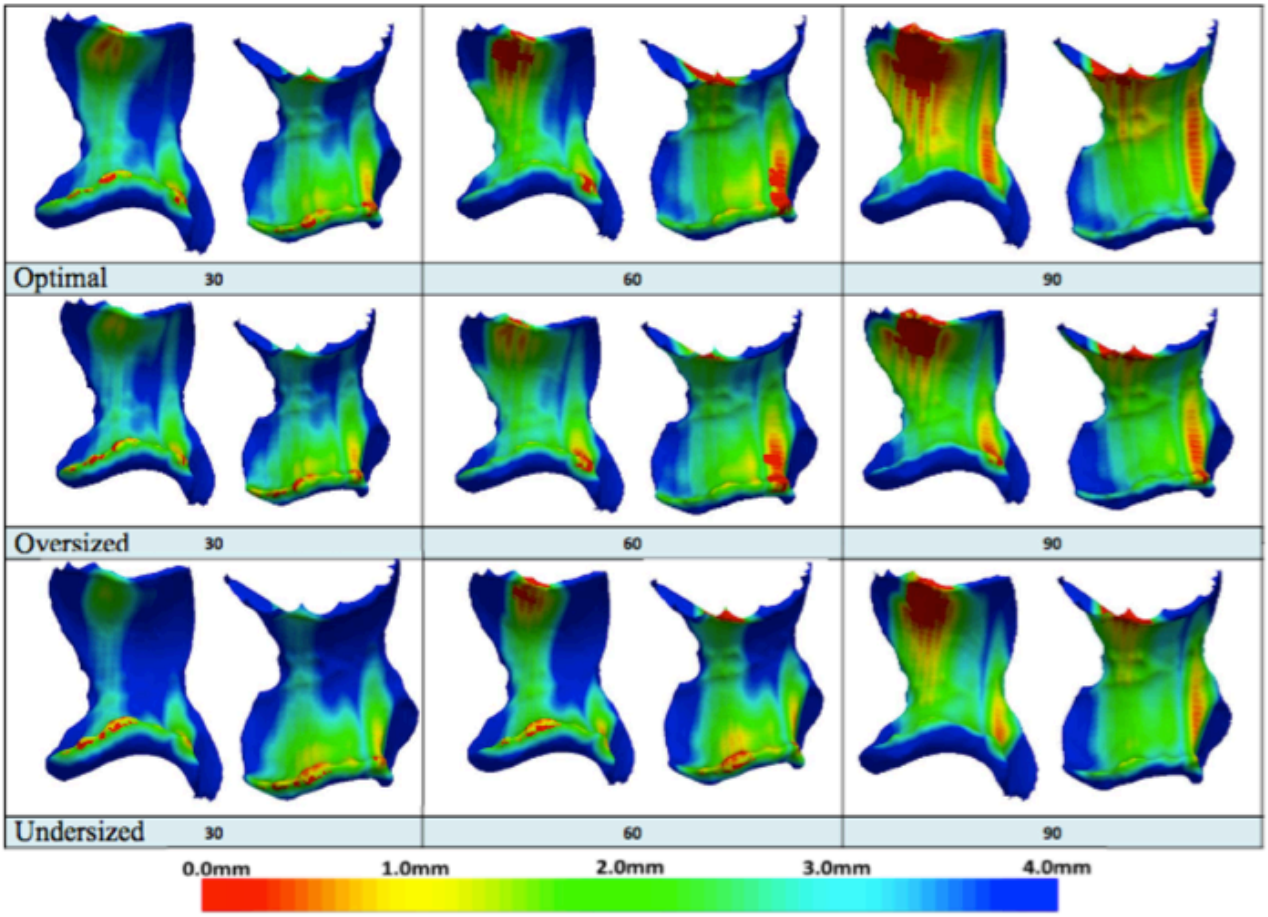

Figure 4.2a: Active Flexion. Example of ulnar proximity maps of a selected specimen at 30, 60 and 90 degrees of active flexion. Inter-bone distances are assigned a colour between blue (4mm) and red (0mm) to demonstrated overall inter-bone distances. Two views of the proximal ulna are presented to better visualize the olecranon and coronoid regions. Significant differences were found between the oversized and undersized implant at all four levels of proximity ($p < 0.05$)

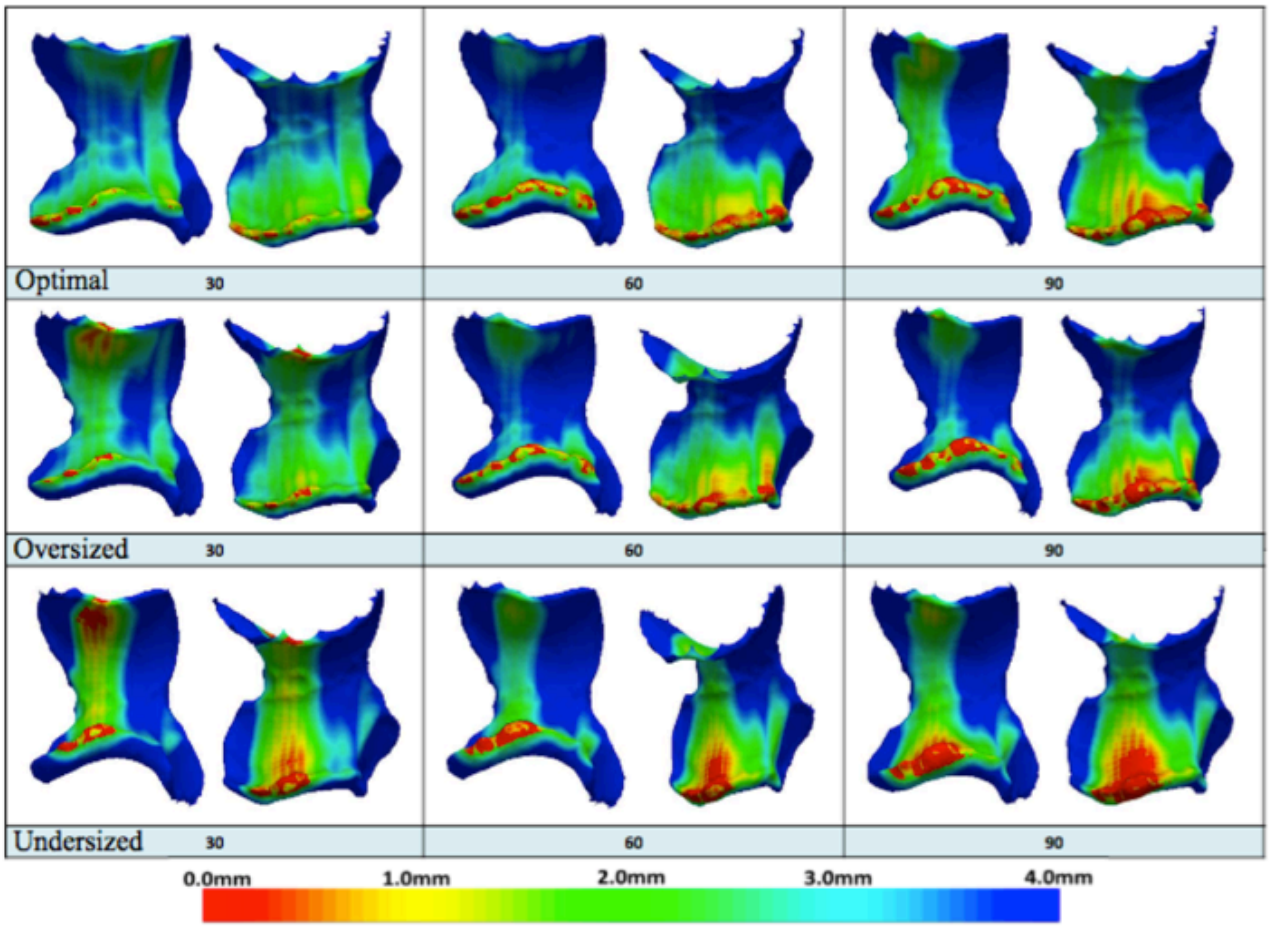

Figure 4.2b: Passive Flexion. Example of ulnar proximity maps of a selected specimen at 30, 60 and 90 degrees of passive flexion. Inter-bone distances are assigned a colour between blue (4mm) and red (0mm) to demonstrated overall inter-bone distances. Two views of the proximal ulna are presented to better visualize the olecranon and coronoid regions. Significant differences were found between the oversized and undersized implant at less than 3.5mm of proximity ($p = 0.016$).

4.3.2 Active vs. Passive Motion

There was a significant effect of loading (active vs. passive motion) on joint congruency at an inter-surface distance less than 3.5mm ($p = 0.018$), 2.5mm ($p = 0.009$), and 1.5mm ($p = 0.045$). Pairwise comparison demonstrated the joint had greater congruency during active versus passive flexion. This indicates that during active flexion the joint is more reduced than in passive flexion.

No difference was found in joint congruency between active and passive motion at an inter-surface distance less than 0.5mm ($p = 0.312$).

4.3.3 Flexion Angle

A significant effect of elbow flexion angle (30-120^{o}) on joint congruency occurred at an inter-surface distance less than 3.5mm ($p = 0.031$), 2.5mm ($p = 0.014$), 1.5mm ($p = 0.004$), and 0.5mm ($p = 0.008$). Pairwise comparisons revealed no significant findings at the various flexion angles. This indicates an overall trend that joint congruency increased at higher angles of flexion.

4.4 Discussion

Distal humeral hemiarthroplasty may be an option in selected patients to avoid the issues of polyethylene wear commonly reported following TEA in younger, higher demand patients. While the risk of implant bearing wear is eliminated, there remain concerns regarding the fate of the adjacent cartilage. Cruess et al. (1984) studied hemiarthroplasty in the hips of dogs, and followed changes in acetabular cartilage up to 24 weeks. They found early loss of proteoglycan, articular damage and progressive degenerative changes. They suggested the articular cartilage maintains its structural integrity for only a brief period following hemiarthroplasty (20). Dalldorf et al. (1995) took biopsy specimens of cartilage and subchondral bone in patients who were undergoing revision from a hemiarthroplasty to a total hip replacement. They also took similar samples from patients of similar age undergoing a total hip replacement for femoral neck fracture. Significant degeneration of acetabular cartilage in those with a previous hemiarthroplasty was found. A direct correlation cartilage degeneration was made with the duration of hemiarthroplasty use (21).

The mechanism of cartilage erosion in hemiarthroplasty is not well defined; however, several possible causes have been proposed. Factors may include improper implant sizing or geometric conformity, abnormal contact pressures and the activity level of the patient (22,23). In their case study, McGibbon et al. (1999) found that areas experiencing increased contact pressures were associated with an increased severity of cartilage degeneration. There is also suggestion that degenerative enzymes may accelerate cartilage breakdown (23). Moon et al. (2008) suggested that abnormal stresses and reduced contact area between the implant and native cartilage promotes the secretion

of degenerative enzymes which induce softening and reduced elasticity in the articular cartilage (24). The resulting biomechanical changes may destroy the existing cartilage, causing further degeneration at the articulation.

The present study examined proximity regions of the ulna using various implant sizes. A previous study by Lapner et al. (2014), examined the effect of hemiarthroplasty and implant size on cartilage contact area, not inter-bone distance, using a vastly different methodology. The study found differences in articular contact with hemiarthroplasty implants, but did not find any effects of implant size. These authors suggested that the implant shape and material are more important than the implant size itself. In the present study, differences in joint congruency were found between implant sizes. The optimally sized and oversized implant consistently demonstrated the highest contact area, while the undersized implant demonstrated the lowest contact area (Figure 4.1).

There are a couple of potential explanations for these findings. First, there are subtle alterations in kinematics between implants sizes. A previous study in our laboratory found that elbow kinematics were most abnormal with the undersized implant, while the optimal and oversized implant best reproduced native elbow kinematics (12). This would suggest that the kinematic alterations present in the undersized implant may contribute to the higher point loading on the ulnar articular cartilage. Lalone et al. (2012) used a similar technique as the current study to quantify articular congruency in both the native elbow and following simulated ligament injury and repair. This study found that even small changes in elbow joint kinematics resulted in relatively large alterations in joint congruency (19). Second, the distal humeral implant does not precisely match the shape of the native distal humerus. Desai et al. (2014) observed differences in distal

humeral morphology when compared to the hemiarthroplasty implant used in the present study (25). This difference in shape may have contributed to the alterations in contact area on the native ulna. This difference in implant shape, as well as altered kinematics, may have exaggerated the surface area contact in the undersized implant condition.

This alteration in contact area on the native ulna with the undersized implant may have harmful consequences on native articular cartilage, especially considering the stiff metallic surface of the hemiarthroplasty implant. In the native elbow, the cartilage possesses viscoelastic properties, which accommodates some joint incongruity. Eckstein et al. (1993) demonstrated that the incongruity between articular surfaces disappears as the joint is loaded. In their study, at 10N of load across the elbow, articular contact was only present ventrally and dorsally in the joint. As the load increased to 640N, the joint surfaces became more congruent. They hypothesized this was a result of the viscoelastic properties of the articular cartilage and subchondral bone (26). This observation of increased contact area at higher loads has been supported in other studies in the literature (27-29). In the present study both active and passive motion were tested. Considering the native elbow becomes more congruent with the greater loads placed in active motion, it would be expected that active motion would have better reduced the joint and subsequently increased joint congruency. The present study confirmed this finding, as there was increased joint congruency at 3.5mm, 2.5mm and 1.5mm levels of proximity in active motion compared to passive motion. With a hemiarthroplasty implant, the accommodation for joint incongruity on the humeral side is not present; therefore, the accommodation occurs on only the ulnar side. As a result, the effects of incongruity with an implant may result in accelerated cartilage wear.

This study has some limitations. First, this study included relatively few cadaveric specimens. Although we found significant differences between implant sizes at certain levels of proximity, further specimens may have revealed further differences between implants at other levels of proximity. Second, we used an in vitro elbow motion simulator, which may not fully replicate the normal clinical scenario. Third, the distal humeral implant was placed under navigation, which has been previously shown to increase accuracy (17). However, there still exists the possibility of errors due to the subjective nature of the navigation. Any errors in navigating the optimal sized stem may exaggerate contact area changes in the undersized and oversized implants.

4.5 Conclusion

This study suggests that an undersized distal humeral hemiarthroplasty implant had the lowest joint congruency when compared to an optimal or oversized implant. An undersized implant has previously been demonstrated to have the greatest alterations in elbow kinematics (12). The present study has further shown that the undersized implant also has the lowest surface area contact. This would suggest that if a surgeon must decide between two sizes of implants, the larger implant should perhaps be favoured. The larger implant would better recreate normal elbow kinematics (12), increase congruency on the native ulna, and presumably reduce wear and delay arthrosis on the native ulna.

4.6 References

1. Athwal GS, Goetz TJ, Pollock JW and Faber KJ. Prosthetic replacement for distal humerus fractures. Orthop Clin North Am. 2008 Apr;39(2):201-12, vi.

2. Adolfsson L and Hammer R. Elbow hemiarthroplasty for acute reconstruction of intraarticular distal humerus fractures. Acta Orthop. 2006;77(5):785-787.

3. Barr JS, Eaton RG. Elbow reconstruction with a new prosthesis to replace the distal end of the humerus: A case report. J Bone and Joint Surg Am. 1965:47:1408-1413.

4. Hohman DW, Nodzo SR, Qvick LM, Duquin TR, Paterson PP. Hemiarthroplasty of the distal humerus for acute and chronic complex intra-articular injuries. J Shoulder Elbow Surg. 2014;23(2):265-72.

5. Malone AA, Zarkadas P, Jansen S, Hughes JS. Elbow hemiarthroplasty for intra-articular distal humeral fracture. J Bone Joint Surg Br 2009;91-B Supp 256

6. Mellex RH, Phalen GS. Arthroplasty of the elbow by replacement of the distal portion of the humerus with an acrylic prosthesis. J Bone Joint Surg Am. 1947;29:348-353.

7. Parsons M, O'Brien R, Hughes J. Elbow hemiarthroplasty for acute and salvage reconstruction of intra-articular distal humerus fractures. Tech Shoulder and Elbow Surg 2005; 6 (2): 87-97.

8. Shifrin PG and Johnson DP. Elbow hemiarthroplasty with 20-year follow-up study. Clin Orthop Relat Res. 1990;254:128-133.

9. Smith GC, Hughes JS. Unreconstructable acute distal humeral fractures and their sequelae treated with distal humeral hemiarthroplasty: a two-year to eleven-year follow-up. J Shoulder Elbow Surg. 2013;22(12):1710-23.

10. Street DM and Stevens PS. A humeral prosthesis for the elbow: results in ten elbows. J Bone Joint Surg Am. 1974;56:1147-1158

11. Swoboda B and Scott R. Humeral hemiarthroplasty of the elbow joint in young patients with rheumatoid arthritis. J of Arthro. 1999;14(5)553-59.

12. Desai SJ, Athwal GS, Ferreira LM, Lalone E, Johnson JA and King GJW. Distal Humerus Hemiarthroplasty: The Effect of Implant Sizing on Elbow Joint Kinematics. J Shoulder Elbow Surg. 2014;23:946-954

13. Howard RF, Ondrovic L, Greenwald DP. Biomechanical analysis of four-strand extensor tendon repair techniques. J Hand Surg Am. 1997;22:838-42.

14. Ferreira, L.M., Johnson, J.A., and King, G.J. Development of an active elbow flexion simulator to evaluate joint kinematics with the humerus in the horizontal position. J.Biomech. 2010;43[11], 2114-2119.

15. Funk DA, An KN, Morrey BF, Daube JR. Electromyographic analysis of muscles across the elbow joint. J Orthop Res. 1987;5:529-38.

16. Johnson, J.A., Rath, D.A., Dunning, C.E., Roth, S.E., King, G.J., 2000. Simulation of elbow and forearm motion in vitro using a load controlled testing apparatus. Journal of Biomechanics 33(5), 635–639.

17. McDonald CP, Peters TM, Johnson JA, King GJ. Stem abutment affects alignment of the humeral component in computer-assisted elbow arthroplasty. J Shoulder Elbow Surg. 2011 Sep;20(6):891-8.

18. Lalone, E.A., Peters, T.M., King, G.W., Johnson, J.A. Accuracy assessment of an imaging technique to examine ulnohumeral joint congruency during elbow flexion. Computer Aided Surgery 2012;17, 142–152.

19. Lalone EA, Giles JW, Alolabi B, Peters TM, Johnson JA, King GJ. Utility of an image-based technique to detect changes in joint congruency following simulated joint injury and repair: an in vitro study of the elbow. J Biomech. 2013a Feb 22;46(4):677-82.

20. Cruess RL, Kwok DC, Duc PN, Lecavalier MA, Dang GT. The response of articular cartilage to weight-bearing against metal. A study of hemiarthroplasty of the hip in the dog. J.Bone Joint Surg.Br. 1984;66:592-7

21. Dalldorf PG, Banas MP, Hicks DG, Pellegrini VD. Rate of degeneration of human acetabular cartilage after hemiarthroplasty. J Bone Joint Surg Am. 1995;77:877-882.

22. McCann L, Ingham E, Jin Z, Fisher J. An investigation of the effect of conformity of knee hemiarthroplasty designs on contact stress, friction and degeneration of articular cartilage: a tribological study. J.Biomech. 2009;42:1326-31

23. McGibbon CA, Krebs DE, Trahan CA, Trippel SB, Mann RW. Cartilage degeneration in relation to repetitive pressure: case study of a unilateral hip hemiarthroplasty patient. J.Arthroplasty 1999;14:52-8.

24. Moon KH, Kang JS, Lee TJ, Lee SH, Choi SW, Won MH. Degeneration of acetabular articular cartilage to bipolar hemiarthroplasty. Yonsei Med.J. 2008;49:719-24

25. Desai SJ, Deluce, S., Johnson JA, Ferreira LM, Leclerc AE, Athwal GS and King JW. An anthropometric study of the distal humerus. J Shoulder Elbow Surg. 2014 Feb;23, 463-469

26. Eckstein F, Lohe F, Schulte E, Miiller-Gerbl M, Milz S, and Peutz R. Physiological incongruity of the humero-ulnar joint: a functional principle of optimized stress distribution acting upon articulating surfaces? Anat Embryol. 1993;188:449M55

27. Eckstein F, Lohe F, Muller-Gerbl M, Steinlechner M, Putz R. 1994. Stress distribution in the trochlear notch. A model of bicentric load transmission through joints. J Bone Joint Surg Br. 76(4):647–653.

28. Goodfellow JW, and Bullough PG. The pattern of aging of the articular cartilage of the elbowjoint. J. Bone Joint Surg. 1967;49B: 174-181.

29. Walker PS. Human joints and their artificial replacements. Springfeld 1977.

Chapter 5

General Discussion, Conclusions and Future Work

Overview

This chapter will review the objectives and hypotheses that were established in Chapter 1. Chapters 2 through 4 will be reviewed in detail, and key findings will be summarized. Future directions for this research will be explored.

.

5.1 Summary of Objectives

Distal humeral hemiarthroplasty is a potential treatment option for elbow pathology that only affects one portion of the elbow joint, including distal humerus fractures, non-unions and avascular necrosis. Currently, there is a lack of literature examining the effect of distal humeral hemiarthroplasty on elbow joint kinematics and congruency. Furthermore, the morphology of the distal humerus has not been well characterized and as such current implant designs may not be optimal.

The objectives of this thesis were:

1. To quantify the osseous anatomy of the distal humerus and define anatomic variability using three-dimensional (3D) imaging techniques;
2. To determine the influence of distal humeral hemiarthroplasty and implant size on joint kinematics and stability *in-vitro*;
3. To determine the influence of distal humeral hemiarthroplasty on joint congruency *in-vitro*.

Correspondingly, the hypotheses were:

1. The morphology of the distal humerus would be consistent in shape but vary in size between elbows. A family of distal humeral implant sizes could be developed to closely replicate the anatomical shape of the distal humerus.
2. An optimally sized distal humeral hemiarthroplasty will best recreate the kinematics and stability of the elbow.
3. Distal humeral hemiarthroplasty with an optimally sized hemiarthroplasty will demonstrate the greatest joint congruency.

5.2 An Anthropometric Study of the Distal Humerus (Chapter 2)

This study set out to quantify the osseous anatomy of the distal humerus and define anatomic variability using 3D imaging techniques. The optimal shape of hemiarthroplasty implants has not been established due to a paucity of data quantifying the morphology of the normal distal humerus (1,2). Anthropometric information is available for the shoulder (3-6). This data played an important role in current designs of shoulder hemiarthroplasty implants. We set out to obtain accurate anthropometric data in order to work towards the creation of a more anatomically shaped distal humeral implant.

Using Visualization ToolKit (VTK) software program, transverse cross sections of the articular surface were automatically segmented at 0.1 mm increments, and then circle-fitted using a least-squares method. A best-fit line through these centers of all the cross sections was generated as per method of Shiba et al. (1), who defined this as the C-Line. The anatomic flexion-extension (FE) axis of the distal humerus was 0.85 ± 0.70 degrees from the C-Line (range 0.07-3.17 degrees) in the coronal plane and 1.57 ± 1.45 degrees (range 0.04-7.47 degrees) in the axial plane. The C-Line was defined using the FE axis as an initial reference direction vector. The difference found between the anatomic FE axis and the C-Line has implications for implant design, as the measurements determined are based off of the C-Line and not the anatomic axis. We have established a data bank of humeral dimensions may be used for the development of future distal humeral hemiarthroplasty implants. With this database, creation of a more anatomic implant should be completed. Because of the difference between the C-Line and the FE axis, basing measurements off the FE-axis would result in non-anatomic

implant surfaces. A more anatomic implant would have to base all measurements off the C-Line to optimize kinematics and joint congruency.

The creation of a more anatomically shaped distal humeral implant is an important future direction based on this work. Further studies to characterize the cartilage thickness distribution are needed. The currently available commercial system used in this study has six different implant sizes (Small, Small plus, Medium, Medium plus, Large and Large plus). This study has demonstrated no morphological differences between men and women, only a difference in overall size between genders. We propose that seven implant sizes would be a reasonable number of options for a surgeon to choose from. We proposed the seven sizes based on the average of all the morphological data that was collected. With seven sizes, 96% of the cadaveric specimens used in this study fell within a 2mm range of the implant sizes. Additionally, the option of reverse engineering implants may also prove beneficial. This would involve obtaining a CT scan of the opposite (unaffected) elbow and engineering a mirrored implant. Patient specific implants would best reproduce native anatomy, and would likely optimize kinematics and joint congruency, however further studies are required to confirm this hypothesis.

5.3 The Effect of Implant Size on Kinematics and Stability

This study sought to determine the effects of distal humeral hemiarthroplasty and the importance of implant size on elbow joint mechanics using *in vitro* techniques. There is currently no literature examining the effects of hemiarthroplasty on elbow mechanics.

The present study demonstrates that distal humeral hemiarthroplasty alters elbow joint kinematics, regardless of the implant size with the arm in both the varus and valgus

positions. These changes could be secondary to errors in implant positioning and/or differences in the shape of the humeral implant relative to the native elbow. Navigation of distal humeral implants has been shown to increase accuracy (7); however, due to the subjective nature of the navigation there was still a possibility of inaccurate placement. The implant was navigated by matching the implant surface with the surface of the virtual distal humerus, not the native FE axis. Even if we had navigated the FE axis of the implant to precisely replicate the native FE axis, the humeral surface would not have been precisely matched. The kinematic effect of a precise match in FE axis but a mismatch in humeral surface is unknown**.** The optimally sized distal humeral implant employed in this study did not precisely match the shape of the native distal humerus, which may further explain the observed changes in joint kinematics.

These changes in joint tracking may cause abnormal articular contact and loading, which may result in pain and cartilage degeneration over time. This has been recently demonstrated by Hughes et al. (2013) who found radiologic evidence of ulnar wear in 50% of patients at an average of five years postoperatively. In addition, they found worse wear was associated with higher American Shoulder and Elbow Society (ASES) scores, lower patient satisfaction and lower EuroQoL Visual Analog Score of quality of life. These authors suggested that implant design was at least partially responsible (8).

5.4 The Effect of Hemiarthroplasty on Joint Congruency

This study sought to determine the effects of hemiarthroplasty and implant size on joint congruency *in vitro*. Joint congruency was determined by proximity mapping

techniques as a surrogate to joint contact, previously described and validated by Lalone et al. (2013) (9,10).

The present investigation demonstrated that distal humeral hemiarthroplasty using the optimal and oversized implants provide the greatest joint congruency, while the undersized implant demonstrated poorest joint congruency. This may be a result of the subtle kinematic differences between implant sizes, which may lead to altered contact stresses. Another likely contributing factor is that the implant shape does not precisely match the shape of the native distal humerus. Undersizing the implant had the largest effect on congruency compared to oversizing the implant. In the previous chapter it was demonstrated that the optimal and oversized implants best recreated native elbow kinematics. The undersized implant poorly recreated normal elbow kinematics, and demonstrated the greatest amount of instability. This increased instability and alterations in kinematics may also be responsible for the alterations found in elbow joint congruency.

This decreased congruency with the undersized implant may cause abnormal articular contact and loading, which may result in pain and accelerated cartilage degeneration over time. Hughes et al. (2013) have demonstrated radiologic evidence of ulnar sided wear in 50% of patients they studied and correlated wear with poor clinical outcomes (8). This study highlights that abnormal congruency can not only cause radiographic deterioration but also poorer clinical outcomes. This suggests that implants which optimize joint congruency would presumably have lower radiographic wear and improved outcomes. Choosing implant sizes intra-operatively, therefore, is an important factor in radiographic and clinical outcomes. Intra-operatively, if the surgeon is deciding

between two sizes, choosing the larger of the two implants will maximize joint congruency and potentially decrease radiographic wear and improve clinical outcomes.

5.5 Conclusion

The results from this work will contribute to the knowledge of distal humeral morphology and the effects of elbow hemiarthroplasty on elbow kinematics and joint congruency. Distal humeral morphology has been accurately defined, which should contribute to the production of more anatomic implants in the future. Based on the results of this *in vitro* study, improvements in the articular shape of distal humeral implants are needed to optimize the outcomes of this procedure. When evaluating the effect of hemiarthroplasty size on joint kinematics and congruency, the undersized implant consistently had the greatest alterations in joint kinematics and the lowest joint congruency when compared to the optimal and oversized implants. This would suggest that intra-operatively, if uncertainty exists in selection of implant size, the larger implant should be used. The oversized implant best recreates normal elbow kinematics, and has comparable joint congruency to the optimal implant.

In summary, this treatise has accurately defined distal humeral morphology and may be used in the development of a more anatomically correct implant in the future. Evaluation of the effects of this implant on kinematics and joint congruency using similar methodology in the present thesis would be beneficial prior to the clinical application of this new design.

5.6 References

1. Shiba R, Sorbie C, Siu DW, Bryant JT, Cooke TDV and Wevers HW. Geometry of the Humeroulnar Joint. J of Orthop Res 1988; 6(6): 897-906

2. Wevers HW, Broekhoven LH, Sorbie C. Resurfacing elbow prosthesis: shape and sizing of the humeral component. J Biomed Eng 1985;7: 241-6.

3. Boileau P, Walch G. The three-dimensional geometry of the proximal humerus. Implications for surgical technique and prosthetic design. J Bone Joint Surg Br 1997;79:857-65

4. Hertel R, Knothe U, Ballmer FT. Geometry of the proximal humerus and implications for prosthetic design. J Shoulder Elbow Surg 2002;11:331-8

5. Pearl ML, Volk AG. Coronal plane geometry of the proximal humerus relevant to prosthetic arthroplasty. J Shoulder Elbow Sur 1996 Jul-Aug;5(4):320-6

6. Robertson DD, Yuan J, Bigliani LU, Flatow EL, Yamaguchi K. Three-dimensional analysis of the proximal part of the humerus: relevance to arthroplasty. J Bone Joint Surg Am 2000;82: 1594-602

7. McDonald CP, Peters TM, Johnson JA, King GJ. Stem abutment affects alignment of the humeral component in computer-assisted elbow arthroplasty. J Shoulder Elbow Surg. 2011 Sep;20(6):891-8

8. Smith GC, Hughes JS. Unreconstructable acute distal humeral fractures and their sequelae treated with distal humeral hemiarthroplasty: a two-year to eleven-year follow-up. J Shoulder Elbow Surg. 2013;22(12):1710-23.

9. Lalone, EA, McDonald, CP, Ferreira, LM, Peters, TM, King, GW & Johnson, JA Development of an image-based technique to examine joint congruency at the elbow, Computer Methods in Biomechanics and Biomedical Engineering, 2013b;16:3, 280-290

10. Lalone, E.A., Peters, T.M., King, G.W., Johnson, J.A. Accuracy assessment of an imaging technique to examine ulnohumeral joint congruency during elbow flexion. Computer Aided Surgery 2012;17, 142–152.

Appendix A: Glossary of Terms

This appendix contains definitions of medical terms used in this thesis. This is meant to provide assistance to the reader who may be unfamiliar with this terminology.

Anatomic variability	Inherent differences in size and shape between the anatomy of humans
Annular ligament	A ligament which encircles the head of the radius ensuring contact between the radius and PRUJ
Anthropometric	Measurement of the human individual
Arthritis	A disorder affecting the joints that can have a variety of causes including inflammation, degeneration, or trauma
Arthroplasty	Surgical reconstruction or replacement of a joint
Articular	Relating to a joint
Aseptic loosening	Loosening of a prosthesis that is not related to infectious causes
Avascular necrosis	Condition in which subchondral bone dies due to an insult to the vascular supply. This leads to loss of mechanical integrity and can lead to collapse and loss of joint congruence
Cadaveric	Part derived from a dead body preserved for research purposes

Capitellum	Smooth rounded surface on the lateral distal humerus which articulates with the radial dish
Capsuloligamentous	Refering to structures around a joint including the joint capsule and ligaments
Cartilage	Smooth, firm connective tissue found on articulating surfaces of joints
Comminuted	Several small fragments
Contact Area	Surface area in contact between two bones
Coronoid	Triangular anterior projection on the proximal ulna which articulates with the radius
CT	Computed tomography, method of x-ray imaging which produces cross section images of the body
Digitization	Acquiring three-dimension location of points relative to an object
Distal	Away from the center of the body
Distal humeral hemiarthroplasty	Prosthetic implant replacing the distal humerus
DRUJ	Distal radioulnar joint, pivot-joint between the distal radius and ulna
Epicondylar Axis	Axis formed between medial and lateral epicondyles of the elbow
Extension	Movement in which two ends of a joint move away from each other
External Rotation	Rotation away from the body

Flexion	Bending movement that decreases angle between two parts
Flexion-extension axis	In elbow, defined as a line between geometric centres of the capitellum and trochlea
Greater Sigmoid Notch	Depression in the ulna formed by the olecranon and the coronoid process. Point of articulation for the trochlea of the humerus
Hemiarthroplasty	Replacement of one surface of a joint with a prosthetic implant
Hemophilia	Bleeding disorder which can cause recurrent bleeds into articular joints and potentially irreversible damage to articular cartilage
Humerus	Bone of the upper arm forming the shoulder and elbow
Internal Rotation	Rotation towards the body
Intramedullary Canal	Marrow cavity of a bone
Kinematics	Study of motion of one part with respect to another
Landmark	Reliably identified feature
Lateral	Away from the middle of the body
Laxity	Looseness
Lesser Sigmoid Notch	Depression on lateral side of coronoid process, allows for articulation with proximal radius
Ligament	Fibrous connective tissue between two bones

LUCL	Lateral ulnar collateral ligament; extends from lateral epicondyle to the coronoid and serves as an important posterolateral rotational stabilizer
Medial	Towards the middle of the body
MCL	Medial collateral ligament; extends from medial epicondyle of humerus to the coronoid providing primary valgus restraint
Morphology	Study of size, shape and structure
Navigation	Use of a tracking system and computer guidance to perform procedures with the goal of increasing accuracy in placement of prosthetic implants
Non-union	Absence of complete healing across a fracture site
ORIF	Open reduction and internal fixation; method for surgically repairing fracure bone using plates and/or screws
Osseous	Relating to bone
Osteology	The scientific study of bones
Posterior	Towards the back of the body
Pronation	Rotation towards the midline
Proximal	Towards the center of the body
Proximal radioulnar joint	Articulation between the proximal aspect of the radius and ulna
Radius	The lateral bone of the forearm articulating with the ulna, humerus and carpal bones

Radiocapitellar joint	Articulation between the radius and the capitellum
Rheumatoid Arthritis	Autoimmune disease that results in chronic systemic inflammation.
RCL	Radial collateral ligament; originates on the lateral epicondyle and inserts into the annular ligament serving as a primary varus stabilizer of the elbow
Stylus	Penlike device used to obtain digitizations
Supination	Rotation away from the midline
Total Elbow Arthroplasty	Prosthesis which replaces the entire elbow joint – distal humerus and proximal ulna (in some designs, radial head is also replaced)
Trochlea	Medial portion of articulating surface of the distal humerus which articulates with the trochlear notch of the ulna
Ulna	The medial bone of the forearm articulating with the radius, humerus, and carpal bones
Ulnohumeral joint	Articulation between the ulna and humerus
Valgus	Displacement of the distal aspect of the bone away from the midline of the body
Varus	Displacement of the distal aspect of the bone towards the midline of the body

Appendix B: Abbreviations List

This appendix contains a list of all abbreviations used throughout this thesis.

3D	Three-dimensional
AL	Alex Leclerc
CAD	Computer-aided design
CD	Capitellar depth
CH	Capitellar height
CT	Computed Tomography
CW	Capitellar width
F-E Axis	Flexion-extension axis
GE	General Electric
HU	Hounsfield Units
Inc	Incorporated
LTD	Lateral trochlear depth
LTH	Lateral trochlear height
LUCL	Lateral ulnar collateral ligament
MCL	Medial collateral ligament
MTD	Medial trochlear depth
MTH	Medial trochlear height

NDI	Northern Digital Inc.
ON	Ontario
pMCL	Posterior band of the medial collateral ligament
SJD	Sagar J. Desai
TEA	Total elbow arthroplasty
TD	Trochlear groove depth
TH	Trochlear height
TW	Trochlear width
TWP	Trochlear width proper
TX	Texas
W	Articular width
USA	United States of America
VTK	Visualization ToolKit
WA	Washington
WI	Wisconsin

Appendix C: Detailed List of Morphologic Measurements

This appendix provides a detailed list of morphologic measurements. Chapter 2 reported on means and standard deviations, but not an inclusive list of all measurements. Each specimen examined has been reported (Specimen defined by Numbers 1-50). Definitions for abbreviations used can be found in Appendix B.

Number	Age	Gender	CW	CH	TW	TWP	LTH
1	48	M	17.7	25.3	27.7	22.7	24.5
2	47	F	17.5	22.4	24.5	20.6	23.5
3	53	M	21.1	26.1	29.6	21.7	24.5
4	76	F	15.6	20.3	22.6	19.1	18.7
5	69	F	15.8	20.5	22.1	18.5	17.4
6	87	F	13.8	19.6	21.5	18.0	18.1
7	77	M	18.2	27.0	28.3	24.0	23.1
8	46	F	14.4	20.2	22.3	18.1	19.3
9	64	F	15.9	21.8	22.5	20.5	19.4
10	93	M	19.8	27.2	33.8	27.4	24.3
11	86	M	17.0	24.9	28.5	23.4	21.7
12	67	F	16.2	22.1	20.5	15.8	21.0
13	61	F	15.9	22.4	23.1	19.5	19.6
14	82	M	15.7	23.3	26.7	22.7	21.6
15	60	M	18.4	25.1	30.0	23.7	25.2
16	60	M	16.6	23.0	27.9	22.7	23.0
17	76	M	17.9	24.6	30.5	23.7	25.0
18	49	M	15.9	21.7	22.3	17.5	21.3
19	72	M	17.3	23.8	28.1	22.2	24.1
20	76	M	17.8	25.6	22.3	18.7	20.7
21	82	M	18.0	24.4	28.2	23.8	23.5
22	82	F	15.0	18.2	19.6	17.1	17.1
23	61	F	15.3	20.1	20.9	17.2	19.6
24	88	F	15.3	21.2	21.5	18.8	19.4
25	59	M	17.2	23.6	23.0	17.2	20.6
26	83	F	15.4	19.3	21.9	18.1	17.2
27	65	M	18.0	25.6	25.8	23.1	21.8
28	66	F	15.7	23.3	25.9	22.1	21.3
29	97	F	12.1	20.8	21.1	16.4	20.3
30	82	M	18.8	24.2	25.0	22.1	21.0
31	57	F	14.2	22.4	21.5	17.6	21.0
32	90	F	16.1	20.5	22.2	19.2	18.2
33	73	M	17.8	22.0	23.3	18.3	21.6
34	81	M	17.4	23.6	27.5	23.4	21.6
35	69	M	18.5	23.2	26.7	21.7	19.7
36	82	M	16.6	22.9	23.4	18.7	23.9
37	80	M	21.1	25.1	26.4	25.9	21.3
38	64	M	19.6	25.9	25.3	21.0	24.8
39	81	M	19.4	27.6	25.5	21.8	24.3
40	73	M	20.7	26.8	27.4	22.1	22.4
41	75	M	16.9	22.0	26.0	21.4	23.6
42	79	M	18.1	27.1	29.8	22.9	22.4
43	75	M	16.7	23.7	27.1	22.6	20.9
44	84	M	17.7	24.1	28.1	22.9	24.0
45	77	M	17.7	20.4	27.2	21.3	20.0
46	78	M	17.6	24.3	25.4	22.4	22.1
47	62	M	17.4	22.1	28.2	23.0	21.9
48	59	M	20.2	26.0	28.3	23.3	24.5
49	78	M	19.4	23.6	24.0	21.2	20.8
50	84	M	17.4	25.1	27.0	21.5	24.0

TH	MTH	lst	mst	mit	lit	alt
18.3	37.3	23.8	42.9	26.1	15.5	14.7
18.2	28.1	17.9	23.8	21.1	15.5	14.5
22.3	34.3	7.0	21.1	21.1	10.0	3.8
15.2	26.3	11.7	24.6	22.7	15.2	10.5
14.8	25.9	7.7	22.7	28.5	12.6	8.4
14.1	24.1	16.8	22.5	24.1	15.5	13.3
19.2	32.3	11.1	24.8	24.7	11.4	14.5
14.9	25.3	14.7	26.7	23.6	18.5	16.9
15.9	25.2	11.0	21.6	22.1	14.9	9.0
20.8	43.6	11.6	43.9	19.2	13.2	15.6
17.9	30.6	11.2	25.5	22.7	13.0	13.9
19.1	27.3	16.7	15.8	24.1	14.0	8.7
16.3	29.5	18.2	27.1	24.4	14.2	7.7
17.3	30.7	10.8	31.0	23.5	14.2	12.3
21.6	31.1	17.5	15.6	16.9	12.8	13.7
19.5	30.7	14.2	21.4	24.1	15.1	10.5
19.2	31.1	13.6	25.0	23.2	21.8	18.2
19.0	27.0	4.7	22.0	24.3	17.9	15.5
19.0	33.8	16.7	33.3	23.8	17.0	13.7
18.1	31.1	7.9	28.9	30.9	11.7	11.5
20.7	30.6	10.1	17.9	20.3	13.9	6.6
13.4	24.0	19.2	21.5	23.8	16.1	7.4
15.0	23.9	14.0	25.1	23.6	22.0	17.0
17.7	23.7	6.8	16.8	18.4	7.0	5.7
16.1	29.0	15.6	25.8	25.6	16.8	14.6
16.4	25.9	3.3	39.5	19.3	10.5	5.6
17.4	28.8	12.5	25.9	24.4	14.2	12.6
16.1	28.9	17.3	25.9	24.1	19.6	11.6
15.8	24.1	23.5	22.7	23.4	18.0	18.6
18.6	30.2	11.4	22.7	22.6	12.2	7.6
18.8	26.8	12.2	16.6	23.3	11.3	8.1
17.1	36.0	11.7	44.2	18.4	7.0	5.4
18.8	29.3	16.1	18.4	24.1	8.5	8.2
18.6	31.5	9.4	28.7	21.6	10.2	7.3
17.5	42.4	16.9	43.6	26.4	8.3	7.7
17.3	27.3	18.4	22.5	25.0	19.6	13.3
14.8	30.8	14.2	29.0	26.0	22.3	14.0
18.4	32.3	15.1	30.8	29.3	20.8	12.7
19.1	30.8	19.3	23.2	21.0	15.3	11.8
18.0	32.4	16.3	25.1	26.8	14.2	15.8
19.8	28.1	9.4	23.6	19.4	15.1	9.3
19.3	34.1	8.6	25.1	23.0	12.1	11.8
17.1	27.6	13.5	19.7	21.4	13.4	14.3
19.6	31.4	14.1	25.7	21.3	14.1	11.9
16.8	27.8	10.7	23.1	26.7	9.6	7.6
18.0	29.4	13.8	28.6	21.0	17.2	13.4
16.1	31.1	19.8	28.8	26.2	18.8	18.3
18.8	31.7	16.8	24.4	22.5	19.8	15.3
18.2	28.3	9.6	20.2	21.4	10.2	4.9
21.2	30.7	8.5	18.5	21.2	11.0	12.4

plt	amt	pmt	CD	LTD	TD	MTD
	34.9	31.2	30.5	9.1	24.6	18.3	37.3
	18.7	23.0	20.1	9.2	23.7	18.2	28.4
	12.5	18.3	23.3	11.4	25.3	22.3	34.4
	14.3	25.5	26.9	7.4	18.7	15.2	26.5
	12.6	25.7	28.5	7.6	17.7	14.8	26.1
	19.3	22.0	24.6	6.9	18.2	14.1	24.1
	11.3	20.6	28.1	9.6	23.2	19.2	32.4
	16.6	24.6	27.7	7.5	19.3	14.9	25.3
	15.3	21.4	23.5	7.8	19.5	15.9	25.2
	9.5	26.3	34.9	10.5	25.0	20.8	43.6
	13.5	19.1	24.8	9.2	21.9	17.8	30.6
	16.4	20.8	21.4	9.7	21.4	18.7	27.3
	23.6	18.3	31.4	9.0	19.9	16.3	29.6
	13.8	23.8	29.5	8.7	21.7	17.2	30.9
	17.0	17.0	15.2	10.8	25.5	21.6	31.1
	15.6	21.6	17.6	9.7	23.0	19.5	31.0
	30.9	18.2	19.7	9.8	25.5	19.1	31.1
	14.3	21.7	17.0	9.1	22.1	18.7	27.0
	25.7	26.6	25.9	9.4	24.2	18.9	33.8
	10.2	27.6	27.0	9.4	20.9	17.9	31.2
	14.4	23.1	17.7	9.9	24.0	20.7	30.6
	32.4	24.2	24.4	7.1	17.4	13.4	24.1
	27.3	25.3	21.0	7.3	19.6	15.0	24.2
	8.1	21.3	11.9	8.4	19.7	17.8	23.8
	24.5	22.6	28.5	8.9	21.8	16.1	29.5
	4.9	20.5	32.0	8.2	17.5	16.4	26.3
	18.2	25.9	20.6	8.4	22.1	17.4	28.8
	22.8	24.1	27.9	8.5	21.3	16.0	28.9
	24.5	22.8	22.7	8.1	20.3	15.7	24.1
	12.2	23.6	22.1	9.3	21.1	18.5	30.2
	11.8	24.2	17.7	9.1	21.4	18.8	27.1
	6.4	22.3	42.6	8.9	18.4	17.2	36.0
	19.9	26.2	19.5	9.5	22.1	18.9	29.9
	19.5	21.9	23.7	9.4	21.7	18.6	31.5
	18.1	26.5	42.7	8.7	19.9	17.5	42.4
	27.9	24.6	23.7	8.5	24.3	17.2	28.1
	20.0	24.2	30.4	7.6	21.3	14.8	30.8
	27.6	28.8	27.2	9.4	25.4	18.4	32.3
	28.3	22.2	22.5	9.8	25.1	19.1	30.9
	31.8	26.3	21.6	8.6	23.2	17.7	32.7
	12.4	17.0	26.0	10.0	23.7	19.9	28.3
	9.9	21.0	27.2	10.5	22.4	19.2	34.7
	14.6	20.7	17.9	8.4	21.0	17.1	27.6
	15.2	19.8	25.2	10.0	24.1	19.6	31.4
	16.8	21.5	27.9	8.7	21.5	16.8	28.0
	20.1	21.1	22.1	9.0	22.5	18.0	29.4
	23.2	21.0	29.4	8.5	22.1	16.1	31.1
	21.6	24.0	24.3	9.4	24.5	18.7	31.8
	14.2	22.5	19.1	9.1	20.9	18.3	28.3
	14.1	19.0	17.9	10.6	24.4	21.2	30.8

it	W		CW/CH	TW/CW	MTH/LTH	W/TH	TW/TH	TWP/TH
	90.0	45.4	0.7	1.5	2.0	2.5	1.51	1.24
	93.5	42.0	0.8	1.3	1.5	2.3	1.35	1.13
	89.1	50.7	0.8	1.3	1.5	2.3	1.32	0.97
	91.7	38.1	0.8	1.5	1.7	2.5	1.48	1.25
	86.5	37.8	0.8	1.5	1.7	2.6	1.49	1.25
	90.0	35.3	0.7	1.5	1.7	2.5	1.52	1.27
	88.3	46.6	0.7	1.5	1.7	2.4	1.47	1.25
	89.1	36.7	0.7	1.5	1.7	2.5	1.50	1.22
	90.9	38.3	0.7	1.4	1.6	2.4	1.41	1.29
	90.0	53.6	0.7	1.6	2.1	2.6	1.62	1.31
	90.0	45.4	0.7	1.6	1.7	2.5	1.59	1.31
	90.0	36.6	0.7	1.1	1.4	1.9	1.07	0.83
	89.2	39.0	0.7	1.4	1.8	2.4	1.42	1.20
	92.4	42.4	0.7	1.5	1.8	2.5	1.54	1.31
	90.0	48.3	0.7	1.4	1.4	2.2	1.38	1.09
	95.3	44.5	0.7	1.4	1.6	2.3	1.43	1.16
	90.0	48.4	0.7	1.6	1.6	2.5	1.58	1.23
	90.0	38.2	0.7	1.2	1.4	2.0	1.18	0.92
	90.0	45.4	0.7	1.5	1.8	2.4	1.48	1.17
	94.9	40.1	0.7	1.2	1.7	2.2	1.23	1.03
	90.0	46.2	0.7	1.4	1.5	2.2	1.36	1.15
	92.5	34.5	0.8	1.5	1.8	2.6	1.46	1.28
	87.3	36.3	0.8	1.4	1.6	2.4	1.39	1.14
	89.1	36.8	0.7	1.2	1.3	2.1	1.21	1.06
	97.8	40.2	0.7	1.4	1.8	2.5	1.43	1.07
	86.7	37.3	0.8	1.3	1.6	2.3	1.34	1.10
	90.0	43.8	0.7	1.5	1.7	2.5	1.48	1.32
	90.0	41.6	0.7	1.6	1.8	2.6	1.61	1.37
	88.3	33.2	0.6	1.3	1.5	2.1	1.33	1.04
	89.1	43.8	0.8	1.3	1.6	2.4	1.34	1.19
	94.9	35.6	0.6	1.1	1.4	1.9	1.14	0.94
	90.0	38.3	0.8	1.3	2.1	2.2	1.30	1.12
	97.0	41.1	0.8	1.2	1.6	2.2	1.24	0.97
	90.8	44.9	0.7	1.5	1.7	2.4	1.48	1.25
	90.0	45.2	0.8	1.5	2.4	2.6	1.52	1.24
	95.2	40.0	0.7	1.4	1.6	2.3	1.36	1.08
	90.9	47.5	0.8	1.8	2.1	3.2	1.78	1.75
	90.0	44.8	0.8	1.4	1.8	2.4	1.37	1.14
	89.1	44.9	0.7	1.3	1.6	2.3	1.34	1.14
	88.3	48.1	0.8	1.5	1.8	2.7	1.52	1.23
	89.1	42.9	0.8	1.3	1.4	2.2	1.31	1.08
	96.2	47.9	0.7	1.5	1.8	2.5	1.55	1.19
	90.0	43.7	0.7	1.6	1.6	2.6	1.59	1.32
	90.0	45.8	0.7	1.4	1.6	2.3	1.44	1.17
	85.4	44.8	0.9	1.6	1.7	2.7	1.62	1.27
	90.0	43.0	0.7	1.4	1.6	2.4	1.41	1.24
	90.0	45.6	0.8	1.7	1.9	2.8	1.75	1.43
	89.1	48.6	0.8	1.5	1.7	2.6	1.51	1.24
	90.0	43.4	0.8	1.3	1.6	2.4	1.31	1.17
	88.3	44.3	0.7	1.3	1.5	2.1	1.27	1.02

APPENDIX D: Congruency Graphs

As discussed in Chapter 4, this appendix presents all congruency graphs for active and passive motion for the optimal, oversized and undersized implants. These figures compliment Figure 1 presented in Chapter 4.

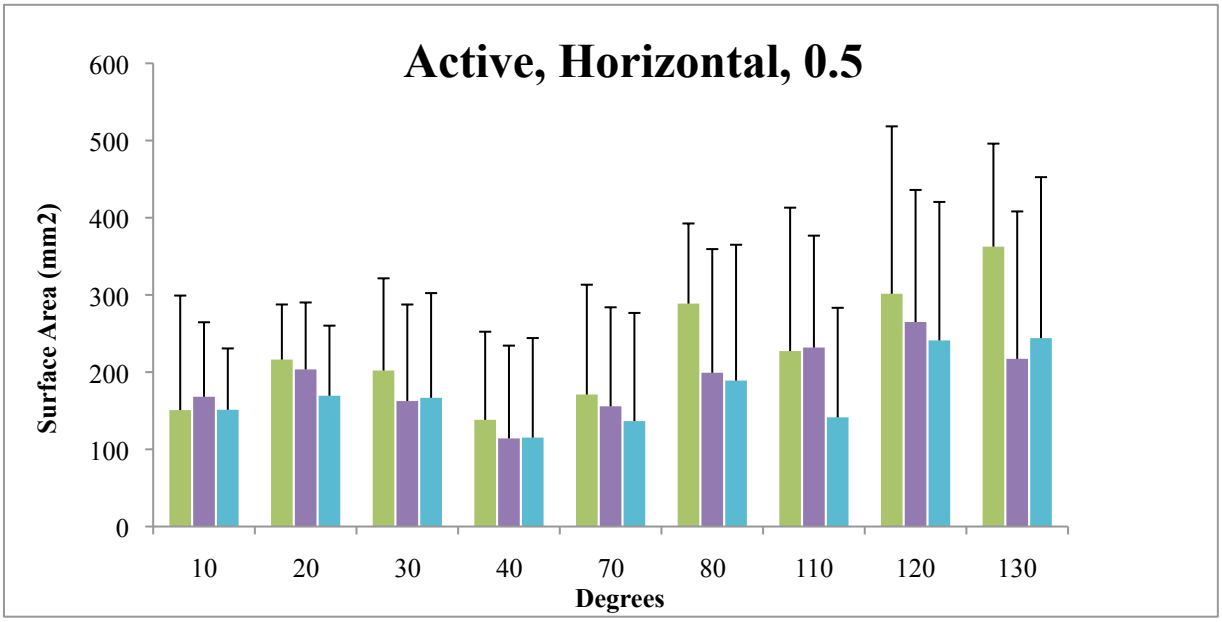
Active, Horizontal, 0.5
Surface Area (mm2)
600
500
400
300
200
100
0
10
20
30
40
70
80
110
120
130
Degrees

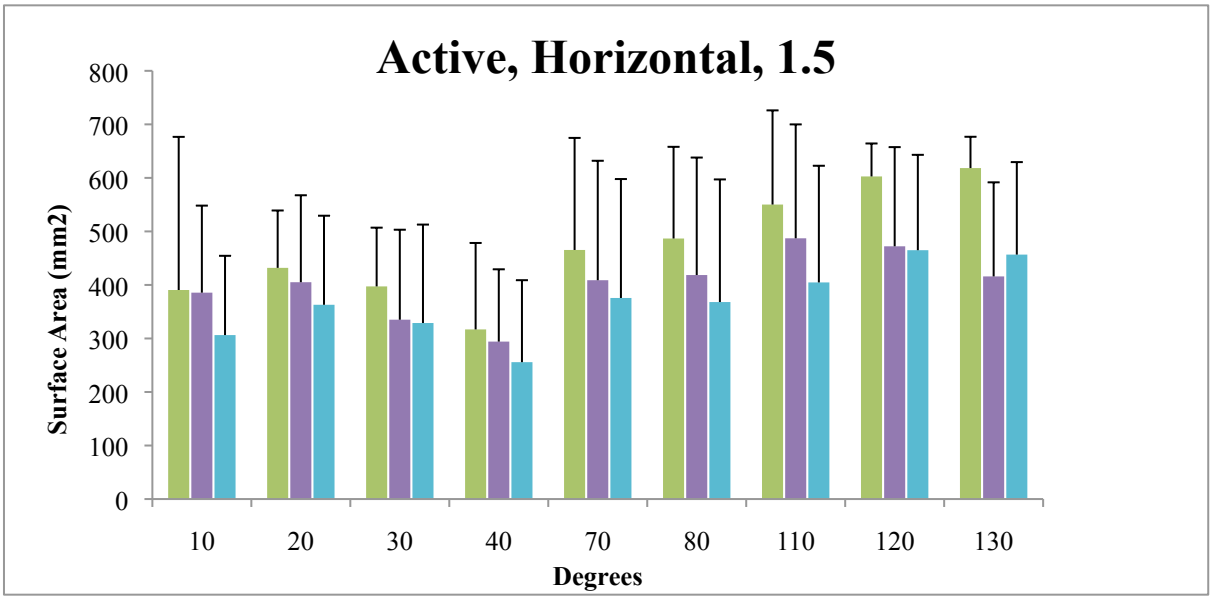
Active, Horizontal, 1.5
Surface Area (mm2)
800
700
600
500
400
300
200
100
0
10
20
30
40
70
80
110
120
130
Degrees

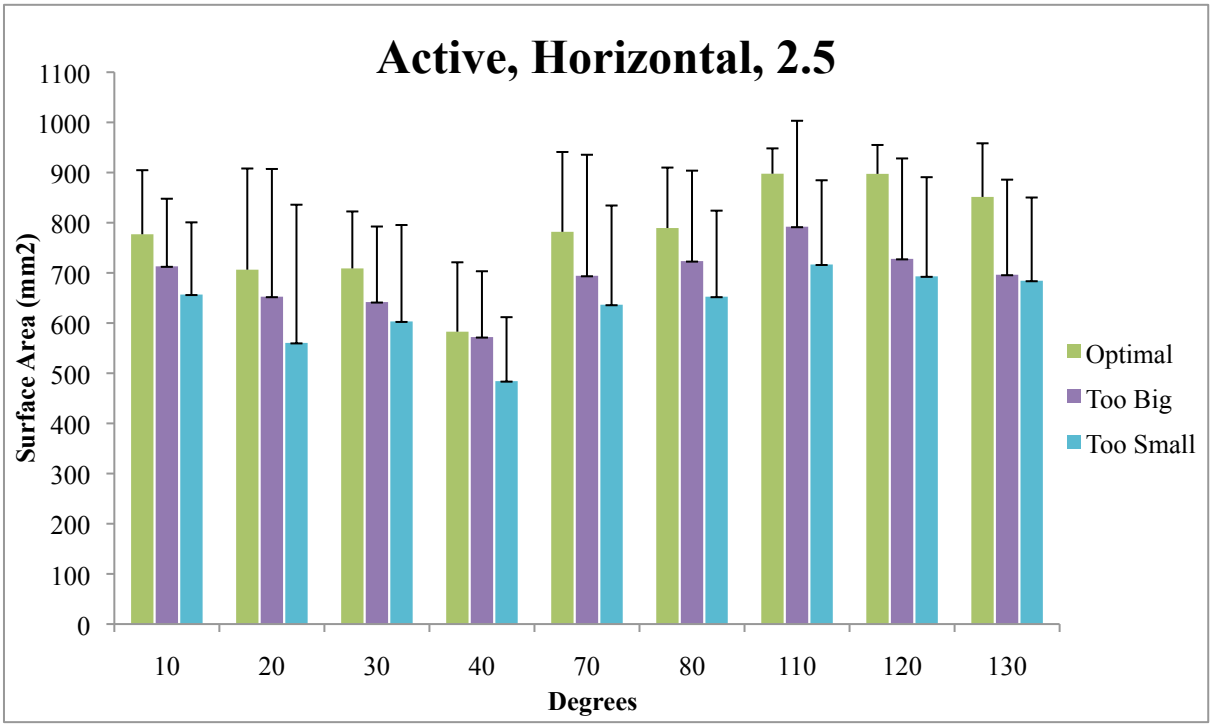
Active, Horizontal, 2.5
Surface Area (mm2)
1100
1000
900
800
700
600
500
400
300
200
100
0
10
20
30
40
70
80
110
120
130
Degrees
Optimal
Too Big
Too Small

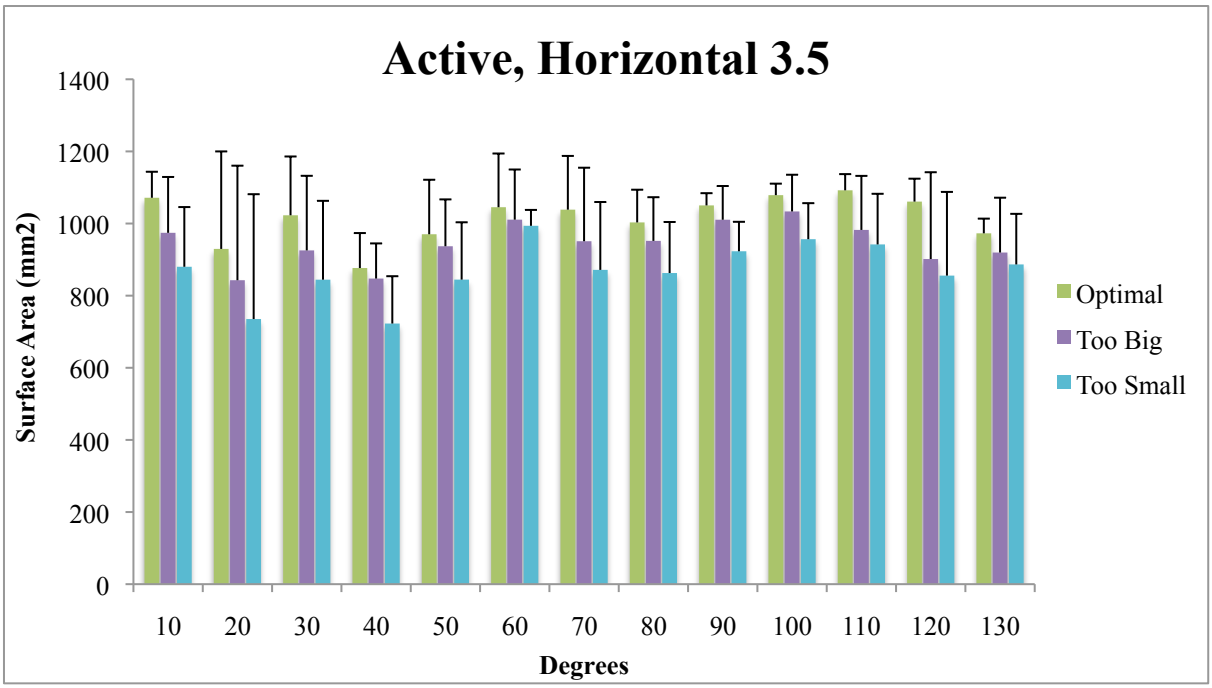
Active, Horizontal 3.5
Surface Area (mm2)
1400
1200
1000
800
600
400
200
0
10
20
30
40
50
60
70
80
90
100
110
120
130
Degrees
Optimal
Too Big
Too Small

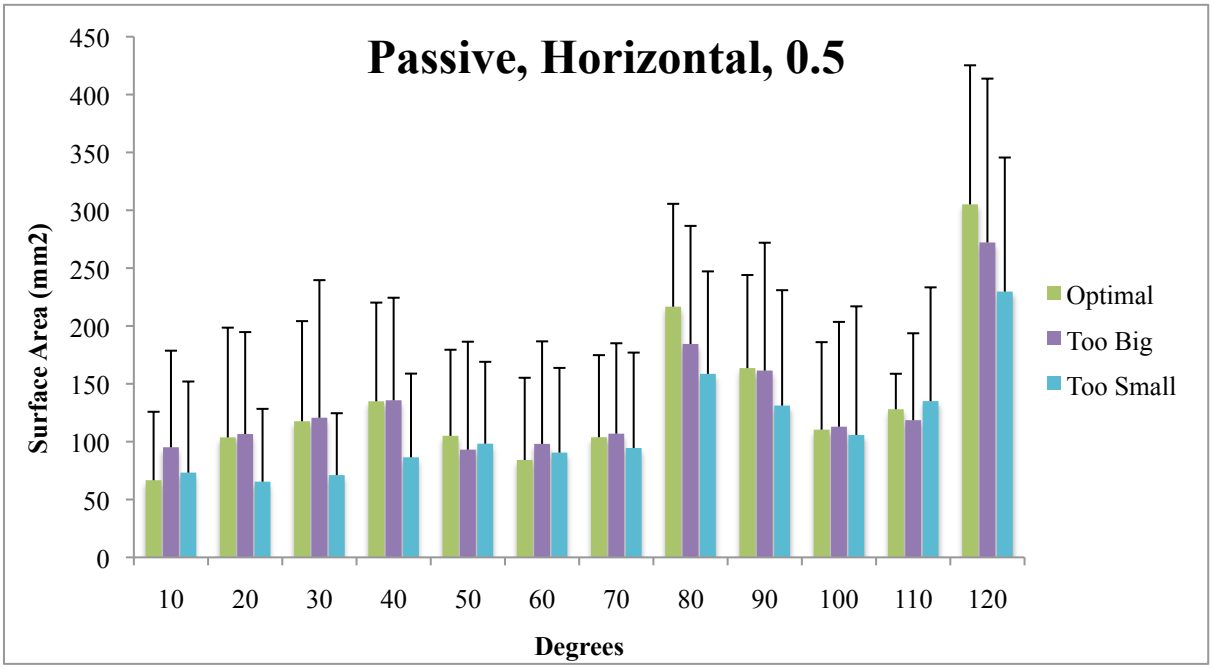
Passive, Horizontal, 0.5
Surface Area (mm2)
450
400
350
300
250
200
150
100
50
0
10
20
30
40
50
60
70
80
90
100
110
120
Degrees
Optimal
Too Big
Too Small

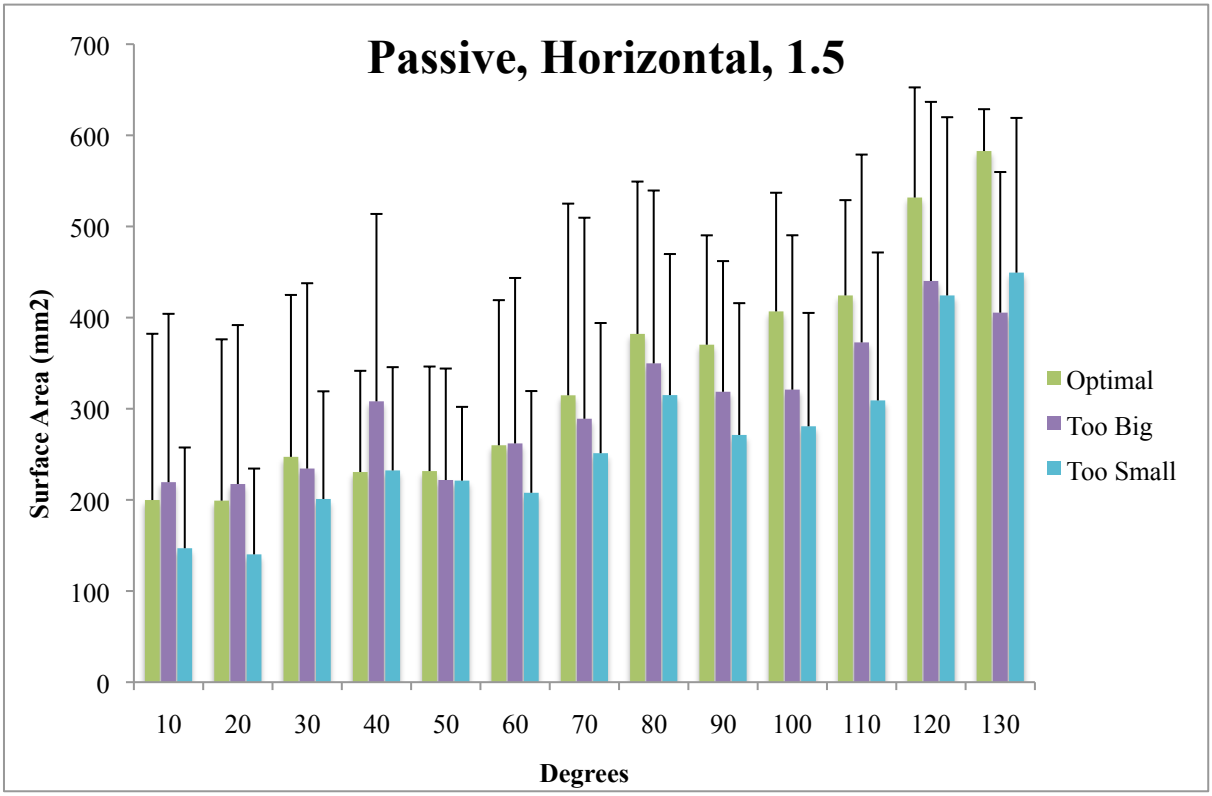
Passive, Horizontal, 1.5
Surface Area (mm2)
700
600
500
400
300
200
100
0
10
20
30
40
50
60
70
80
90
100
110
120
130
Degrees
Optimal
Too Big
Too Small

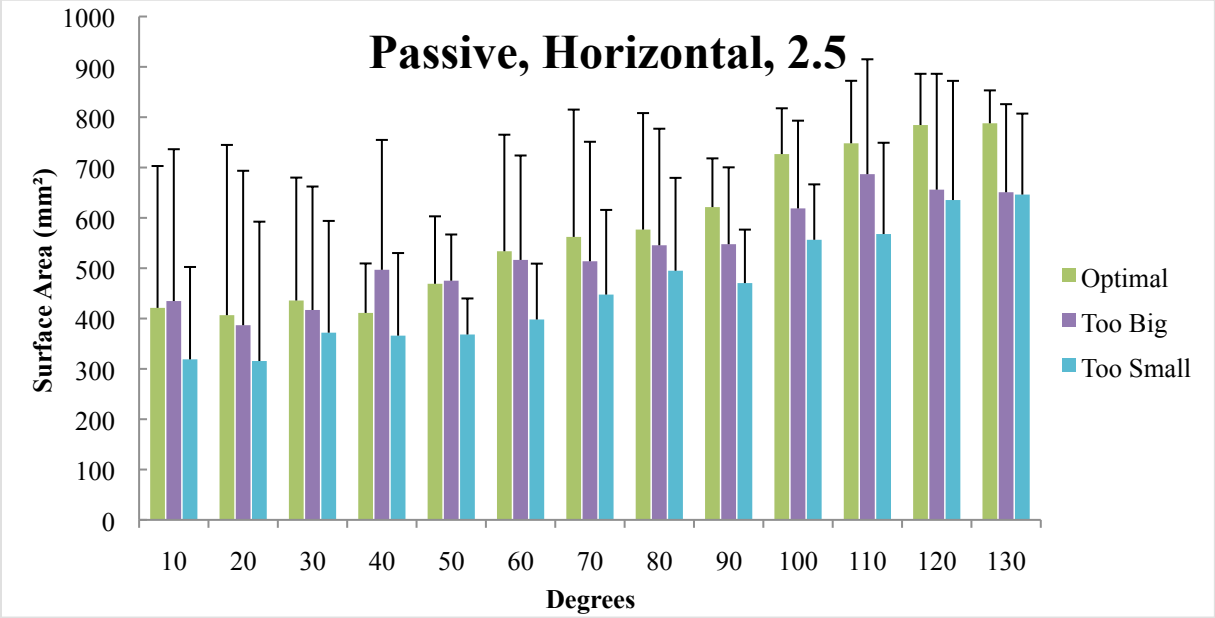
Passive, Horizontal, 2.5
Surface Area (mm²)
1000
900
800
700
600
500
400
300
200
100
0
10
20
30
40
50
60
70
80
90
100
110
120
130
Degrees
Optimal
Too Big
Too Small

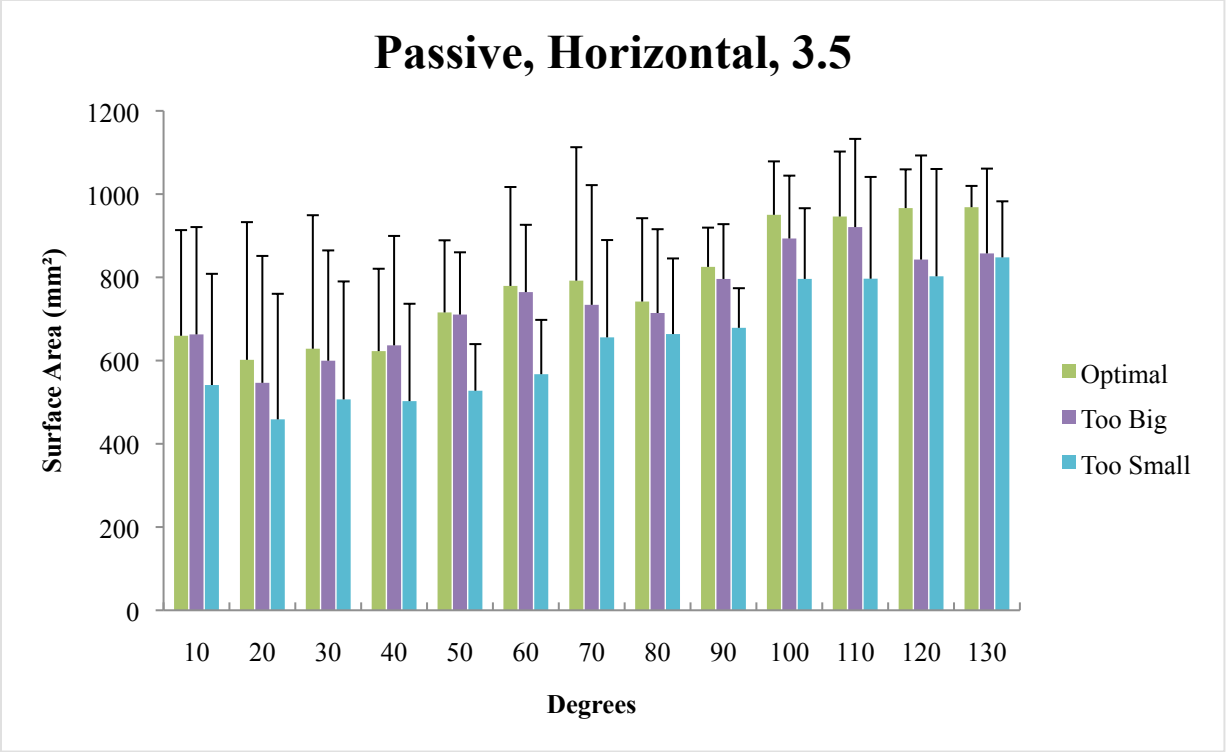
Passive, Horizontal, 3.5
Surface Area (mm²)
1200
1000
800
600
400
200
0
10
20
30
40
50
60
70
80
90
100
110
120
130
Degrees
Optimal
Too Big
Too Small

Appendix E: Copyright Permission

The work presented in Chapter 2 and Chapter 3 has been published in the Journal of Shoulder and Elbow Surgery, which an Elsevier publication. This appendix provides copyright permission information from the Elsevier website which outlines that authors may use their accepted manuscript or final published article for inclusion in a thesis or dissertation.

Excerpt from http://www.elsevier.com/journal-authors/author-rights-and-responsibilities#author-use

Author Rights

Elsevier supports the need for authors to share, disseminate and maximize the impact of their research. We take our responsibility as stewards of the online record seriously, and work to ensure our policies and procedures help to protect the integrity of scholarly works.

Author's rights to reuse and post their own articles published by Elsevier are defined by Elsevier's copyright policy. For our proprietary titles, the type of copyright agreement used depends on the author's choice of publication:

For subscription articles: These rights are determined by a copyright transfer, where authors retain scholarly rights to post and use their articles.

For open access articles: These rights are determined by an exclusive license agreement, which applies to all our open access content.

In both cases, the fundamental rights needed to publish and distribute an article remain the same and Elsevier authors will be able to use their articles for a wide range of scholarly purposes.

Details on how authors can reuse and post their own articles are provided below.

How authors can use their own journal articles

Authors can use their articles for a wide range of scholarly, non-commercial purposes as

outlined below. These rights apply for all Elsevier authors who publish their article as either a subscription article or an open access article.

We require that all Elsevier authors always include a full acknowledgement and, if appropriate, a link to the final published version hosted on Science Direct.

For open access articles these rights are separate from how readers can reuse your article as defined by the author's choice of Creative Commons user license options.

Authors can use either their accepted author manuscript or final published article for:	
	Use at a conference, meeting or for teaching purposes
	Internal training by their company
	Sharing individual articles with colleagues for their research use* (also known as 'scholarly sharing')
	Use in a subsequent compilation of the author's works
	Inclusion in a thesis or dissertation
	Reuse of portions or extracts from the article in other works
	Preparation of derivative works (other than for commercial purposes)

Curriculum Vitae

Sagar J. Desai

Department of Surgery, Division of Orthopedic Surgery

Schulich School of Medicine

Western University

London, Ontario, Canada

Education

2008-2013	**Fellow of the Royal College of Surgeons of Canada - Orthopaedic Surgery** University of Western Ontario (UWO), London, Ontario
2012-present	**Masters of Science - Medical Biophysics** University of Western Ontario (UWO), London, Ontario
2004-2008:	**Doctor of Medicine** University of Toronto Medical School, Toronto, Ontario
2000-2004:	**Honours Bachelor of Sciences in Kinesiology** University of Western Ontario (UWO), London, Ontario

Awards and Accomplishments

2014 **Alan C. Groom Seminar Award Nominee** – Top Medical Biophysics Presentation at Graduate Seminar

2012 **AOA-OREF Resident Leadership Award** – Top PGY 4 resident, elected by the UWO Orthopaedic Surgery Division.

2011 **W. H. Bailey Award** – UWO Orthopaedic Surgery resident who best exemplifies teaching and mentorship to fellow residents and students.

2011 **Resident/Fellow Research Travel Award** – For presentation of research at the 2011 Canadian Orthopaedic Association Annual Meeting.

2010 **Sandy Kirkley Clinical Research Award** – Top clinical research at UWO's Annual Research Day, October 13th, 2010.

2009 **Craig Boydell Award** - Excellence in sport, scholarship and community service. Has been presented to 7 members of the Western Mustangs Basketball program (since 1919).

2008 **Mary Cassidy Award** – Participation in extra-curricular activities during medical school.

2008 **Medical Society Honours Award** – For serving as Class President during medical school.

2008 **Gladwin-Ridings Memorial Scholarship** – 3rd year medical student who possesses good academic standing, practicality, modesty, sensitivity and reverence for human life.

2006 **Robert J. Ginsberg Research Award** – Top research project at the 2006 Canadian Association of Thoracic Surgeons Conference, Calgary, Alberta.

2006 **Canadian Medical Association (CMA) 2006 Leadership Innovation Award** – Development of Medical Fitness Initiative: *"Practice What You Preach" Promoting a Healthy and Active Lifestyle for medical students and residents.*

2006 **Comprehensive Research Experience for Medical Students (CREMS) Summer Scholarship** - *Video Assisted Thoracic Surgery Lobectomy – Closed-Chested Dissection Technique and Initial Results.*

2005 **Dr. Jean Hogarth Scholarship** – University of Toronto Medical School – Academic achievement and extra-curricular activities.

2005 **UWO Kinesiology 494: Sport and Community Service** – Fourth year Kinesiology course founder.

2004 **Team Captain** – 2003-2004 UWO Varsity Men's basketball team.

2004 **Honourable G. Howard Ferguson Award** – Top UWO graduating student combining athletics, academics, and contribution to college life.

2004 **Canadian Interuniversity Sport (CIS) Top 8 Academic All-Canadian** – Top 8 varsity athletes in Canada who best combine athletics, academics, and community service.

2004 **Kinesiology Student of Excellence Award** – Greatest overall contribution to UWO Kinesiology.

2004 **Ontario University Athletics (OUA) Ken Shields Award** – Top Ontario varsity basketball player combining athletics, academics and community service.

2004 **Henry Wu Memorial Scholarship** – Top UWO student combining extracurricular activities and academic achievement.

2004 **Scholar's Electives Scholarship** – Top UWO student combining extracurricular activities, leadership.

2004 **Dean's Honour List** – Academic achievement in Kinesiology Bachelor of Science program at the UWO (2001, 2002, 2003 and 2004).

2004 **Canadian Interuniversity Sport (CIS) Academic All-Canadian Roll** – Varsity athletics and 80% academic average (2001, 2002, 2003 and 2004).

2004 **Ontario University Athletics Academic Achievement Award** – OUA varsity athletics, 80% plus academic average in Honours program (2001, 2002, 2003 and 2004).

2004 **School of Kinesiology Honours Award** – 80% plus academic average in UWO Kinesiology Program (2001, 2002, 2003 and 2004).

2003 **Bronze "W" Award** – UWO varsity athlete who has exhibited commitment and dedication to the varsity athletics program.

2003 **Gordon Risk Award** – Top UWO student-athlete combining academic achievement and athletic leadership.

2003 **Bob Gage Award** – Top UWO student-athlete combining athletic leadership and academic achievement.

2001 **UWO School Letter** – UWO student combining academic and athletic commitment.

2000 **UWO Academic Entrance Scholarship** – High school academic average over 90%.

Committees and Extracurricular Activities

2013 2013 **Fellowship Committee Member** – U of T Orthopaedic Surgery Postgraduate Department

2012 **Chief Resident** – UWO Orthopaedic Surgery Program

2012 **Program Training Committee member** - UWO Orthopaedic Surgery Program (2009-2010, 2011-2012 and 2012-2013)

2012 **Admissions committee resident member** – UWO Orthopaedic Surgery Program (2009-2010, 2011-2012 and 2012-2013)

2012 **Editor – WesternOrtho Orientation Manual**

2012 **Medical Reconciliation Task Group** - London Health Science Centre (2011-2012)

2010 **Junior Chief Resident** – UWO Orthopaedic Surgery Program (2009-2010)

2008 **Editor** - Canadian Medical School Residency Guide

2008 **Curriculum Review Steering Committee** – committee reviewing Undergraduate Medical Program at the University of Toronto

2008 **Class President** - U of T Medical School Class of 2008

Research Grants

2011-2012 **Physicians' Services Incorporated Foundation (PSI) Research Grant** – $19,500/one year. For project "Hemi-Arthroplasty of the Elbow: The Effect of Implant Sizing on Joint Kinematics and Contact Mechanics" Supervisors: Graham King, George Athwal and James Johnson.

Publications, Presentations and Abstracts

Peer-reviewed Papers (6)

1) **Desai SJ**, Wood KS, Marsh J, Bryant D, Abdo H, Lawendy AR and Sanders DW. Factors Affecting Transfusion Requirement After Hip Fracture: Can We Reduce the Need for Blood? Can J Surg. 2014 Oct;57(5):342-8.
2) **Desai SJ**, Athwal GS, Ferreira LM, Lalone E, Johnson JA and King GJW. Distal Humerus Hemiarthroplasty: The Effect of Implant Sizing on Elbow Joint Kinematics. J Shoulder Elbow Surg. 2014 *In press*
3) **Desai SJ**, Deluce, S., Johnson JA, Ferreira LM, Leclerc AE, Athwal GS and King JW. An anthropometric study of the distal humerus. J Shoulder Elbow Surg. 2014 *In press*
4) **Desai SJ**, Patel J, Abdo H, Lawendy AR and Sanders DW. A Comparison of Surgical Delays in Directly Admitted vs. Transferred Patients with Hip Fractures: Opportunities for Improvement? Can J Surg. 2014 Feb;57(1):40-3.

5) **Desai SJ** and Daniels T. Calcaneal Fractures - Long-term Outcomes: What Can Patients Expect? COA Bulletin 2013. pg 42-33.
6) Leclerc AE, Deluce S, Ferreira L, **Desai SJ**, King GJ and Athwal GS. Measurements of the Ipsilateral Capitellum Can Reliably Predict the Diameter of the Radial Head. J Shoulder Elbow Surg. 2013 Dec;22(12):1724-8.

Published Abstracts (8)

1) **Desai SJ**, Deluce S, Johnson JA, Ferreira LM, Leclerc AE, Athwal GS and King GJ. An anthropometric study of the distal humerus. Proceedings COA 2013
2) **Desai SJ**, Patel J, Abdo H, Lawendy AR and Sanders DW. A Comparison of Surgical Delays in Directly Admitted vs Transferred Patients with Hip Fractures: Opportunities for Improvement? Proceedings COA 2013.
3) Preston S, **Desai SJ**, Somerville L, Angevine D, Sanders, DW, Howard JL. The Implications of Clopidogrel on the Management of Hip Fractures: An Institutional Review. Proceedings COA 2013.
4) **Desai SJ**, Athwal GS, Ferreira LM, Johnson JA, Welsh M, Lalone E and King GJW. Distal Humerus Hemiarthroplasty: The Effect of Implant Sizing on Elbow Joint Kinematics. Proceedings COA 2012.
5) Lerclerc A, **Desai SJ**, Deluce S, Ferreira LM, King GJW and Athwal GS. Measurements of the Ipsilateral Capitellum can Reliably Predict the Diameter of the Radial Head. Proceedings COA 2012.
6) **Desai SJ**, Sanders DW, Wood K and Bryant D. Wait times and transfusion requirements in hip fractures. J Bone Joint Surg Br 2012 vol. 94-B no. SUPP XXXVIII 130
7) **Desai SJ**, Sanders DW, Ferriera L and Giles J. The Mechanical Effect of Locking and Blocking Screws in Distal Femur Fractures. J Bone Joint Surg Br 2011 vol. 93-B no. SUPP IV 582
8) **Desai SJ**, Sanders DW, Ferriera L and Giles J. The Mechanical Effect of Locking and Blocking Screws in Distal Femur Fractures. Proceedings OTA 2010.

Book Chapters (1)

1) **Desai, SJ,** Gerth, S. & Yathindra, Y. "Orthopaedic Surgery." Toronto Notes 2008 Edition. Somogyi R and Colman R (ed). McGraw-Hill, pgs. 554-600, Montreal, 2008

Peer-reviewed Presentations – National and International (15)

1) Lau JTC and **Desai SJ**. High Ankle Sprains. Ontario Medical Association Sport Med 2014. Toronto, Ontario. January 31st, 2014.
2) **Desai SJ**, Deluce S, Johnson JA, Ferreira LM, Leclerc AE, Athwal GS and King GJ. An anthropometric study of the distal humerus. Canadian Orthopaedic Association Annual Meeting, Winnipeg, Manitoba, June 20-22, 2013.
3) **Desai SJ**, Patel J, Abdo H, Lawendy AR and Sanders DW. A Comparison of Surgical Delays in Directly Admitted vs Transferred Patients with Hip Fractures: Opportunities for Improvement? Canadian Orthopaedic Association Annual Meeting, Winnipeg, Manitoba, June 20-22, 2013.
4) Preston S, **Desai SJ**, Somerville L, Angevine D, Sanders, DW, Howard JL. The Implications of Clopidogrel on the Management of Hip Fractures: An Institutional Review. Canadian Orthopaedic Association Annual Meeting, Winnipeg, Manitoba, June 20-22, 2013.
5) **Desai SJ**. Management of Pelvic Fractures. 27th Annual Canadian Orthopaedic Nurses Association Conference, London, Ontario, October 25th, 2012
6) **Desai SJ**, Donohoe E, Abdo H, Lawendy AR. Paediatric Compartment Syndrome. 3rd Annual Paediatric "Talk Trauma" Conference, London. Ontario, September 28th, 2012.
7) Athwal GS and **Desai SJ**. Hemiarthroplasty of the distal humerus. 8th Annual Meeting of the Association of Clinical Elbow & Shoulder Surgeons. Whitefish, Montana, USA, August 3-5, 2012.
8) **Desai SJ**, Athwal GS, Ferreira LM, Johnson JA, Welsh M, Lalone E and King GJW. Distal Humerus Hemiarthroplasty: The Effect of Implant Sizing on Elbow Joint Kinematics. Canadian Orthopaedic Association Annual Meeting, Ottawa, Ontario, Canada, June 8-10th, 2012.

9) Leclerc A, **Desai SJ**, Deluce S, Ferreira LM, King GJW and Athwal GS. Measurements of the Ipsilateral Capitellum can Reliably Predict the Diameter of the Radial Head. Canadian Orthopaedic Association Annual Meeting, Ottawa, Ontario, Canada, June 8-10th, 2012.
10) **Desai SJ**. Traumatic Amputations. "Talk Trauma" Conference, London, Ontario, Canada, April 26th, 2012.
11) **Desai SJ**, Sanders D, Wood K and Bryant D. Wait times and transfusion requirements in hip fractures. Canadian Orthopaedic Association Annual Meeting, St. John's, Newfoundland, Canada, July 7-9, 2011.
12) **Desai SJ**, Sanders D, Wood K and Bryant D. Transfusion requirements in hip fractures. 25th Annual Canadian Orthopaedic Nurses Association Conference, London, Ontario, Canada, October 28, 2010.
13) **Desai SJ**, Sanders D, Ferriera L and Giles J (2009) The Mechanical Effect of Locking and Blocking Screws in Distal Femur Fractures. Orthopaedic Trauma Association Annual Meeting, Baltimore, Maryland, USA, October 13, 2010.
14) **Desai SJ**, Sanders D, Ferriera L and Giles J (2009) The Mechanical Effect of Locking and Blocking Screws in Distal Femur Fractures. Canadian Orthopaedic Association Annual Meeting, Edmonton, Alberta, Canada, June 17-20, 2010.
15) Lee A, **Desai SJ**, Inculet R, Fortin D and Malthaner R. (2006) Video Assisted Thoracic Surgery Lobectomy – Closed-Chested Dissection: Technique and Initial Results: The London, Ontario Experience. Canadian Association of Thoracic Surgeons Conference at the Canadian Surgery Forum in Calgary, Alberta, Canada **First Prize Award Winning Paper.**

Peer-reviewed Presentations – Local (25)

1) **Desai SJ**, Deluce, S., Johnson JA, Ferreira LM, Leclerc AE, Athwal GS and King JW. An anthropometric study of the distal humerus. UWO Medical Biophysics Conference. London, Ontario. February 6, 2014.
2) **Desai SJ** and Lau JT. Fibular Hemimelia: Ball and Socket Ankle. UofT Foot and Ankle Citywide Grand Rounds. January 10th, 2014
3) **Desai SJ** and Daniels TR. Valgus deformity post Total Ankle Replacement. UofT Foot and Ankle Citywide Grand Rounds. January 10th, 2014

4) **Desai SJ** and Lau JT. Recurrent Claw Toe Deformity. UofT Foot and Ankle Citywide Grand Rounds. September 20th, 2013.
5) Dhillon N and **Desai SJ**. Osteonecrosis of the hip following corticosteroid therapy. Rheumatology Grand Rounds. July 30th, 2013
6) **Desai SJ** and Athwal GS. Facioscapulohumeral Muscular Dystrophy. Orthopaedic Surgery City-Wide Grand Rounds, June 18th, 2013
7) **Desai SJ**, Athwal GS, Ferreira L, Johnson JA, Welsch M, Lalone E and King JW. Hemi-Arthroplasty of the Elbow: The Effect of Implant Sizing on Joint Kinematics. UWO Medical Biophysics Conference. April 25th, 2013
8) Smit K and **Desai SJ**. Fractures of the Pelvis. "Talk Trauma" Conference, London, Ontario, Canada, April 25th, 2013.
9) **Desai SJ**, Abdo H, Patel J, Lawendy AR and Sanders DW. A Comparison of Outcomes Between Transfer and Non-Transfer Patients with Hip Fractures. UWO Annual Orthopaedic Surgery Research Day, October 9th, 2012
10) **Desai SJ**, Athwal GS, Ferreira L, Johnson JA, Welsch M, Lalone E and King JW. Hemi-Arthroplasty of the Elbow: The Effect of Implant Sizing on Joint Kinematics. UWO Annual Orthopaedic Surgery Research Day, September 27th, 2011.
11) **Desai, SJ** and MacDonald, SJ. Broken Femoral Stem in Total Hip Arthroplasty. UWO Orthopaedic Surgery City-Wide Grand Rounds, November 23rd, 2011.
12) **Desai, SJ** and Naudie, DD. Tracheal Injury Following Hip Arthroscopy under General Anesthesia. UWO Orthopaedic Surgery City-Wide Grand Rounds, November 23rd, 2011.
13) **Desai SJ** and Sanders, DW. Hip Fractures and Fragility Fractures. UWO Orthopaedic Surgery Program, October 19, 2011.
14) **Desai SJ** and Naudie, DD. Periprosthetic Fractures Above Total Knee Arthroplasty. UWO Orthopaedic Surgery City-Wide Grand Rounds, October 5, 2011
15) **Desai SJ** and Carey, TP. Paediatric Musculoskeletal Infections. UWO Orthopaedic Surgery Program, February 16, 2011.

16) **Desai SJ** and Lebel ME. Polyarticular Septic Arthritis. UWO Orthopaedic Surgery Grand Rounds, October 26th, 2010.
17) **Desai SJ**, Sanders D, Wood K and Bryant D. Wait times and transfusion requirements in hip fractures. UWO's Annual Orthopaedic Surgery Research Day, October 13th, 2010. **First Prize Award Winning Paper**
18) **Desai SJ** and King, GJ. Posteromedial Elbow Instability. UWO Orthopaedic Surgery City-Wide Grand Rounds, May 12th, 2010.
19) **Desai, SJ**. Neurologic Injury Following Pelvic Trauma. UWO Physical Medicine and Rehabilitation Grand Rounds. December 18th, 2009.
20) **Desai, SJ**. Acute Management of Pelvic Fractures. UWO Critical Care Trauma Meeting, October 9th, 2009.
21) **Desai SJ**, Sanders DW, Ferriera L and Giles J (2009) The Mechanical Effect of Locking and Blocking Screws in Distal Femur Fractures. UWO Annual Orthopaedic Surgery Research Day, October 6th, 2009.
22) **Desai SJ**. Ankle Syndesmosis Injuries. UWO Department of Radiology, April 15th, 2009.
23) **Desai SJ**. Pelvic Trauma. UWO Division of Traumatology Meeting, February 12th, 2009.
24) **Desai SJ** and Sanders DW. Calcaneus Fractures. UWO Orthopaedic Surgery City-Wide Grand Rounds, December 10, 2008.
25) **Desai SJ**. & Lemon, P. Effects of Cyclical Caloric Intake on Resting Metabolic Rate. UWO Kinesiology department, 2004.

Poster Presentations (2)

1) **Desai SJ**, Welsh M, Athwal GS, Ferreira LM, Johnson JA, Lalone E and King GJW. Distal Humerus Hemiarthroplasty: The Effect of Implant Sizing on Elbow Joint Kinematics. Orthopaedic Research Society Annual Meeting, San Antonio, Texas, January 26-29, 2013
2) Lee A, **Desai SJ**, Inculet R, Fortin D and Malthaner R. (2006) Video Assisted Thoracic Surgery Lobectomy – Closed-Chested Dissection: Technique and Initial Results. CREMS Research Day, January 18th, 2007, University of Toronto, Toronto, Ontario.

Meetings/Conferences Attended

November 15-16, 2013	Advances in Foot and Ankle Surgery. New York, New York.
October 25-26, 2013	Emerging Techniques and Biologic Solutions for Foot and Ankle Surgery: Foot and Ankle Surgeon Lab Experience. Clearwater, Florida
June 20-22, 2013	Canadian Orthopaedic Association Annual Meeting. Winnipeg, Manitoba, Canada
April 5-8, 2013	11th Annual Canadian Orthopaedic Resident Forum. Calgary, Alberta, Canada
March 13-15, 2013	26th Sainte-Justine Paediatric Orthopaedic Review Course. Montreal, Quebec, Canada
January 17-19, 2013	Canadian Orthopaedic Resident Review (CORR) Recon Course. Mississauga, Ontario, Canada
November 22-24, 2012	Canadian Orthopaedic Resident Review (CORR) Trauma Course. Mississauga, Ontario, Canada
September 28, 2012	29th Western Homecoming Sports Medicine Symposium: Care of the High Level Athlete. London, Ontario, Canada.
June 26-27, 2012	American Orthopaedic Association-Orthopaedic Research and Education Foundation Resident Leadership Conference, Washington, DC, USA
June 8-10, 2012	Canadian Orthopaedic Association Annual Meeting. Ottawa, Ontario, Canada
May 10-12, 2012	Orthopaedic Trauma Review Course. Kingston, Ontario, Canada
April 26, 2012	Talk Trauma Conference, London, Ontario, Canada
April 20-21, 2012	Canadian Orthopaedic Foot and Ankle Society Annual Meeting, Toronto, Ontario, Canada
February 7-11, 2012	American Academy of Orthopaedic Surgeons (AAOS) Annual Meeting, San Francisco, California
November 11-12, 2011	Advances in Foot and Ankle Surgery. New York, New York.

July 7-9, 2011	Canadian Orthopaedic Association Annual Meeting. St. John's, Newfoundland, Canada
April 28-30, 2011.	Orthopaedic Trauma Association Comprehensive Fracture Course for Residents. Schaumburg, Illinois
November 5-7, 2010.	American Academy of Hip and Knee Surgeons Annual Meeting. Dallas, Texas